AN IMPROVED PROFILE OF THE RAILWAY WHEEL TO MINIMIZE RESIDUAL STRESSES AFTER SEVERE DRAG BRAKING

by

Syed M. Badruddin

A RESEARCH THESIS
IN THE
FACULTY OF ENGINEERING

Presented in partial fullfilment of the
requirements for the degree of
MASTER OF ENGINEERING
at
Concordia University
Montreal, Quebec, Canada

April 1982

ABSTRACT

AN IMPROVED PROFILE OF RAILWAY WHEEL TO MINIMIZE RESIDUAL STRESSES AFTER DRAG BRAKING

Syed M. Badruddin

The objective of this thesis is to study the behavior of elasto-plastic stresses under severe drag braking. Attempt is made here to find an improved fillet profile of the wheel with the intention of minimizing high tensile residual stresses.

A railway wheel performs three tasks, aiding in train movement, supporting the car load and also act as brake drum. In its service life it encounters both mechanical and thermal stresses. Thermal stresses are caused by brake application. Very high thermal stresses are observed under severe drag braking, causing yielding and wheel failure.

Finite element computer programs are developed for both temperature calculations and elasto-plastic stress analysis. Three new fillet profiles for the wheel are tested. A penalty function is used as a criteria for comparison of stresses between the new designs and the old design. The design with the least penalty is chosen to be the improved one.

ACKNOWLEDGEMENTS

The author wishes to express his appreciation to his supervisors, Drs. S. V. Hoa and R. M. H. Cheng, for their encouragement and guidence throughout all stages of this work.

CONTENTS

LIST OF TABLES

LIST OF FIGURES

LIST OF SYMBOLS

$[B]$ = matrix relating stress and strain.

$[C]$ = capacitance matrix.

c = heat capacitance, $J/kg^{\circ}C$.

$[D]$ = elasticity matrix.

$[D]_{ep}$ = elasto-plastic matrix.

E = modulus of elasticity, MPa.

$\{F\}$ = force vector.

H' = plastic modulus, MPa .

h = convection coefficient, $W/m^2-{}^{\circ}K$.

i, j, k = nodes of a triangle.

l_r, l_z = direction cosines.

L_{ij} = length of side i-j, m..

$[K]$ = stiffness matrix.

K_r, K_z = thermal conductivity in r and z directions, $W/m^{\circ}K$.

$[N]$ = shape function of the element.

$\{P\}$ = vector containing nodal forces.

Q = internal heat generated per unit volume, W/m^3 .

q = heat flux, W/m^2 .

r = radial direction.

S, s = surface.

T = temperature, $^{\circ}K$.

T_{∞} = ambient temperature, $^{\circ}K$.

Δt = time increment, seconds.

V = volume, m^3 .

u = displacements in radial direction.

v = displacements in axial direction.

W_t = weight assigned to tangential stress.

W_r = weight assigned to radial stress.

Y = yield criteria.

z = axial direction.

α = coefficient of thermal expansion, $in/in^{\circ}K$.

γ = shear strain.

θ = tangential direction.

δ_{ij} = kronecker delta.

$\{\delta\}$ = displacements.

ε_r, ε_z, ε_θ = normal strain in r, z and θ directions.

$\hat{\varepsilon}$ = equivalent strain.

Δ = area of triangular element, m^2 .

ρ = density of the material, kg/m^3 .

ε_o = thermal strain.

σ_r, σ_z, σ_θ = normal stress in r, z and θ directions.

σ_o = initial stress, MPa .

$\hat{\sigma}$ = equivalent stress, MPa.

$\bar{\sigma}$ = yield stress, MPa .

τ = shear stress, MPa .

1. INTRODUCTION

Since the time of the first steam engine to the present day the railway system has evolved considerably. From the premitive slow moving engines of the past to the high speed engines of today, trains have gone through a great deal of research and development, to keep pace with the changing needs of society, which has kept it competetive, and in many cases economical, to other transportation systems.

Increasing demand of high speed and heavy loads has led to occasional accidents. According to statistics on accidents, compiled by the U. S. Federal Railroad Administration, there were a total of 324 reportable derailments (causing railroad property damage in excess of $750.00) due to wheel defects and failure during 1973. This number represents about 20% of the total equipment-related derailments [11]. In another report Carter et al.[3] summarize the reported wheel failures between 1968-1972, shown in Table 1 (page 2). Cracked or broken plate consistently contributes to one-fifth to one quarter of the causes of failure. Cracked or broken rims constitute about 20% of the reported wheel failures. These failures are mainly due to thermal stresses. This follows the trend of

Date	Number of failures reported	Causes of failures(%)							
		Cracked or broken plate	Cracked or broken flange	Cracked or broken rim	Thermal cracks	Burst hubs	Shattered rim	Tread shelled	Susurface defect
1968	251 25% cast 75% wrought	19.5	4.25	14	17	0.5	33	0.5	4.25
1969	419 14.3% cast 85.7% wrought	17	6	13.5	3	0.75	54	0	2
1970	354 25.5% cast 74.5% wrought	19	2.5	24	7	1	45	1	1
1971	348 36.2% cast 63.8% wrought	20	4	39	6.5	1.5	20	2	7
1972	710 27.3% cast 72.7% wrought	24	2.5	26	10.5	0.8	35	0.2	1

Table 1. Summary of wheel failures reported to AAR for period 1968-1972. [3]

increasing frequency in accidents that has been established in recent years. The matter is of concern to engineers, since future demand on the railway system is expected to lead to more serious and frequent accidents.

1.1 WHEEL DESIGN

Figure 1 (page 4). shows the nomenclature of a wheel. Although the basic design of all railroad wheels follow dimensional requirements set by the Association of American Railroads, there is actually a wide variety of wheels with different cross-sections and material properties. For example H36, J36 and K36 are intended for same weight range of 70 to 100 tons car capacity and have same overall dimensions except the rim, as shown in Table 2 (page 5). For H36 minimum rim thickness is 3.8 cms (1.5 inches), for J36 it is 5 cms (2 inches) and for K36, 6.4 cms (2.5 inches). Similarly the wheel material can have different chemical composition, with carbon content ranging from 0.47% to 0.77%, and the rim can be hardened, with hardness ranging from 197 B.H.N. to 363 B.H.N. or they may be untreated. The factors influencing these varieties are the manufacturing process, the intended application and the desired service life.

The first factor, the manufacturing process, divides the wheel into two main categories; parabolic plate wheels and

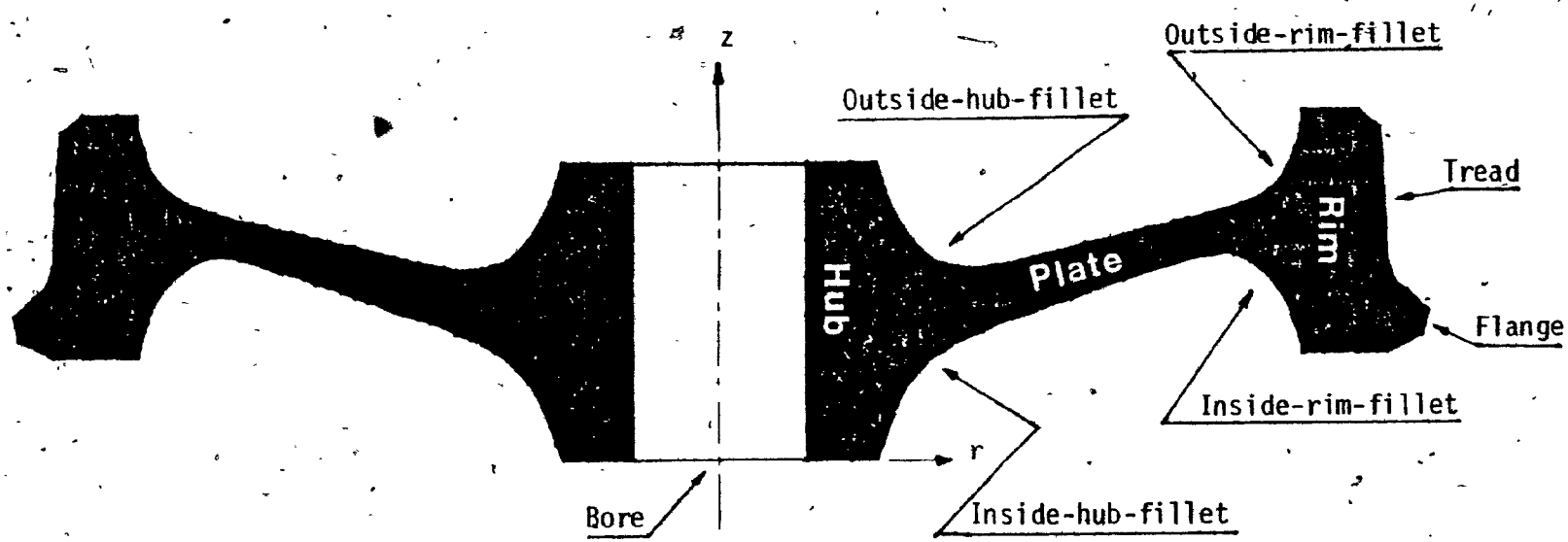

Figure 1. Wheel Nomenclature

Table 2

AAR STANDARD DESIGN — WROUGHT STEEL WHEELS

WIDE FLANGE WHEELS — FOR FREIGHT CARS

Design	Intended Freight Car Capacity	Intended Max. Axle Size (Roller Bearing) (Ins.)	Min. Rim Thickness (Ins.)	Min. Hub Diameters (Ins.)	Max. Finish Bore (Ins.)	Nominal Weight (Lbs.)
ONE WEAR						
D 28	Not over 22,400 lbs. per wheel	6 x 11	1-1/2	10-5/8	8-3/8	550
A 33	40 and 50 ton	5-1/2 x 10	1-1/4	9-11/16	7-11/16	580
J 33	70 ton	6 x 11	1-1/4	10-5/8	8-3/8	630
H 36	Over 70 to 100 ton	6-1/2 x 12	1-1/2	11-1/8	8-7/8	765
B 36	Not over 39,375 lbs. per wheel	7 x 12	1-1/2	12-1/8	9-5/8	850
TWO WEAR						
K 33	40 and 50 ton	5-1/2 x 10	2	9-11/16	7-11/16	685
M 33	70 ton	6 x 11	2	10-5/8	8-3/8	720
J 36	Over 70 to 100 ton	6-1/2 x 12	2	11-1/8	8-7/8	835
C 36	Not over 39,375 lbs per wheel	7 x 12	2	12-1/8	9-5/8	925
MULTIPLE WEAR						
A 28	70 to 100 ton	6-1/2 x 12	2-1/2	11-1/8	8-7/8	725
A 30	70 to 100 ton	6-1/2 x 12	2-1/2	11-1/8	8-7/8	760
G 33	100 ton	6-1/2 x 12	2-1/2	11-1/2	9-1/4	870
N 33	40 and 50 ton	5-1/2 x 10	2-1/2	9-11/16	7-11/16	780
R 33	70 ton	6 x 11	2-1/2	10-5/8	8-3/8	800
K 36	Over 70 to 100 ton	6-1/2 x 12	2-1/2	11-1/8	8-7/8	900

[12]

Table 3

CHEMICAL ANALYSIS AND HARDNESS, AAR SPECIFICATION M-107

		Class U	Class L	Class A	Class B	Class C
Carbon	%	.65-.80	.47(Max.)	.47-.57	.57-.67	.67-.77
Manganese	%	.60-.85	.60-.85	.60-.85	.60-.85	.60-.85
Phosphorus(Max.)	%	.05	.05	.05	.05	.05
Sulphur (Max.)	%	.05	.05	.05	.05	.05
Silicon (Max.)	%	.15	.15	.15	.15	.15
Rim Hardness Range (B.H.N)		not specified	197-277	255-321	277-341	321-363

[12]

straight plate wheels. Presently there are two basic methods employed in wheel manufacturing process, namely forging and casting. Casting is used in manufacturing of parabolic plate wheels, Figure 2 (page 7), while forging results in straight plate wheels, Figure 3 (page 7). Both parabolic and straight plate wheels are used in North American railways.

The second factor relates to the type and severity of application. As one expects, a higher load would require larger diameter to keep the rail contact stress within acceptable limits. Thus, the nominal diameter of wheels range from 0.71 to 1.06 meters (28 to 42 inches); corresponding to load ranging from 96081. N to 15235. N (21600. lbs. to 34900. lbs.).

The third influencing factor is the desired life. About 85% of the wheels in service are designed for single tread life which is called one-wear wheel. On the other hand life of a wheel can be extended by making the rim thick enough to allow remachining of the rim after service wear, to restore the original profile. Wheels with this capabilities are designed as either two-wear or multiple-wear wneels, depending on the rim thickness. The specification of the Association of American Railroads for rim thickness for one-wear, two-wear and multiple-wear wheels are minimum of 3.17, 5.08 and 6.35 cms. (1.25, 2.0 and 2.5 inches) respectively.

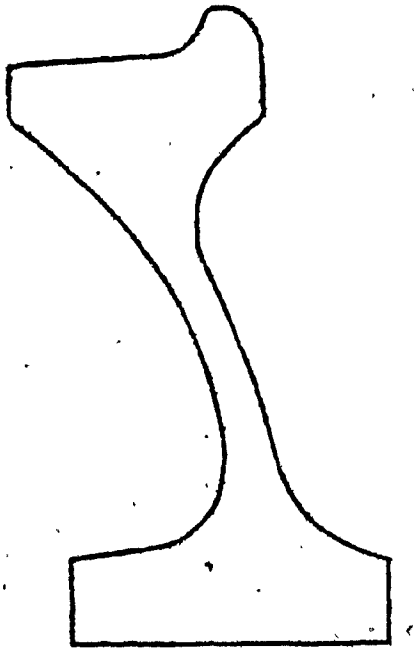

Figure 2.
Parabolic Plate Wheel.

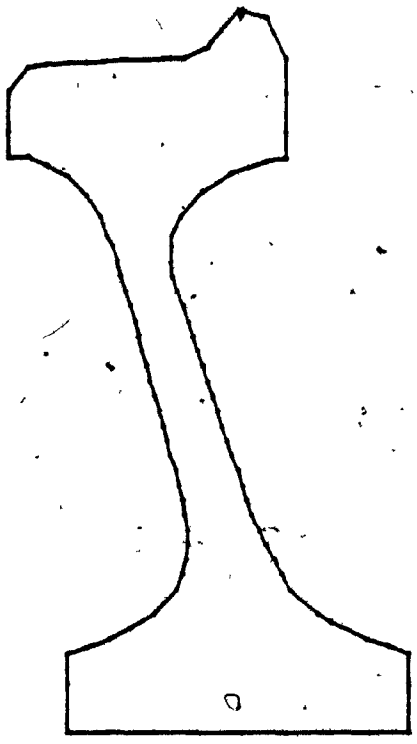

Figure 3.
Straight Plate Wheel.

AAR has further classified wheels into 5 categories, class U, L, A, B and C. Class U has no heat treatment. While class L, A, B and C have varying degrees of heat treatment. Their chemical compositions are shown in Table 3 (page 5). The service for which they are intended are as follows: [12]

Class U - General service where an untreated wheel is satisfactory.

Class L - High speed service, with more severe braking conditions than other classes, and with light wheel loads.

Class A - High speed service with severe braking conditions, but with moderate wheel loads.

Class B - High speed service with severe braking conditions and heavier wheel loads.

Class C - (1) Service with light braking conditions and high wheel loads.
(2) Service with heavier braking conditions where off-tread brakes are employed.

1.2 SERVICE CONDITIONS

Besides being an integral part of the train motion, railway wheels are required to perform two main functions in

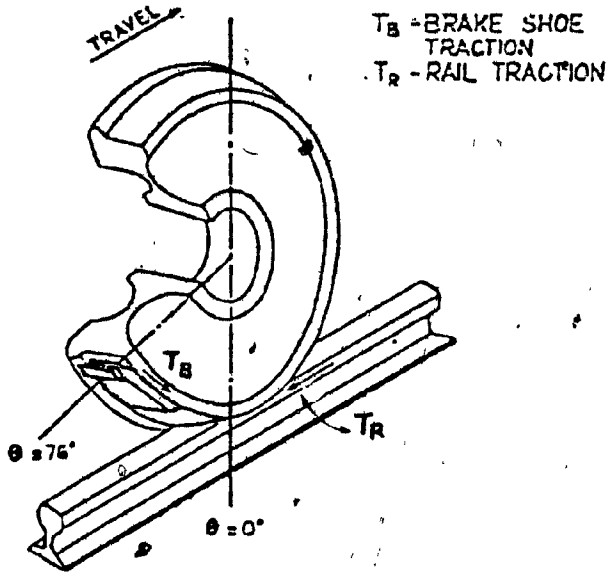

Figure 4. Coordinate (θ) system illustrating the location of the wheel-brake shoe (θ = 76 deg.) and wheel-rail (θ = 0 deg.) planes. [17]

railroad service, one is to support the weight of the vehicle, and the other is to provide a brakedrum, as shown in Figure 4 (page 9). So during its service life a wheel encounters different types of wear and tear such as shelling, thermal cracking, spalling, overheating etc.

Shelling is caused by fatigue failure of tread due to repeated overstressing by heavy wheel loads. The condition is characterized by the expulsion of metal from tread in rail contact area, as shown in Figure 5 (page 11). Contributing factor to this type of failure include poor tracks, excessive speed, high loads, or use of wheels with insufficient hardness.

Thermal cracks are caused by intense brake heating. They are usually confined to tread or flange, but in extreme cases, may go through the entire rim and into the plate, as shown in Figures 6 and 7 (pages 11 & 12). Thermal cracking is a serious condition at any stage of development, and such cases should be immediatly removed from service. Radial cracks on inside and outside face of the rim tend to progress and can lead to wheel failure. Many shallow thermal cracks can be removed by machining, but care must be taken to make certain that the cracks have been completely eliminated.

Spalling develops from service conditions such as wheel slipping, skidding or sliding. These conditions produce brief intense heating of wheel tread surface in rail contact

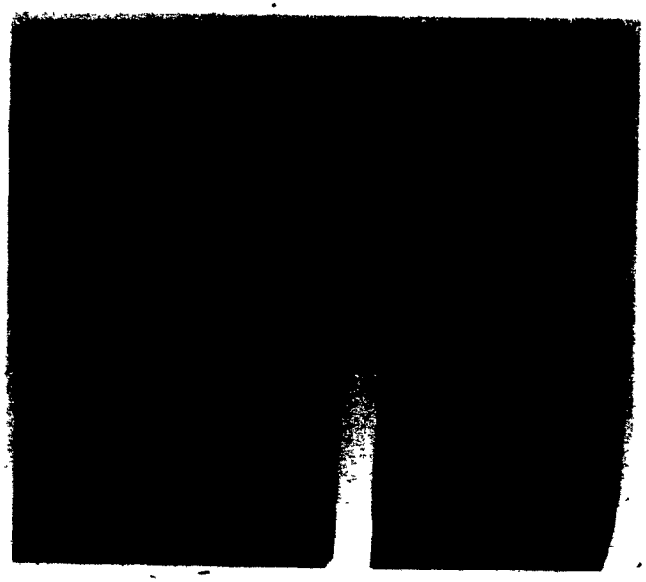

Figure 5. Shelled tread. [23]

Figure 6. Thermal cracks in tread of wheel. [23]

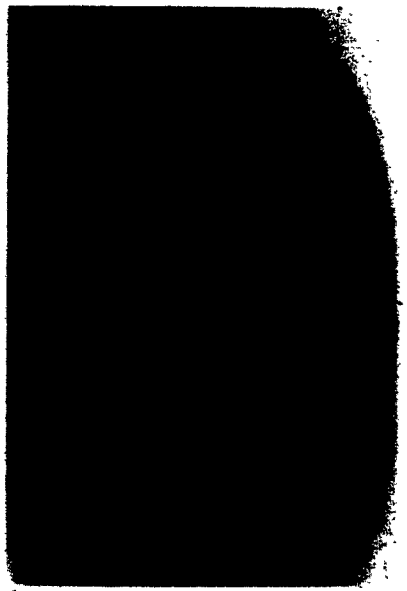

Figure 7. Wheel which failed through a thermal crack. [23]

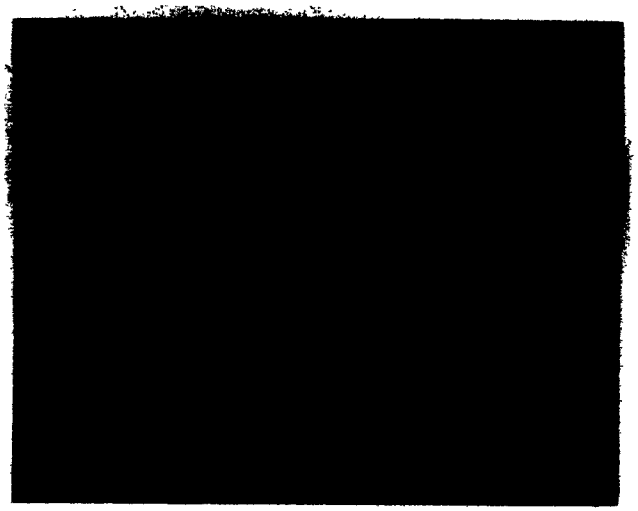

Figure 8. Cross-section ofwheel tread with spalling. Magnification 15X. [23]

area, leading to the development of small traverse thermal cracks, as shown in Figure 8 (page 12). With repeated rail contact under load, fractures may progress beneath the layers affected by heat and portions of tread surface between the thermal cracks may fall away.

A very important category of wheel failure is overheating due to drag braking or stuck brakes. Prolonged application of the brake causes heat to spread deep inside the plate. Such wheels are potentially dangerous because the high tensile stresses that are developed can lead to sudden failure in the presence of even small thermal cracks.

1.3 SERVICE STRESSES

The stresses experienced in wheels during service result primarily from the following conditions.

i) Vertical loads due to equipment and car load. These loads are applied cyclically along the wheel tread, and may be accelerated by dynamic effects due to track deviation and operating conditions.

ii) Lateral loads applied against the front of the flange as a result of curve negotiation, hunting etc. These loads occur less frequently

than vertical loads but also tend to fluctuate.

iii) Thermal gradient effects, resulting from conversion of kinetic energy of the train into heat, when the brake shoes are applied to the wheel tread. The stress caused by braking can be considered to be of a steady nature. They do not fluctuate during each revolution.

Maximum wheel load allowed in design is the static gross weight of the car, but dynamic effect can increase the wheel load by a factor of about 2 times [3]. Stresses developed due to the dynamic loads vary considerably along the section of the wheel.

Rusin et al.[20] have analysed a 84 cms (33 inch) wheel subjected to 244,200. N (55,000 lbs.) vertical load, which is twice the allowed static load. The maximum Von Mises stress developed is about 75 MPa around the section of inside-rim-fillet and outside-hub-fillet. In another report Carter et al.[3] has reported that for a 91.5 cms (36 inch) wheel with 266,400. N (60,000. lbs.) vertical load the highest stresses occur in the radial direction. At the inside-rim-fillet the highest radial stress is +21.36MPa (+3100 psi), and that at outside-hub-fillet is +26.87MPa (+3900 psi), both at 180 degrees from the load line. Lateral load of 88,800. N (19,900. lbs.) and up are also observed elsewhere in practice [3], which produce radial stress of

+68MPa around outside-hub-fillet.

Stresses due to brake application vary depending upon the amount of heat energy dissipated. Although the rate of energy dissipation is much higher in emergency braking than drag braking, the extended duration of the latter is such that the wheel is heated to a considerably greater depth below the tread. This causes the stresses in the plate regions of the wheel to be considerably higher than those produced under emergency braking. Stresses due to drag braking have been experienced to have crossed the yield limit of 400 MPa.

1.4 PREVIOUS STRESS ANALYSIS ON RAILWAY WHEELS

Wheel failure phenomenon has been under investigation for the past few decades. Both experimental and theoratical results have been reported showing the temperature and stress distribution in a wheel during its service life. It has been generally agreed by most investigators [15,17,25] that the most severe damage to a wheel is due to thermal stresses.

Novak and Stone[16] have analysed a 36 inch straight plate wheel under a vertical load of 312,000. N (70,000. lbs.) and a lateral load of 89000N with 55 seconds of 0.62 MPa (90 psi) brake cylinder pressure application normally used for emergency braking. It is observed that as

rim thickness decreases, stresses in the rim-plate-fillet and hub-plate-fillet tend to increase.

In another report Novak et al. [14,17] have reported experimental temperature distribution on 36 inch deep dish parabolic and straight plate wheels subjected to emergency braking, which show high temperature gradient in rim sections. Also stresses due to a vertical load of 212,000. N (47,500. lbs.) on static wheel are compared with stresses in a wheel with 127km/hr (79mph) velocity under the same load, it is observed that stresses decrease by more than 15% in the wheel with 127km/hr velocity.

Wetenkamp and Kipp[26] has done experimental and theoretical analysis on 33 inch parabolic plate wheel. A three dimensional finite element model has been developed. For a 88,800. N (19,900. Lbs) vertical load the maximum Von Mises stress is observed to be 25MPa (3628 psi) at outside-hub-fillet at 0 degrees from load line, which is 7% of the value of yield limit.

Rusin et al.[20] has analysed a 33 inch straight plate wheel and proposed a new design, which is similar to parabolic plate wheel. The fourier series is used to model the point load on an axisymmetric formulation. The results are found to be in close agreement with those obtained using the three dimensional general purpose finite element program "Superb". Upto 30% of reduction in thermal stresses are

observed in the new design in fillet regions where high Von Mises stresses are high, but a slight increment is found in these regions under mechanical loading.

All the work mentioned above has examined wheel stresses using elastic analysis. Johnson et al.[9] has done plastic analysis on 36 inch one-wear, two-wear and worn straight plate wheels, under severe drag brake conditions of 20hp, 30hp and 40hp of braking for 60 minute. Plastic stress and residual stress distribution are obtained across the plate thickness near the hub and rim regions. High compressive radial residual stresses are observed in plate regions, but nothing is mentioned about tangential residual stresses in plates. Both radial and tangential residual stresses are important in the study of fatigue life of wheel, specially if tangential stresses are tensile in the critical fillet regions as is observed in our study.

1.5 SCOPE OF WORK

In reality, wheels under severe drag braking do go into plastic deformation. Few investigators have worked in this area to predict plastic stresses and the consequent residual stresses. Tensile residual stresses occur in regions of high stress concentration [9], which explains why cracks often begin in those regions. These cracks lead to fatigue

failures of wheels, and the presence of tensile residual stresses tend to reduce their fatigue life.

The purpose of the present work is to study the behavior of elasto-plastic and residual stresses due to severe drag braking, and to reduce tensile residual stresses in regions of stress concentration by modifying the wheel profile, without significantly changing the wheel weight, and load-bearing capacity. Previous attempts by Rusin et al. [20] for an improved profile of a straight plate wheel resulted in a parabolic plate wheel. Since the manufacturing processes of both parabolic and straight plate wheels are considerably different, and a large number of wheel manufacturers are producing straight plate wheels, attempt is made here for the reduction of stress concentration in a straight plate wheel with modification in the fillet profiles only.

1.6 METHOD OF SOLUTION

The irregular shape of wheel makes it impossible to obtain a closed form solution of any comprehensive analytical model of it. Numerical methods are therefore used to obtain approximate solutions. Two of the possible methods are the finite difference and the finite element methods.

In the finite difference method the solution region is divided into an array of uniform grid points, while in the finite element method the solution region is composed of interconnected subregions or elements. The finite difference method is used quite commonly to solve fairly difficult problems, but becomes difficult to implement in problems with irregular geometries and unusual boundary conditions. As an example, consider the study of a turbine blade. In Figure 9(a) (page 20), the turbine blade is divided in uniform finite difference mesh, but the boundaries are approximated by vertical and horizontal lines. On the other hand, the finite element method gives a better approximation to the region and requires fewer nodes as shown in Figure 9(b), it also gives better results for its boundary, since the curved boundary is represented by a series of straight line segments [8]. Based on these considerations finite element method is used for the present investigation, since the geometry of the wheel involves many curved boundaries.

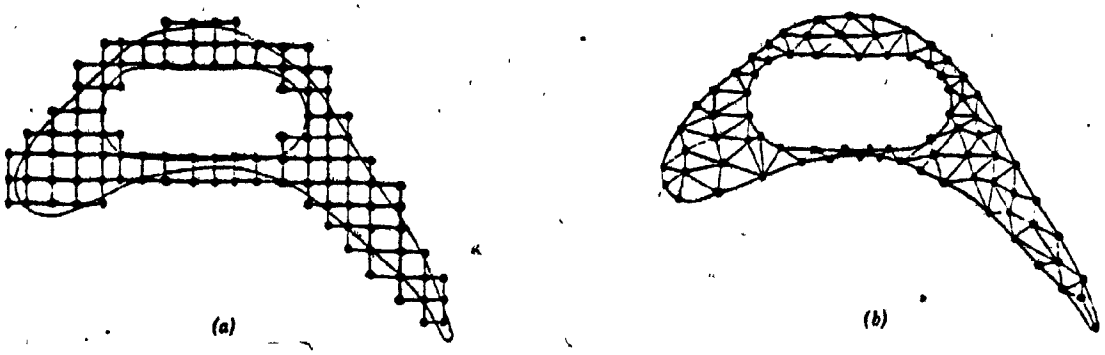

Figure 9. Finite difference (a) and finite element (b) discretization of a turbine blade profile. [8]

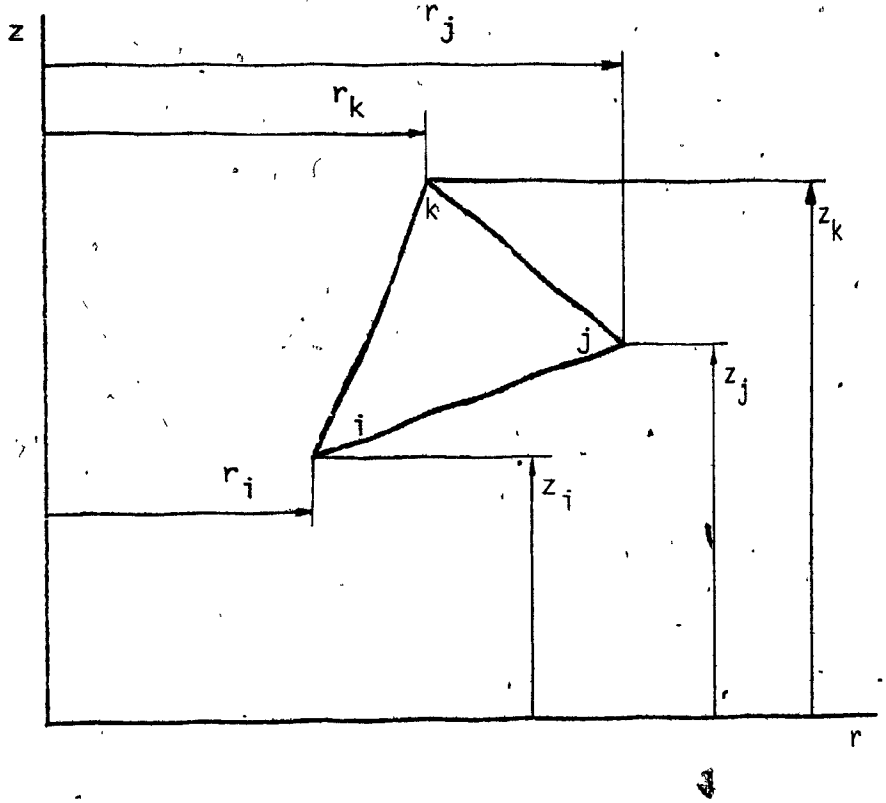

Figure 10. A typical triangular finite element.

2 THE FINITE ELEMENT METHOD

The finite element method which was initially used in structural analysis is now being used for a wide range of continuum mechanics problems such as fluid mechanics, heat transfer, lubrication etc. A great deal of work about the method is available in the literature [8,21,28]. Recent advancements in digital computer, probably, have been the most important driving force in the fast development of the finite element method, since it is tedious to solve by hand the large number of element equations.

The elements can be of different shapes, triangular, rectangular, quadrilateral, three-dimensional, isoparametric etc. Constant strain triangular elements are used in this analysis. The selection of this element is based upon its simplicity and its ability to model curved contours of the wheel shape by using trianlges of sufficiently short sides. The accuracy of the mesh is achieved by its progressive refinement.

2.1 ELEMENT SHAPE FUNCTION

For thermal stress analysis, even though the heat input from braking is a point source, this heat input can be

considered axisymmetric since the wheel is rotating at a sufficiently high speed. The geometry of the wheel is also axisymmetric. These two conditions would permit the use of the simplified axisymmetric finite element formulation. The same mesh is used for both temperature and stress calculations.

At this stage let us define interpolation, or shape function, for a triangular element. Shape function is a continuous function which defines the behavior of the field variable, e.g. temperature or displacements etc., over the element in terms of the nodal values of the element. Let T_i, T_j and T_k be temperatures at the nodes i, j and k respectively of the triangle shown in Figure 10 (page 20). Where r represents the radial direction and z the axial direction of the wheel. The temperature distribution over the element can be represented by:

$$T = \begin{bmatrix} N_i & N_j & N_k \end{bmatrix} \begin{Bmatrix} T_i \\ T_j \\ T_k \end{Bmatrix} = [N] \{T\} \qquad (2.1)$$

N_i N_j and N_k are called the shape functions. [N] is a 1x3 matrix and {T} is a 3x1 vector.

The shape function can be shown to be: [21]

$$N_i = \frac{1}{2\Delta}\left[r_j z_k - r_k z_j + \left(z_j - z_k\right)r + \left(r_k - r_j\right)z \right] \qquad (2.2)$$

$$N_j = \frac{1}{2\Delta}\left[r_k z_i - r_i z_k + \left(z_k - z_i\right)r + \left(r_i - r_k\right)z \right]$$

$$N_k = \frac{1}{2\Delta}\left[r_i z_j - r_j z_i + \left(z_i - z_j\right)r + \left(r_j - r_i\right)z \right]$$

where

r_i, z_i = nodal values of r and z coordinates of node i respectively, (see Figure 10).

Δ = area of the triangular element.

Similarly displacements in the element can be represented as a function of nodal displacements of the element by:

$$u = \begin{bmatrix} N_i & N_j & N_k \end{bmatrix} \begin{Bmatrix} u_i \\ u_j \\ u_k \end{Bmatrix} = [N]\{u\} \qquad (2.3)$$

$$v = \begin{bmatrix} N_i & N_j & N_k \end{bmatrix} \begin{Bmatrix} v_i \\ v_j \\ v_k \end{Bmatrix} = [N]\{v\}$$

where u and v represent displacements along radial and axial directions respectively.

2.2 TEMPERATURE DISTRIBUTION

The duration of time involved in brake application makes it a transient problem. The finite element formulation is outlined in the book of Segerlind [22], but for the sake of

completeness, the relevent portions are repeated here.

The general heat transfer equation for axisymmetric solids is:[8]

$$K_r \frac{\partial^2 T}{\partial r^2} + \frac{K_r}{r} \frac{\partial T}{\partial r} + K_z \frac{\partial^2 T}{\partial z^2} + Q = \rho c \frac{\partial T}{\partial t} \qquad (2.4)$$

with boundary conditions:[20]

$$K_r \frac{\partial T}{\partial r} l_r + K_z \frac{\partial T}{\partial z} l_z + q + h(T - T_\infty) = 0 \qquad (2.5)$$

where

K_r, K_z = conduction coefficient in r and z directions respectively

Q = heat generated per unit volume.

c = heat capacity.

ρ = density.

T = temperature

t = time

q = heat flux per unit area.

l_r, l_z = directions cosines.

h = convection coefficient.

T_∞ = ambient temperature.

It can be shown by calculus of variation that the solution to the above differential equation (2.4) and boundary condition (2.5) can be obtained by minimizing a corresponding funtional χ . The formulation of χ is

outlined below.

We seek a functional, X, of equations 2.4 and 2.5, such that its first variation with respect to T be zero. Equations 2.4 and 2.5 can be written as:

$$-K_r\, r\, \frac{\partial^2 T}{\partial r^2} - K_r \frac{\partial T}{\partial r} - K_z\, r\, \frac{\partial^2 T}{\partial z^2} - r\left(Q - \rho c \frac{\partial T}{\partial t}\right) = 0 \qquad (2.6)$$

and

$$K_r\, r\, \frac{\partial T}{\partial r}\, l_r + K_z\, r\, \frac{\partial T}{\partial z}\, l_z + rq + rh(T - T_\infty) = 0 \qquad (2.7)$$

Multiply equations 2.6 and 2.7 by the first variation of T, δT, and integrate over the domain, we get:

$$\delta X = \int_V \left[-K_r\, r\, \frac{\partial^2 T}{\partial r^2} - K_r \frac{\partial T}{\partial r} - K_z\, r\, \frac{\partial^2 T}{\partial z^2} - r\left(Q - \rho c \frac{\partial T}{\partial t}\right)\right] \delta T\, dV$$

$$+ \int_S \left[K_r\, r\, \frac{\partial T}{\partial r}\, l_r + K_z\, r\, \frac{\partial T}{\partial z}\, l_z + rq + rh(T - T_\infty)\right] \delta T\, dS \qquad (2.8)$$

re-arranging the above equation 2.8, we get:

$$\delta X = \int_S K_r\, r\, \frac{\partial T}{\partial r}\, l_r\, \delta T\, dS - \int_V K_r\, r\, \frac{\partial^2 T}{\partial r^2}\, \delta T\, dV - \int_V K_r \frac{\partial T}{\partial r}\, \delta T\, dV$$

$$+ \int_S K_z\, r\, \frac{\partial T}{\partial z}\, l_z\, \delta T\, dS - \int_V K_z\, r\, \frac{\partial^2 T}{\partial z^2}\, \delta T\, dV - \int_V r\left(Q - \rho c \frac{\partial T}{\partial t}\right) \delta T\, dV$$

$$+ \int_S rq\, \delta T\, dS + \int_S rh(T - T_\infty)\, \delta T\, dS \qquad (2.9)$$

using Green's (Divergence) theorem, we can write:

$$\int_S K_r\, r\, \frac{\partial T}{\partial r}\, l_r\, \delta T\, dS = \int_V K_r\, r\, \frac{\partial^2 T}{\partial r^2}\, \delta T\, dV + \int_V K_r\, \frac{\partial T}{\partial r}\, \delta T\, dV + \int_V \frac{K_r}{2}\, r\, \delta\left(\frac{\partial T}{\partial r}\right)^2 dV \tag{2.10}$$

and

$$\int_S K_z\, r\, \frac{\partial T}{\partial z}\, l_z\, \delta T\, dS = \int_S K_z\, r\, \frac{\partial^2 T}{\partial z^2}\, \delta T\, dV + \int_S \frac{K_z}{2}\, r\, \delta\left(\frac{\partial T}{\partial z}\right)^2 dV \tag{2.11}$$

substituting equations 2.10 and 2.11 in equation 2.9, we get:

$$\delta\chi = \int_V \frac{K_r}{2}\, r\, \delta\left(\frac{\partial T}{\partial r}\right)^2 dV + \int_V \frac{K_z}{2}\, r\, \delta\left(\frac{\partial T}{\partial z}\right)^2 dV - \int_V r\, \delta T\, (Q - \rho c\, \frac{\partial T}{\partial t})\, dV + \int_S rq\, \delta T\, dS + \int_S \frac{rh}{2}\, \delta(T - T_\infty)^2\, dS \tag{2.12}$$

which can be written as:

$$\delta\chi = \int_V \delta\left[\frac{K_r}{2}\, r\, \left(\frac{\partial T}{\partial r}\right)^2 + \frac{K_z}{2}\, r\, \left(\frac{\partial T}{\partial z}\right)^2 - rT(Q - \rho c\, \frac{\partial T}{\partial t})\right] dV + \int_S \delta\left[rqT + \frac{rh}{2}\, (T - T_\infty)^2\right] dS \tag{2.13}$$

the δ can be removed out of the integral sign, hence the functional:

$$\chi = \int_V \left[\frac{K_r}{2}\, r\, \left(\frac{\partial T}{\partial r}\right)^2 + \frac{K_z}{2}\, r\, \left(\frac{\partial T}{\partial z}\right)^2 - rT(Q - \rho c\, \frac{\partial T}{\partial t})\right] dV + \int_{S1} rqT\, dS + \int_{S2} \frac{rh}{2}\, (T - T_\infty)^2\, dS \tag{2.14}$$

S1 is the surface with heat flux and S2 is the surface with convection.

To show that the funtional, equation 2.14, is the funtional equivalent of equations 2.4 and 2.5, we use Euler-Lagrange formula. The equation 2.14 is of the form:

$$\chi = \int_V f(r, z, \phi, \phi_r, \phi_z)\, dV + \int_S \left[rq\phi + \frac{rh}{2}(\phi - \phi_\infty)^2 \right] dS \qquad (2.15)$$

where $\phi = T$, $\phi_r = \frac{\partial T}{\partial r}$, $\phi_z = \frac{\partial T}{\partial z}$, $\phi_\infty = T_\infty$

According to Euler's theorem of variational calculus, [32], the function f that minimizes the functional χ should satisfy:

$$\frac{\partial f}{\partial \phi} - \frac{\partial}{\partial r}\left(\frac{\partial f}{\partial \phi_r} \right) - \frac{\partial}{\partial z}\left(\frac{\partial f}{\partial \phi_z} \right) = 0 \qquad (2.16)$$

over the volume, and

$$l_r \frac{\partial f}{\partial \phi_r} + l_z \frac{\partial f}{\partial \phi_z} + rq + rh(\phi - \phi_\infty) = 0 \qquad (2.17)$$

over the surface.

Applying the equations 2.16 and 2.17 we obtain equations 2.4 and 2.5 , which shows that the functional, equation 2.14, and the governing equation with boundary conditions, equations 2.4 and 2.5 are equivalent.

Using equations 2.1 and 2.2 let us define two matrices [A] and [G] :

$$\begin{Bmatrix} \frac{\partial T}{\partial r} \\ \frac{\partial T}{\partial z} \end{Bmatrix} = \begin{bmatrix} \frac{\partial N_i}{\partial r} & \frac{\partial N_j}{\partial r} & \frac{\partial N_k}{\partial r} \\ \frac{\partial N_i}{\partial z} & \frac{\partial N_j}{\partial z} & \frac{\partial N_k}{\partial z} \end{bmatrix} \begin{Bmatrix} T_i \\ T_j \\ T_k \end{Bmatrix} = [A] \{T\} \tag{2.18}$$

$$[G] = \begin{bmatrix} r K_r & 0 \\ 0 & r K_z \end{bmatrix} \tag{2.19}$$

From the same equation 2.1, we can also write:

$$\frac{\partial T}{\partial t} = [N] \frac{\partial \{T\}}{\partial t} \tag{2.20}$$

where

$$\frac{\partial \{T\}}{\partial t} = \left\{\frac{\partial T}{\partial t}\right\} = \begin{Bmatrix} \frac{\partial T_i}{\partial t} \\ \frac{\partial T_j}{\partial t} \\ \frac{\partial T_k}{\partial t} \end{Bmatrix}$$

Substituting equation 2.18, 2.19 and 2.20 in equation 2.14, we get :

$$\chi = \int_V \tfrac{1}{2}\{T\}^T [A]^T [G] [A] \{T\}\, dV - \int_V r\left(Q - \rho c [N]\left\{\frac{\partial T}{\partial t}\right\}\right)[N] \{T\}\, dV + \int_{S1} qr[N] \{T\}\, dS + \int_{S2} \frac{rh}{2} \{T\}^T [N]^T [N] \{T\}\, dS - \int_{S2} rh T_\infty [N] \{T\}\, dS + \int_{S2} \frac{rh}{2} T_\infty^2\, dS \qquad (2.21)$$

The above functional, equation 2.21, is continuous only over the individual element and not over the region, since the shape function [N] is defined over the element.

Minimizing the functional with respect to {T}, wich will yield a stationary value that will satisfy the governing equation and the boundary conditions, we get :

$$\frac{\partial \chi}{\partial \{T\}} = 0$$

therefore

$$\int_V [A]^T [G] [A] \{T\}\, dV - \int_V Qr[N]^T dV + \int_V \rho c r[N]^T [N] \left\{\frac{\partial T}{\partial t}\right\} dV + \int_{S1} qr[N]^T dS + \int_{S2} hr[N]^T [N] \{T\}\, dS - \int_{S2} rhT_\infty [N]^T dS = 0 \qquad (2.22)$$

equation 2.22 can be written as:

$$\left[\int_V [A]^T [G] [A]\, dV + \int_{S2} hr[N]^T [N]\, dS\right] \{T\} + \left[\int_V \rho cr[N]^T [N]\, dV\right] \left\{\frac{\partial T}{\partial t}\right\}$$

$$= \int_V Qr[N]^T dV - \int_{S1} q\, r[N]^T dS + \int_{S2} hT_\infty r[N]^T dS \qquad (2.23)$$

or

$$[C] \left\{\frac{\partial T}{\partial t}\right\} + [K] \{T\} = \{F\} \qquad (2.24)$$

where

$$[C] = \int_V \rho c\, r[N]^T [N]\, dV$$

$$[K] = \int_V [A]^T [G] [A]\, dV + \int_{S2} hr[N]^T [N]\, dS$$

$$\{F\} = \int_V Qr[N]^T dV - \int_{S1} q\, r[N]^T dS + \int_{S2} hT_\infty r[N]^T dS$$

FORMULATION OF [K] MATRIX

$$[K] = \int_V [A]^T [G] [A]\, dV + \int_{S2} hr[N]^T [N]\, dS \qquad (2.25)$$

$$= [K_k] + [K_h]$$

where

$$[K_k] = \int_V [A]^T [G] [A]\, dV = [A]^T [G] [A] \int_V dV \qquad (2.26)$$

for an axisymmetric cylinder the approximate volume integral is:

$$\int_V dV = 2\pi \bar{r} \Delta \qquad (2.27)$$

where

$\bar{r} = \frac{r_i + r_j + r_k}{3}$ and Δ = Area of the triangular element.

therefore

$$[k_k] = \frac{2\pi(\bar{r})^2 K_r}{4\Delta} \begin{bmatrix} b_i b_i & b_i b_j & b_i b_k \\ b_j b_i & b_j b_j & b_j b_k \\ b_k b_i & b_k b_j & b_k b_k \end{bmatrix} + \frac{2\pi(\bar{r})^2 K_z}{4\Delta} \begin{bmatrix} c_i c_i & c_i c_j & c_i c_k \\ c_j c_i & c_j c_j & c_j c_k \\ c_k c_i & c_k c_j & c_k c_k \end{bmatrix} \quad (2.28)$$

where

$$b_i = z_j - z_k \quad , \quad c_i = r_k - r_j$$

$$b_j = z_k - z_i \quad , \quad c_j = r_i - r_k$$

$$b_k = z_i - z_j \quad , \quad c_k = r_j - r_i$$

Also

$$[K_h] = \int_{S2} h\, r [N]^T [N]\, dS = h \int_{S2} r [N]^T [N]\, dS \quad (2.29)$$

Matrix $[K_h]$ is due to surface convection. If none of the sides of the element is convecting heat, $[K_h]$ will be zero. For the sides with convection $[K_h]$ is dependent on the side. Using area coordinate system to find surface integral of equation 2.29, we get [22] :

For convection on side i-j :

$$[K_h]_{ij} = \bar{r}\frac{2\pi hL}{12}{}_{ij} \begin{bmatrix} 3r_i+r_j & r_i+r_j & 0 \\ r_i+r_j & 3r_j+r_i & 0 \\ 0 & 0 & 0 \end{bmatrix} \qquad (2.30)$$

similarly for convection on side j-k :

$$[K_h]_{jk} = \bar{r}\frac{2\pi hL}{12}{}_{jk} \begin{bmatrix} 0 & 0 & 0 \\ 0 & 3r_j+r_k & r_j+r_k \\ 0 & r_j+r_k & 3r_k+r_j \end{bmatrix} \qquad (2.31)$$

and for convection on side i-k :

$$[K_h]_{ik} = \bar{r}\frac{2\pi hL}{12}{}_{ik} \begin{bmatrix} 3r_i+r_k & 0 & r_i+r_k \\ 0 & 0 & 0 \\ r_i+r_k & 0 & 3r_k+r_i \end{bmatrix} \qquad (2.32)$$

where L_{ij} = length of the side i-j, etc.

FORMULATION OF [C] MATRIX

$$[C] = \int_V \rho c\, r [N]^T [N]\, dV = \rho c \int_V r [N]^T [N]\, dV \qquad (2.33)$$

using the volume coordinate system to integrate over the volume, we get [22] :

$$[C] = \frac{4\pi\rho cA\bar{r}}{120}\begin{bmatrix} 6r_i+2r_j+2r_k & 2r_i+2r_j+r_k & 2r_i+r_j+2r_k \\ 2r_i+2r_j+r_k & 2r_i+6r_j+2r_k & r_i+2r_j+2r_k \\ 2r_i+r_j+2r_k & r_i+2r_j+2r_k & 2r_i+2r_j+6r_k \end{bmatrix} \quad (2.34)$$

FORMULATION OF {F} VECTOR

$$\{F\} = \int_V Q r[N]^T dV - \int_{S1} q r[N]^T dS + \int_{S2} hT_\infty r[N]^T dS \quad (2.35)$$

$$= \{F\}_Q - \{F\}_q + \{F\}_h$$

where

$$\{F\}_Q = \frac{\bar{r}2\pi QA}{12}\begin{Bmatrix} 2r_i+r_j+r_k \\ r_i+2r_j+r_k \\ r_i+r_j+2r_k \end{Bmatrix} \quad (2.36)$$

$\{F\}_q$ is dependent on the side with heat flux.

So for side i-j :

$$\{F\}_{q_{ij}} = \frac{\bar{r}2\pi}{6} q_{ij} L_{ij} \begin{Bmatrix} 2r_i+r_j \\ r_i+2r_j \\ 0 \end{Bmatrix} \quad (2.37)$$

for side j-k :

$$\{F\}_{q_{jk}} = \frac{\bar{r}2\pi}{6} q_{jk} L_{jk} \begin{Bmatrix} 0 \\ 2r_j+r_k \\ r_j+2r_k \end{Bmatrix} \tag{2.38}$$

and for side i-k :

$$\{F\}_{q_{ik}} = \frac{\bar{r}2\pi}{6} q_{ik} L_{ik} \begin{Bmatrix} 2r_i+r_k \\ 0 \\ r_i+2r_k \end{Bmatrix} \tag{2.39}$$

Similarly $\{F\}_h$ is dependent on the sides with convection.

So for side i-j :

$$\{F\}_{h_{ij}} = \frac{\bar{r}2\pi h T_\infty L_{ij}}{6} \begin{Bmatrix} 2r_i+r_j \\ r_i+2r_j \\ 0 \end{Bmatrix} \tag{2.40}$$

for side j-k :

$$\{F\}_{h_{jk}} = \frac{\bar{r}2\pi h T_\infty L_{jk}}{6} \begin{Bmatrix} 0 \\ 2r_j+r_k \\ r_j+2r_k \end{Bmatrix} \tag{2.41}$$

for side i-k :

$$\{F\}_{h_{ik}} = \bar{r}\frac{2\pi h T_\infty L_{ik}}{6}\begin{Bmatrix} 2r_i + r_k \\ 0 \\ r_i + 2r_k \end{Bmatrix} \qquad (2.42)$$

Equation 2.24 can be solved by taking finite increment of time and finding values at mid-point.

$$\left\{\frac{\partial T}{\partial t}\right\} = \frac{\{T_1\} - \{T_0\}}{\Delta t} \qquad (2.43)$$

$$\{T\} = \frac{\{T_1\} + \{T_0\}}{2} \qquad (2.44)$$

Substituting equation 2.43 and 2.44 in equation 2.24, we get

$$\left(\frac{[C]}{\Delta t} + \frac{[K]}{2}\right)\{T_1\} = \left(\frac{[C]}{\Delta t} - \frac{[K]}{2}\right)\{T_0\} + \{F\} \qquad (2.45)$$

which can be written as

$$[C']\left\{T_1\right\} = [K']\left\{T_0\right\} + \{F\} \qquad (2.46)$$

where

$$[C'] = \left(\frac{[C]}{\Delta t} + \frac{[K]}{2}\right)$$

$$[K'] = \left(\frac{[C]}{\Delta t} - \frac{[K]}{2}\right)$$

$\{T_0\}$ = vectors containing nodal temperatures at the begining of the time increment.

$\{T_1\}$ = vector containing nodal temperatures at the end of the time increment.

Δt = time increment.

A time increment of 2 minutes is used for the analysis. Smaller time increment have been tried out but they did not show any significant improvement in the results, variation of temperature with different time increment is shown in Figure 11. Material properties shuch as thermal conductivity, heat capacitance convection coefficient etc., which are temperature dependent, are updated for each increment.

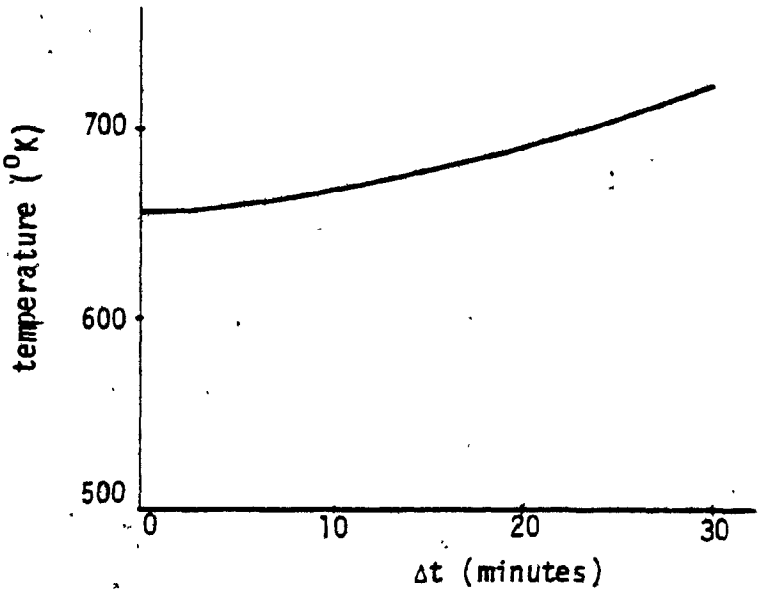

Figure 11. Plot of temperature (at point B of Figure 17) versus Δt for 40hp and 30 minutes of brake application.

2.3 STRESS ANALYSIS

Axisymmetric finite element formulation is obtained by minimization of potential energy "Π":

$$\Pi = \text{strain energy (U)} - \text{work done (W)}$$

$$= \left[\int_V \left(\tfrac{1}{2}\{\varepsilon\}^T [D] \{\varepsilon\} - \{\varepsilon\}^T [D] \{\varepsilon_o\} + \{\varepsilon\}^T \{\sigma_o\} \right) dV \right] - \left[\int_S \{F_s\} \{\delta\} \, dS + \{P\} \{\delta\} \right] \qquad (2.47)$$

where

$\{\varepsilon\}$ = vector containing strains.

$[D]$ = matrix relating stresses and strains.

$\{\varepsilon_o\}$ = thermal strains.

$\{\sigma_o\}$ = initial stresses.

$\{F_s\}$ = surface forces.

$\{\delta\}$ = nodal displacements.

$\{P\}$ = external nodal forces.

The total potential energy for an element is approximated by assuming the displacements within the element to have the form as shown in equation 2.3.

For an axisymmetric body, the strain expressions are:

$$\{\varepsilon\} = \begin{Bmatrix} \varepsilon_z \\ \varepsilon_r \\ \varepsilon_\theta \\ \gamma_{rz} \end{Bmatrix} = \begin{Bmatrix} \frac{\partial v}{\partial z} \\ \frac{\partial u}{\partial r} \\ \frac{u}{r} \\ \frac{\partial u}{\partial z} + \frac{\partial v}{\partial r} \end{Bmatrix} \tag{2.48}$$

using the interpolation functions, equation 2.3 , we get:

$$\{\varepsilon\} = [B]\{\delta\} \tag{2.49}$$

where

$$[B] = \frac{1}{2\Delta} \begin{bmatrix} 0 & c_i & 0 & c_j & 0 & c_k \\ b_i & 0 & b_j & 0 & b_k & 0 \\ \frac{a_i+b_i+c_i z}{r} & 0 & \frac{a_i+b_j+c_j z}{r} & 0 & \frac{a_k+b_k+c_k z}{r} & 0 \\ c_i & b_i & c_j & b_j & c_k & b_k \end{bmatrix}$$

$$\{\delta\} = \begin{Bmatrix} u_i \\ v_i \\ u_j \\ v_j \\ u_k \\ v_k \end{Bmatrix}$$

$$a_i = r_j z_k - r_k z_j$$

$$a_j = r_k z_i - r_i z_k$$

$$a_k = r_i z_j - r_j z_i$$

b_i , c_i etc. are given on page 31.

Stress strain relationship for an axisymmetric body is given by:

$$\{\sigma\} = [D]\left(\{\varepsilon\} - \{\varepsilon_o\}\right) \tag{2.50}$$

where

$$\{\varepsilon_o\} = \begin{Bmatrix} \varepsilon_{z_o} \\ \varepsilon_{r_o} \\ \varepsilon_{\theta o} \\ \gamma_{rz_o} \end{Bmatrix} = \begin{Bmatrix} \alpha\Delta T \\ \alpha\Delta T \\ \alpha\Delta T \\ 0 \end{Bmatrix}$$

$$[D] = \frac{E}{(1+\nu)(1-2\nu)} \begin{bmatrix} 1-\nu & \nu & \nu & 0 \\ \nu & 1-\nu & \nu & 0 \\ \nu & \nu & 1-\nu & 0 \\ 0 & 0 & 0 & \frac{1-2\nu}{2} \end{bmatrix}$$

The minimization process gives us:

$$\left(\int_V [B]^T [D] [B] \, dV\right) \{\delta\} = \int_S [N]^T \{F_s\} \, dS + \int_V [B]^T [D] \{\varepsilon_o\} \, dV - \int_V [B]^T \{\sigma_o\} \, dV + \{P\} \tag{2.51}$$

Equation 2.51 for an element can be written as:

$$[K]_e \{\delta\}_e = \{F\}_e \tag{2.52}$$

where

$$\{F\}_e = \int_S [N]^T \{F_s\} \, dS + \int_V [B]^T [D] \{\varepsilon_o\} \, dV - \int_V [B]^T \{\sigma_o\} \, dV + \{P\}$$

$$[K]_e = \int_V [B]^T [D] [B] \, dV$$

Once the element stiffness matrix and force vector have been formulated, they are assembled in a global stiffness matrix [K] and global force vector {F}. Since:

$$[K] \{\delta\} = \{F\} \tag{2.53}$$

the nodal displacements can be obtained by:

$$\{\delta\} = [K]^{-1} \{F\} \tag{2.54}$$

individual nodal displacements are then extracted from the global displacement vector and are used to find element strains and stresses, using equations 2.5 and 2.6 respectively. The procedure for computer implementation is given in the flowchart in section 2.6.

PLASTIC ANALYSIS

In plastic region the strains in general are not uniquely determined by the stresses but depend on the entire histony of incremental loading. The total elasto-plastic strain increment, $d\varepsilon_{ij}$, is the sum of elastic strain, $d\varepsilon^e_{ij}$, and plastic strain, $d\varepsilon^p_{ij}$, i.e. in tensor form:

$$d\varepsilon_{ij} = d\varepsilon^{e}_{ij} + d\varepsilon^{p}_{ij} \tag{2.55}$$

where the elastic strain increment is equal to:

$$d\varepsilon^{e}_{ij} = \frac{1+\nu}{E} d\sigma_{ij} - \frac{\nu}{E} d\sigma_{kk}\,\delta_{ij} = [D]^{-1} d\sigma_{ij} \tag{2.56}$$

$\sigma_{kk} = (\sigma_z + \sigma_r + \sigma_\theta)$

[D] is defined in equation 2.50. δ_{ij} = Kronecker delta $= \begin{cases} 1 & i = j \\ 0 & i \neq j \end{cases}$

The plastic strain increment is based on the generally accepted hypothesis, that:

$$d\varepsilon^{p}_{ij} = \lambda \frac{\partial Y}{\partial \sigma_{ij}} \tag{2.57}$$

where λ is a proportionality constant and Y is the yield criteria. Yielding can occur only if the stress $\{\sigma\}$ satisfy the general yield criteria:

$$Y(\{\sigma\},k) = 0 \tag{2.58}$$

where k is a work-hardening parameter. Distortion energy theory (Von Mises) is used as the yield criteria, which says that yielding will occur when equivalent stress, $\hat{\sigma}$, is greater than uniaxial yield stress, $\bar{\sigma}$. That is: [4]

$$Y = \hat{\sigma} - \bar{\sigma} \tag{2.59}$$

where

$$\hat{\sigma} = \left[\tfrac{1}{2}(\sigma_r - \sigma_z)^2 + \tfrac{1}{2}(\sigma_z - \sigma_\theta)^2 + \tfrac{1}{2}(\sigma_\theta - \sigma_r)^2 + 3\tau^2_{r\theta} + 3\tau^2_{\theta z} + 3\tau^2_{rz}\right]^{\frac{1}{2}}$$

$\bar{\sigma}$ = uniaxial yield stress.

$\sigma_r, \sigma_z, \sigma_\theta$ = normal stresses in r, z and θ directions respectively.

$\tau_{rz}, \tau_{r\theta}, \tau_{\theta z}$ = shear stresses

for an axisymmetric solid, $\tau_{r\theta} = \tau_{\theta z} = 0$. [23]

If for an element, from equation 2.59

$Y > 0$ ..... stresses in the element has exceeded yield point.

$Y < 0$ ..... stresses in the element are below yield point.

The plastic stress-strain relationship is based on Levy-Mises criteria, that is:

$$d\varepsilon^p_{ij} = \frac{3}{2}\frac{d\hat{\varepsilon}}{\hat{\sigma}}\sigma'_{ij} \qquad (2.60)$$

where

$$\sigma'_{ij} = \sigma_{ij} - \frac{(\sigma_z + \sigma_r + \sigma_\theta)}{3}\delta_{ij}$$

$$\hat{\varepsilon} = \frac{\sqrt{2}}{3}\left[(\varepsilon_z - \varepsilon_r)^2 + (\varepsilon_r - \varepsilon_\theta)^2 + (\varepsilon_\theta - \varepsilon_z)^2 + 6\gamma^2_{zr} + 6\gamma^2_{r\theta} + 6\gamma^2_{\theta z}\right]^{\frac{1}{2}}$$

The term $\hat{\sigma}/d\hat{\varepsilon}$ is the variable plastic modulus, H'. If a plot of plastic stress strain curve is given, $\hat{\sigma}/d\hat{\varepsilon}$ represents the slope of that curve at a particular $\hat{\sigma}$.

Substitution of equation 2.56 and 2.60 in equation 2.55 will yield the total elasto-plastic stress-strain relationship, also known as Prandtl-Reuss equation:

$$d\varepsilon_{ij} = \frac{1+\nu}{E}d\sigma_{ij} - \frac{\nu}{E}d\sigma_{kk}\delta_{ij} + \frac{3}{2}\frac{d\hat{\varepsilon}}{\hat{\sigma}}\sigma'_{ij}$$

$$= [D]^{-1}d\sigma_{ij} + \lambda\frac{\partial Y}{\partial\sigma_{ij}} \qquad (2.61)$$

When plastic yield is occuring the stresses are on the yield surface, given by equation 2.58. Differentiating this we get:

$$\frac{\partial Y}{\partial \sigma_z} d\sigma_z + \frac{\partial Y}{\partial \sigma_r} d\sigma_r + \frac{\partial Y}{\partial \sigma_\theta} d\sigma_\theta + \frac{\partial Y}{\partial \tau_{rz}} d\tau_{rz} + \frac{\partial Y}{\partial k} dk = 0$$

$$\text{or} \quad \left\{\frac{\partial Y}{\partial \{\sigma\}}\right\}^T d\{\sigma\} + A\lambda \qquad (2.62)$$

$$\text{where} \quad A = \frac{\partial Y}{\partial k} dk \cdot \frac{1}{\lambda}$$

Equation 2.61 and 2.62 can be written in a single matrix form as:

$$\begin{Bmatrix} d\varepsilon_z \\ d\varepsilon_r \\ d\varepsilon_\theta \\ d\gamma_{rz} \\ 0 \end{Bmatrix} = \begin{bmatrix} & & & \frac{\partial Y}{\partial \sigma_z} \\ & [D]^{-1} & & \frac{\partial Y}{\partial \sigma_r} \\ & & & \frac{\partial Y}{\partial \sigma_\theta} \\ & & & \frac{\partial Y}{\partial \tau_{rz}} \\ \frac{\partial Y}{\partial \sigma_z} & \frac{\partial Y}{\partial \sigma_r} & \frac{\partial Y}{\partial \sigma_\theta} \quad \frac{\partial Y}{\partial \tau_{rz}} & A \end{bmatrix} \begin{Bmatrix} d\sigma_z \\ d\sigma_r \\ d\sigma_\theta \\ d\tau_{rz} \\ \lambda \end{Bmatrix} \qquad (2.63)$$

Zienkiewicz [33] has shown that λ can be eleminated, and equation 2.63 can be written as $\{\sigma\} = [D]_{ep} \{\varepsilon\}$

$$[D]_{ep} = [D] - [D] \left\{\frac{\partial Y}{\partial \{\sigma\}}\right\} \left\{\frac{\partial Y}{\partial \{\sigma\}}\right\}^T [D] \left[A + \left\{\frac{\partial Y}{\partial \{\sigma\}}\right\}^T [D] \left\{\frac{\partial Y}{\partial \{\sigma\}}\right\} \right]^{-1} \qquad (2.64)$$

and, also, for Prandtl-Reuss equation:

$$A = H' \qquad (2.65)$$

where

$$\frac{\partial Y}{\partial \{\sigma\}} = \begin{Bmatrix} \frac{\partial Y}{\partial \sigma_z} \\ \frac{\partial Y}{\partial \sigma_r} \\ \frac{\partial Y}{\partial \sigma_\theta} \\ \frac{\partial Y}{\partial \tau_{rz}} \end{Bmatrix} = \frac{3}{\theta} \begin{Bmatrix} \frac{\sigma'_z}{2} \\ \frac{\sigma'_r}{2} \\ \frac{\sigma'_\theta}{2} \\ \tau_{rz} \end{Bmatrix}$$

where primes ($'$) are deviatoric stresses, e.g.

$$\sigma'_{ij} = \sigma_{ij} - \left(\frac{\sigma_z + \sigma_r + \sigma_\theta}{3}\right) \delta_{ij}$$

The non-linearity of material in plastic region is evident from equation 2.64, where the elasto-plastic stiffness matrix is dependent on the state of total stress. The solution requires incremental elasticity approach. The method is based on Zienkiewicz's "initial stress" process.

First a purely elastic load increment is applied, and elastic problem is solved determining an increment of strain $\{\Delta\varepsilon'\}$ and stress $\{\Delta\sigma'\}$ at every point of the structure. The non-linearity implies that the strain $\{\Delta\varepsilon'\}$ and stress $\{\Delta\sigma'\}$ found are not correct. If the true stress possible for a

given strain is $\Delta\{\sigma\}$ then the situation can only be maintained by a set of "body forces" equilibrating the "initial stress" $(\Delta\{\sigma\}' - \Delta\{\sigma\})$.

"At the second stage of computation this body force can be removed by allowing the structure (with unchanged elastic properties) to deform further. An additional set of strain and corresponding stress increment is caused. Once again these are likely to exceed those permissible by the non-linear relationship and the redistribution of equilibrating body forces has to be repeated"[33]. This process is stopped when the body forces become sufficiently small.

The solution steps during a typical load increment can be summerized as follows: [33]

1. Apply load increment and determine elastic increments of strain $\{\Delta\varepsilon'\}$ and stress $\{\Delta\sigma'\}$.
2. Add $\{\Delta\sigma'\}$ to stresses $\{\sigma_o\}$ existing at the start of the increment, to obtain $\{\sigma'\}$. Check weather $Y\{\sigma'\} < 0$. If, $Y\{\sigma'\} < 0$, then the stresses are within elastic region, and the process is stopped, if not proceed to 3.
3. If $Y\{\sigma'\} \geq 0$ and $Y\{\sigma_o\} = 0$ (i.e. Element was in yield at the start of increment) find $\{\Delta\sigma\}_1$ by equation 2.64.

$$\{\Delta\sigma\}_1 = [D]_{ep} \{\Delta\varepsilon'\}_1$$

with $[D]_{ep}$ computed from equation 2.64 with

stresses $\{\sigma'\}$.

Evaluate stresses which has to be supported by body forces:

$$\{\Delta\sigma''\}_1 = \{\Delta\sigma'\}_1 - \{\Delta\sigma\}_1$$

store current stresses $\{\sigma\} = \{\sigma'\} - \{\Delta\sigma''\}_1$

4. If $Y\{\sigma'\} > 0$ but $Y\{\sigma_o\} < 0$, find the intermidiate stress value at which yield begins and compute increment $\{\Delta\sigma\}_1$ by equation 2.64 starting from that point. Then proceed as in 3.

5. Compute nodal forces corresponding to the equilibrating body forces. These are given for any element by:

$$\{P\}_1 = \int_V [B]^T \{\Delta\sigma''\}_1 \, dV$$

6. Resolve using original elastic properties and the load system $\{P\}$ to find $\{\Delta\sigma'\}_2$ and $\{\Delta\varepsilon'\}_2$.

7. Find current value of H'.

8. Repeat step 2 to 6, etc.

The cycling is terminated when the nodal forces of step 5 reach sufficiently small values. The process is illustrated graphically in a two dimentional stress space in Figure 12. Note that after a few cycle the resulting stress is always brought back to the yield surface.

In this thesis, the stress strain curve is assumed to be bilinear (Figure 15, page 52), in that the value of H' is constant for the whole plastic region.

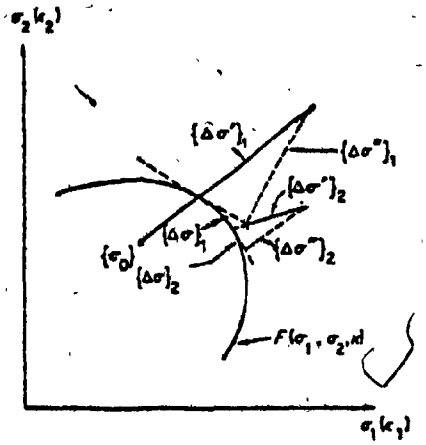

Figure 12. Graphical interpretation of the 'initial stress' process. [33]

2.4 FINITE ELEMENT MESH AND COMPUTER IMPLEMENTATION

The wheel is divided into more than 430 elements, as shown in Figure 13 (page 49). A finer mesh is used around the areas of stress concentrations, such as fillet regions etc. Further refinement of the mesh is not possible due to the limitations in the computer memory allowed. The same mesh is used for both temperature and stress calculations. Nodal temperatures obtained from the program TEMPCAL, given in appendix A, are stored on tape and later used in the program PLASTIC, given in appendix B, to calculate stresses.

For temperature calculation each node has one degree-of-freedom, one temperature, and for stress calculations it has two degrees-of-freedom, one displacement 'u' in r direction and the other 'v' in z direction. The total degrees-of-freedom for stress calculation is more than 500, that is, more than 500 simultaneous equations, which are in matrix form:

$$[K]\{\delta\} = \{F\} \qquad (2.19)$$

A great part of the matrix [K] contain zeros. So to minimize the storage of zeros the [K] matrix is stored in band storage mode. The element stiffness matrix is accumulated directly in global stiffness matrix in band storage, minimizing the use of computer memory and time. Numbers are assigned to the nodes with care so as to minimize

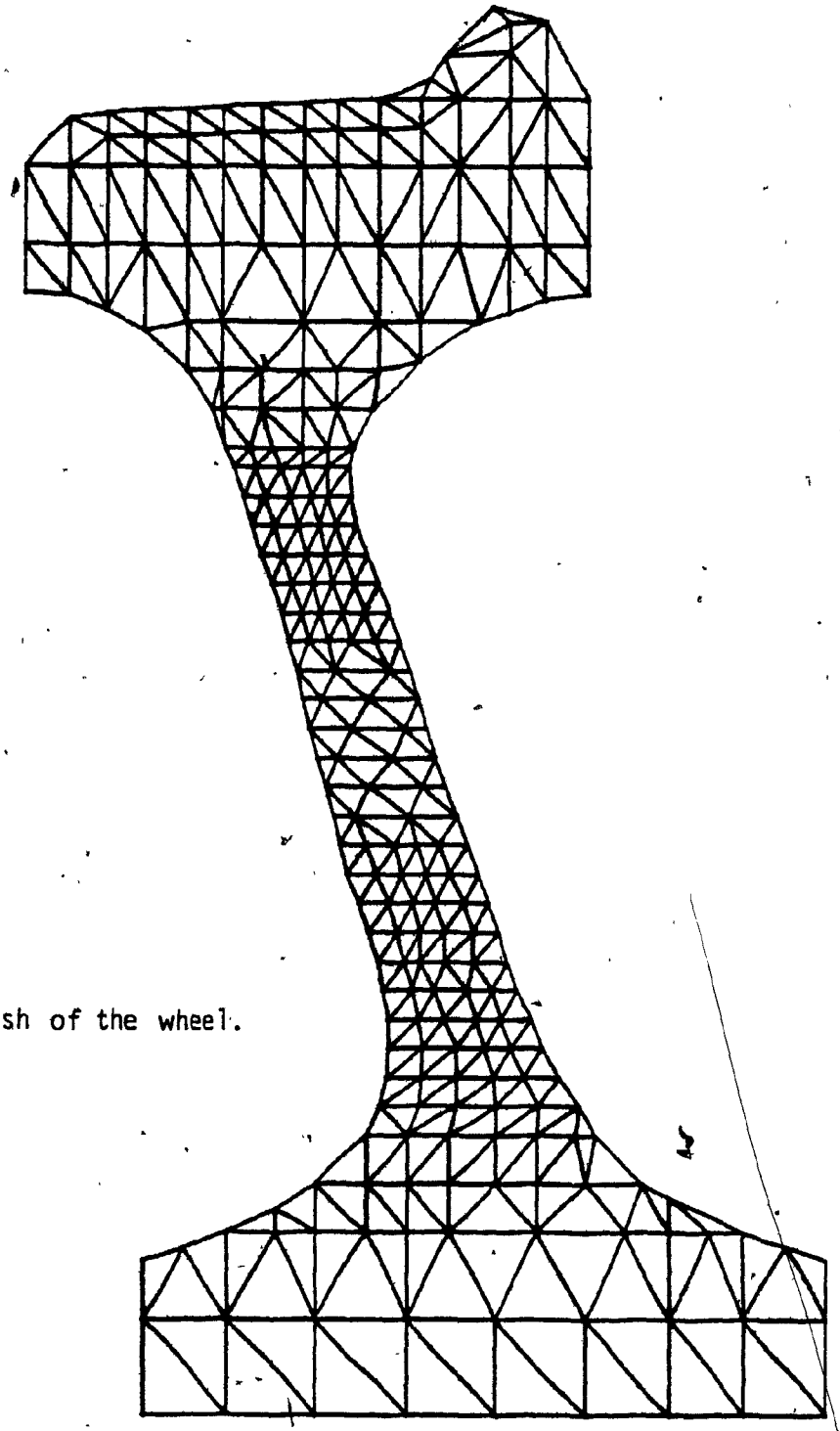

Figure 13.
Finite element mesh of the wheel.

the band width of the [K] matrix. IMSL routines from computer library are used for the solution of these simultaneous equations. The value of convection coefficient (h) is taken to be 19.87 W/m K. [20]

2.5 MATERIAL PROPERTIES

Class U steel wheel is used for analysis, with the following properties:

Thermal conductivity (k)[9] = 30-5.5(TR/1000) Btu/hrft ^{0}R

= 29-0.0095(TK) W/m ^{0}C

Where TR and TK are temperatures in degree Rankin and degree Kelvin, respectively.

Heat capacity (c) [9] = 0.07+0.06(TR/1000) BTU/lb ^{0}R

= 160+0.25(TK) J/Kg ^{0}C

Wheel density (ρ) [20] = 7833 Kg/m^{3}

Poisson's ratio (ν) = 0.3

Ambient temperature (T_∞) = 297 ^{0}K

Modulus of elasticity (E) and plasticity (H') and coefficient of thermal expansion (α) are obtained as a

function of temperature, as shown in Figure 14, 15 and 16 (page 52) respectively. They are incorporated in computer program by Lagrange polynomials of interpolation. A series of n points, x_i , were chosen, for which the value of funtion, $f(x_i)$, were obtained from the graphs. The Lagrange polynomial is obtained by:

$$f(x) = \sum_{j=1}^{n} f(x_j)\, P_j(x)$$

where

$$P_j(x) = \frac{\prod_{\substack{i=1 \\ i \neq j}}^{n} (x - x_i)}{\prod_{\substack{i=1 \\ i \neq j}}^{n} (x_j - x_i)}$$

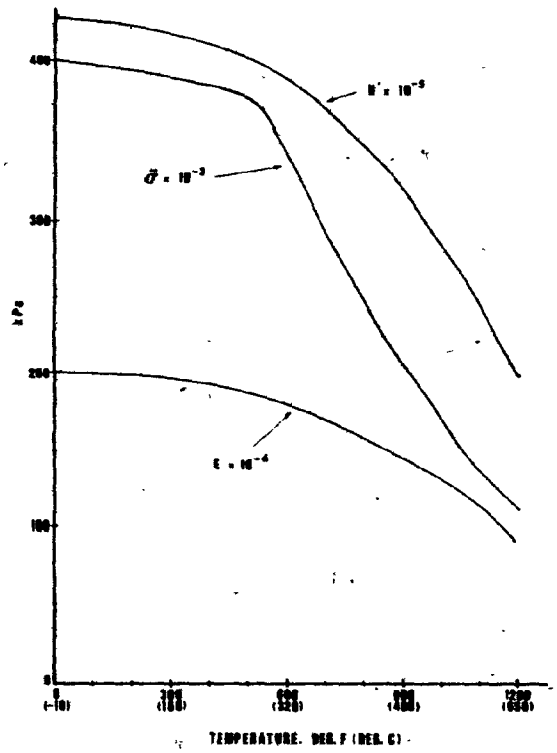

Figure 14. Assumed variation of E, H′ and $\bar{\sigma}$ with temperature. [9]

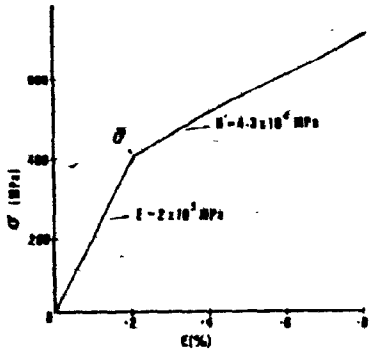

Figure 15. Bilinear representation of stress-strain curve for class U wheel steel. [9]

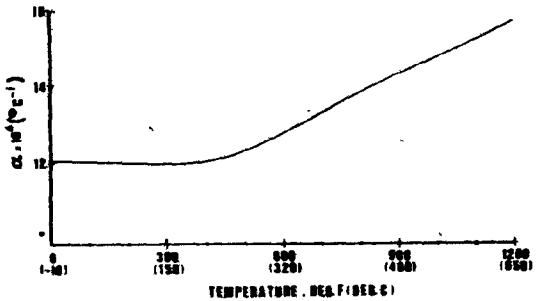

Figure 16. Assumed Variation of coefficient of thermal expansion, α, with temperature. [9]

2.6 FLOW CHART OF COMPUTER PROGRAM FOR STRESS ANALYSIS

Flow chart for finite element, axisymmetric, elasto-plastic stress analysis: (the temperature distribution is obtained from finite element program for temperature, using the same mesh)

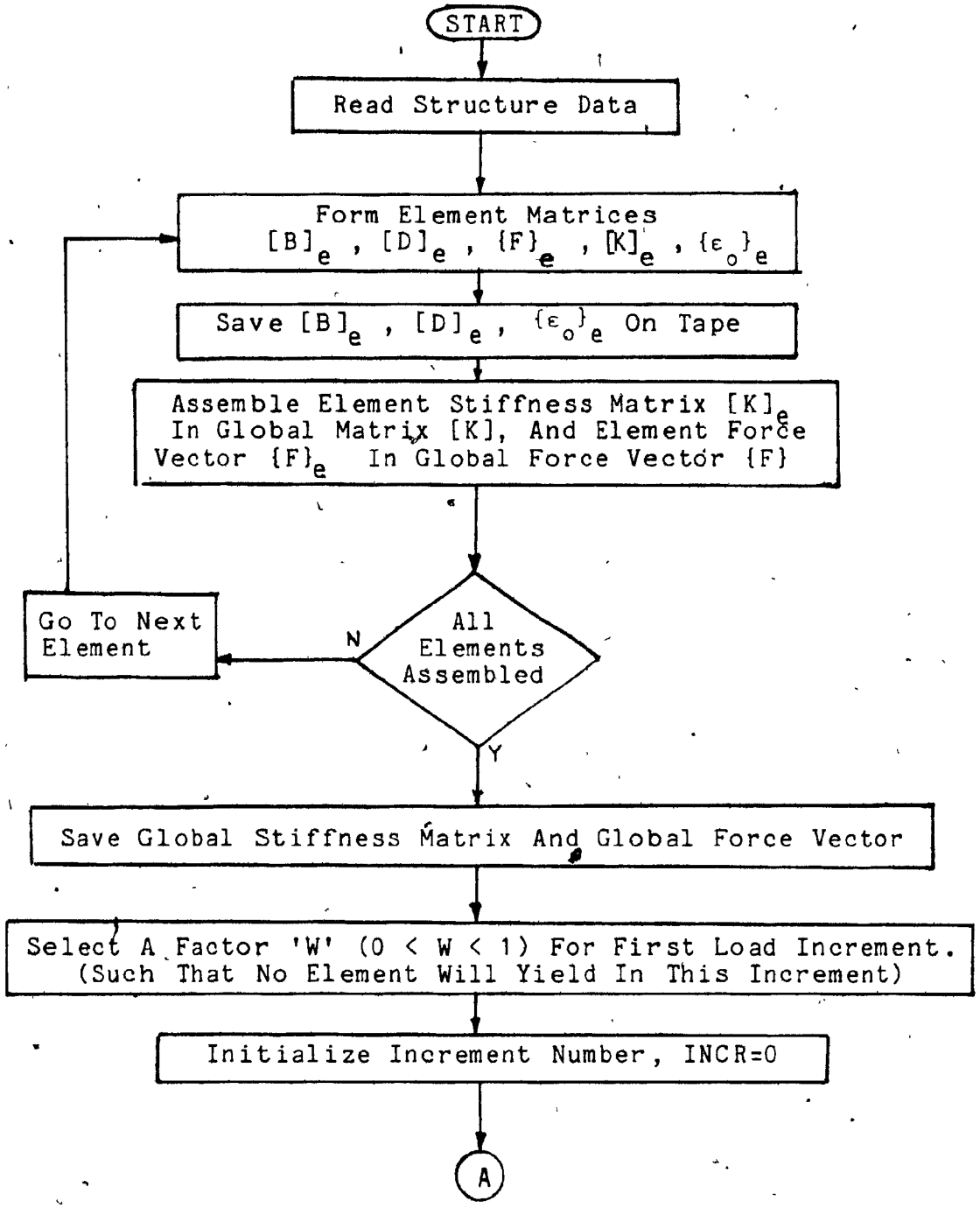

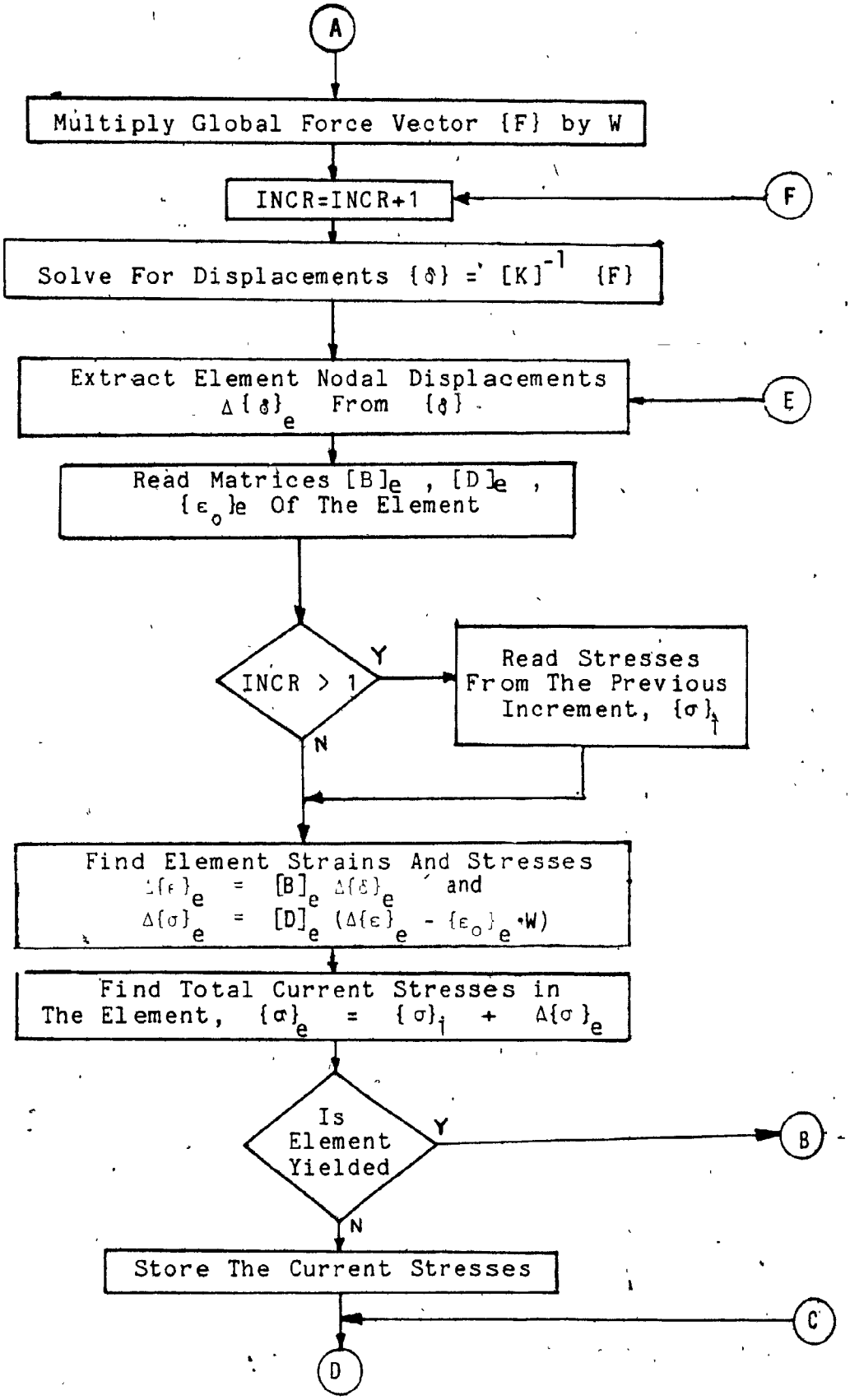
A
Multiply Global Force Vector {F} by W
INCR=INCR+1
F
Solve For Displacements {δ} = [K]^-1 {F}
Extract Element Nodal Displacements Δ{δ}e From {δ}
E
Read Matrices [B]e , [D]e , {εo}e Of The Element
INCR > 1
Y
N
Read Stresses From The Previous Increment, {σ}i
Find Element Strains And Stresses Δ{ε}e = [B]e Δ{δ}e and Δ{σ}e = [D]e (Δ{ε}e - {εo}e •W)
Find Total Current Stresses in The Element, {σ}e = {σ}i + Δ{σ}e
Is Element Yielded
Y
B
N
Store The Current Stresses
C
D

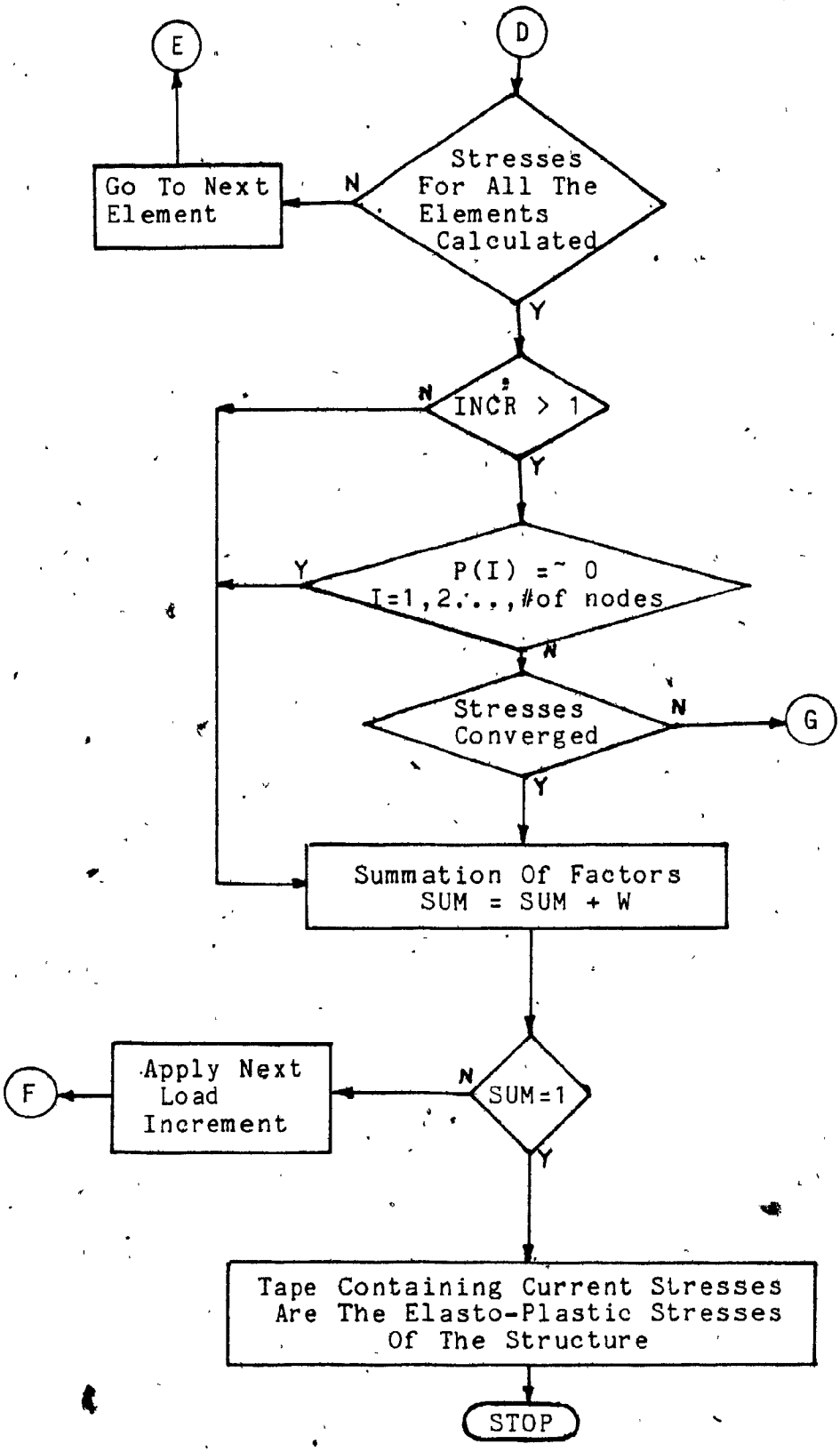
D
E
Stresses For All The Elements Calculated
N
Go To Next Element
Y
INCR > 1
N
Y
P(I) =~ 0 I=1,2...,#of nodes
Y
N
Stresses Converged
N
G
Y
Summation Of Factors SUM = SUM + W
SUM=1
N
Apply Next Load Increment
F
Y
Tape Containing Current Stresses Are The Elasto-Plastic Stresses Of The Structure
STOP

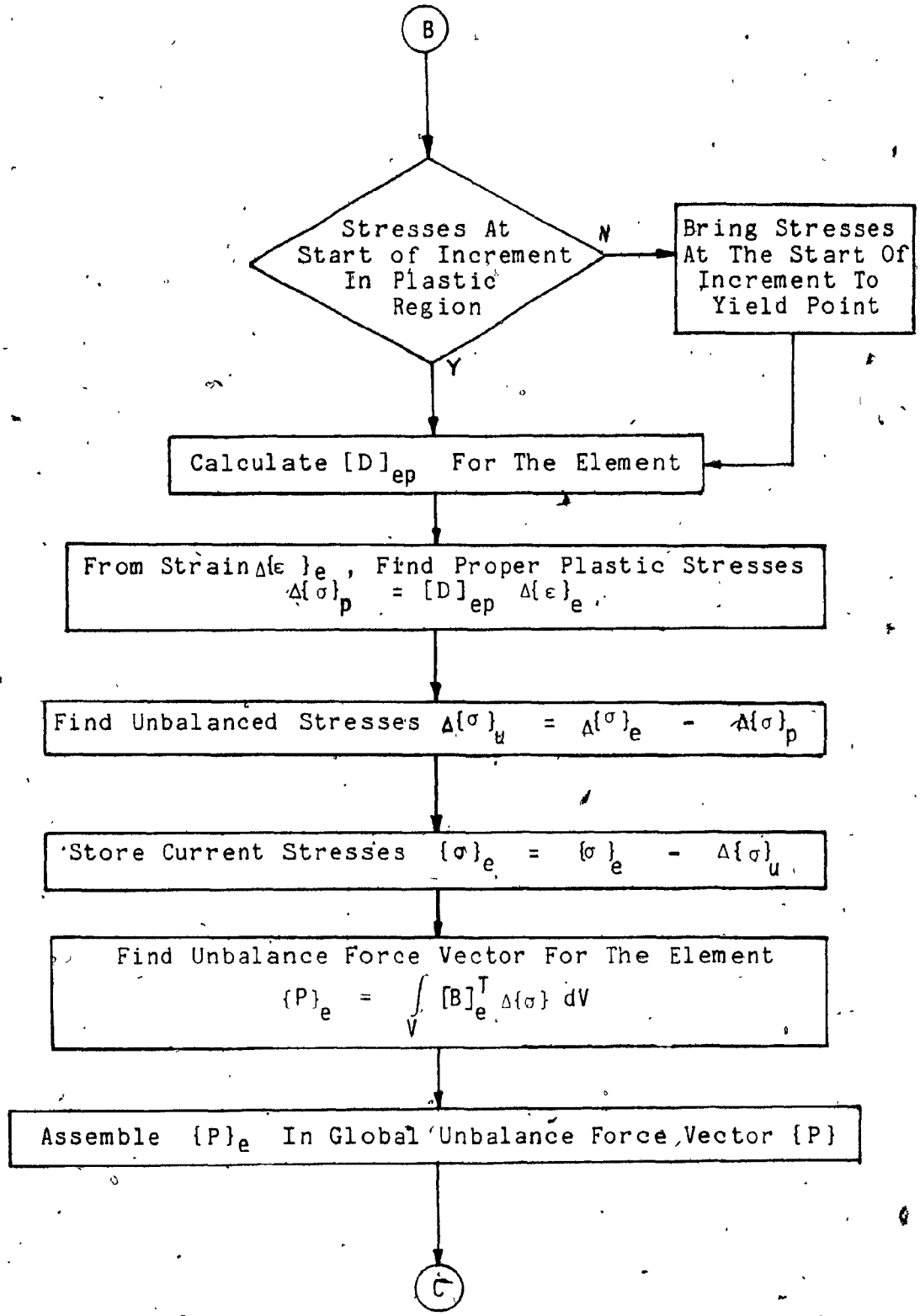
B
Stresses At Start of Increment In Plastic Region
N
Bring Stresses At The Start Of Increment To Yield Point
Y
Calculate $[D]_{ep}$ For The Element
From Strain $\Delta\{\epsilon\}_e$, Find Proper Plastic Stresses $\Delta\{\sigma\}_p = [D]_{ep}\ \Delta\{\epsilon\}_e$
Find Unbalanced Stresses $\Delta\{\sigma\}_u = \Delta\{\sigma\}_e - \Delta\{\sigma\}_p$
Store Current Stresses $\{\sigma\}_e = \{\sigma\}_e - \Delta\{\sigma\}_u$
Find Unbalance Force Vector For The Element
$\{P\}_e = \int_V [B]_e^T \Delta\{\sigma\}\, dV$
Assemble $\{P\}_e$ In Global Unbalance Force Vector $\{P\}$
C

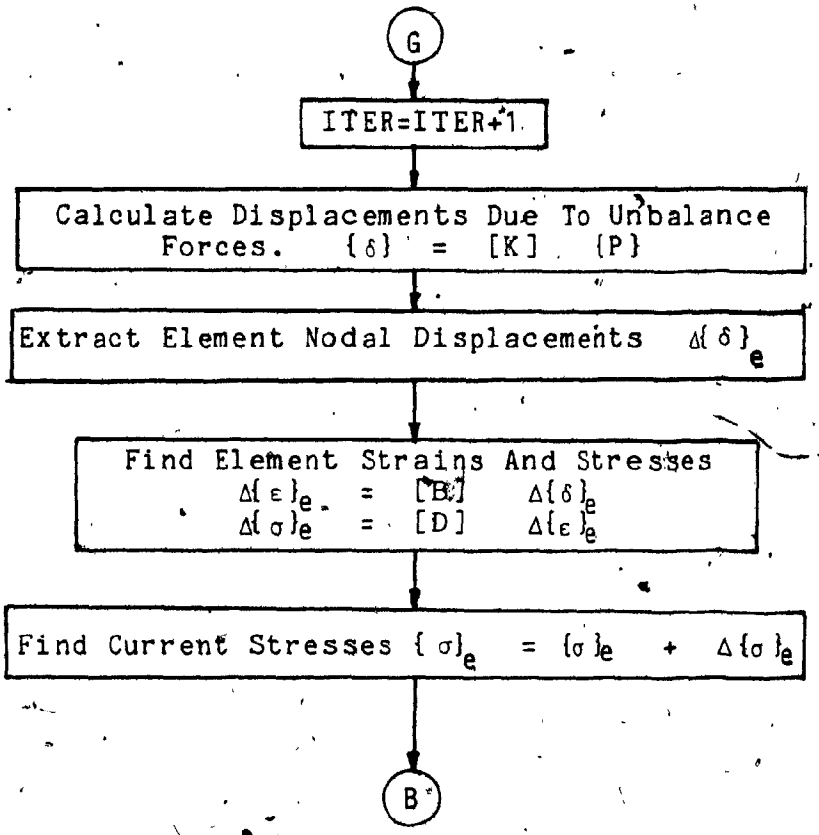
G
ITER=ITER+1
Calculate Displacements Due To Unbalance Forces. {δ} = [K] {P}
Extract Element Nodal Displacements Δ{δ}e
Find Element Strains And Stresses
Δ{ε}e = [B] Δ{δ}e
Δ{σ}e = [D] Δ{ε}e
Find Current Stresses {σ}e = {σ}e + Δ{σ}e
B

3 RESULTS AND DISCUSSIONS

3.1 TEMPERATURE AND DISPLACEMENTS

A standard J36 wheel is used in the analysis. Temperature distribution due to drag brake application of 20hp, 30hp and 40hp for 60 minutes are obtained, which are shown in Figure 17. Similar brake powers have been used by previous investigators [9], which represent the extreme cases of drag braking. Higher brake horsepower has resulted in higher rim temperatures. A temperature gradient of 80 degrees (ie. Difference between the maximum and the minimum temperature) is observed in the rim region for brake application of 20hp for 60 minutes, while almost double the temperature gradient, 160 degrees, is observed in the same region for 40hp for 60 minutes.

Across the rim along section A-A in Figure 17, the temperature at point B is higher than that at point C, resulting in reduction of tread taper angle, as shown in Figure 18. Similar trend is observed across the plate along section D-D and E-E, in Figure 17. High temperature gradient is observed along the plate. High temperature near the rim and low temperature near the hub region, causing reduction in

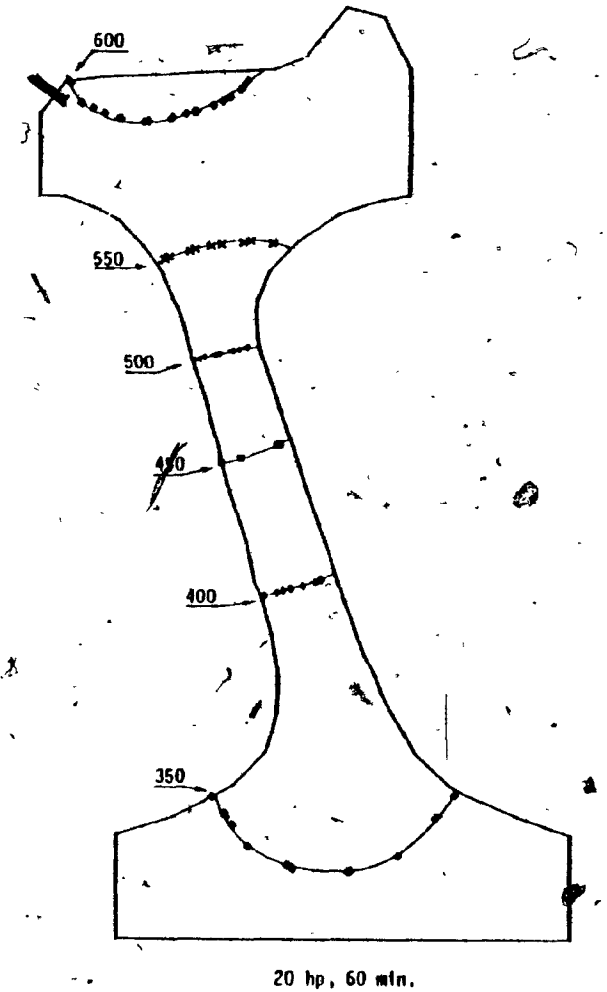

20 hp, 60 min.

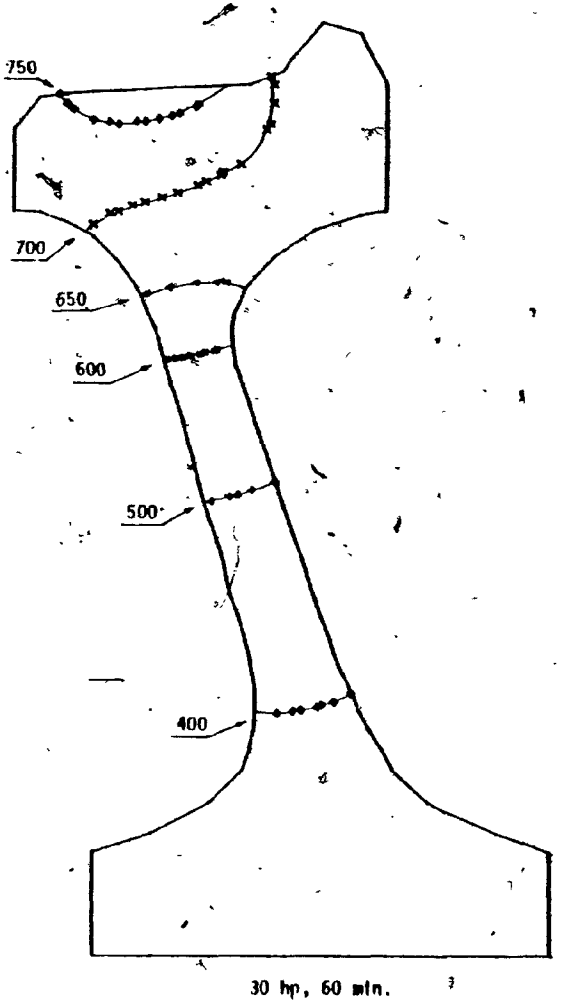

30 hp, 60 min.

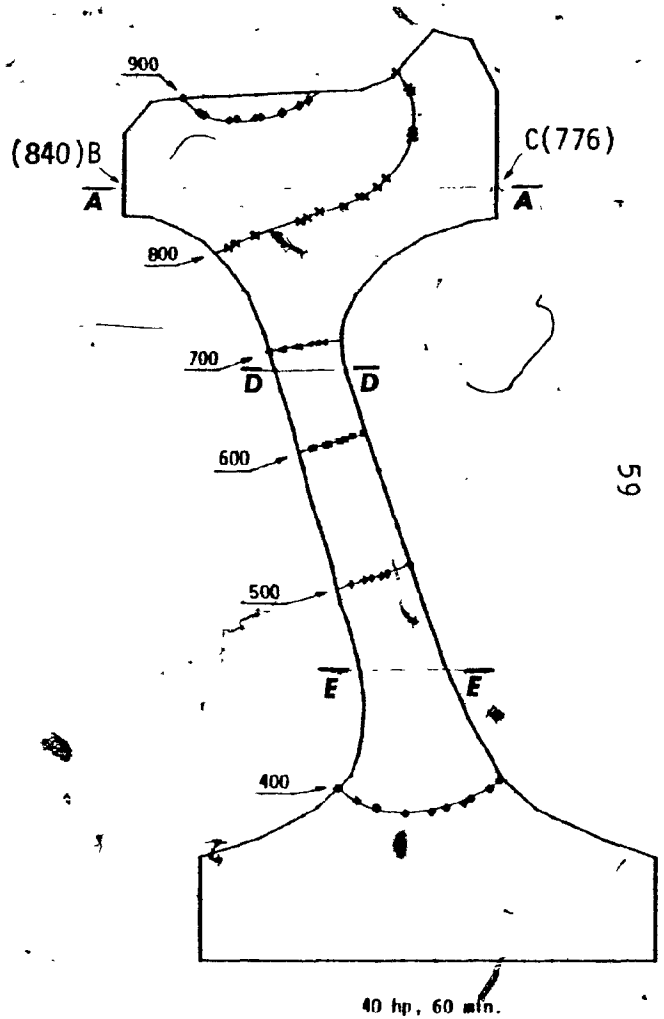

40 hp, 60 min.

Figure 17. Temperature distribution in wheel after 20hp, 30hp and 40hp brake application for 60 minutes. All values in degree Kelvin.

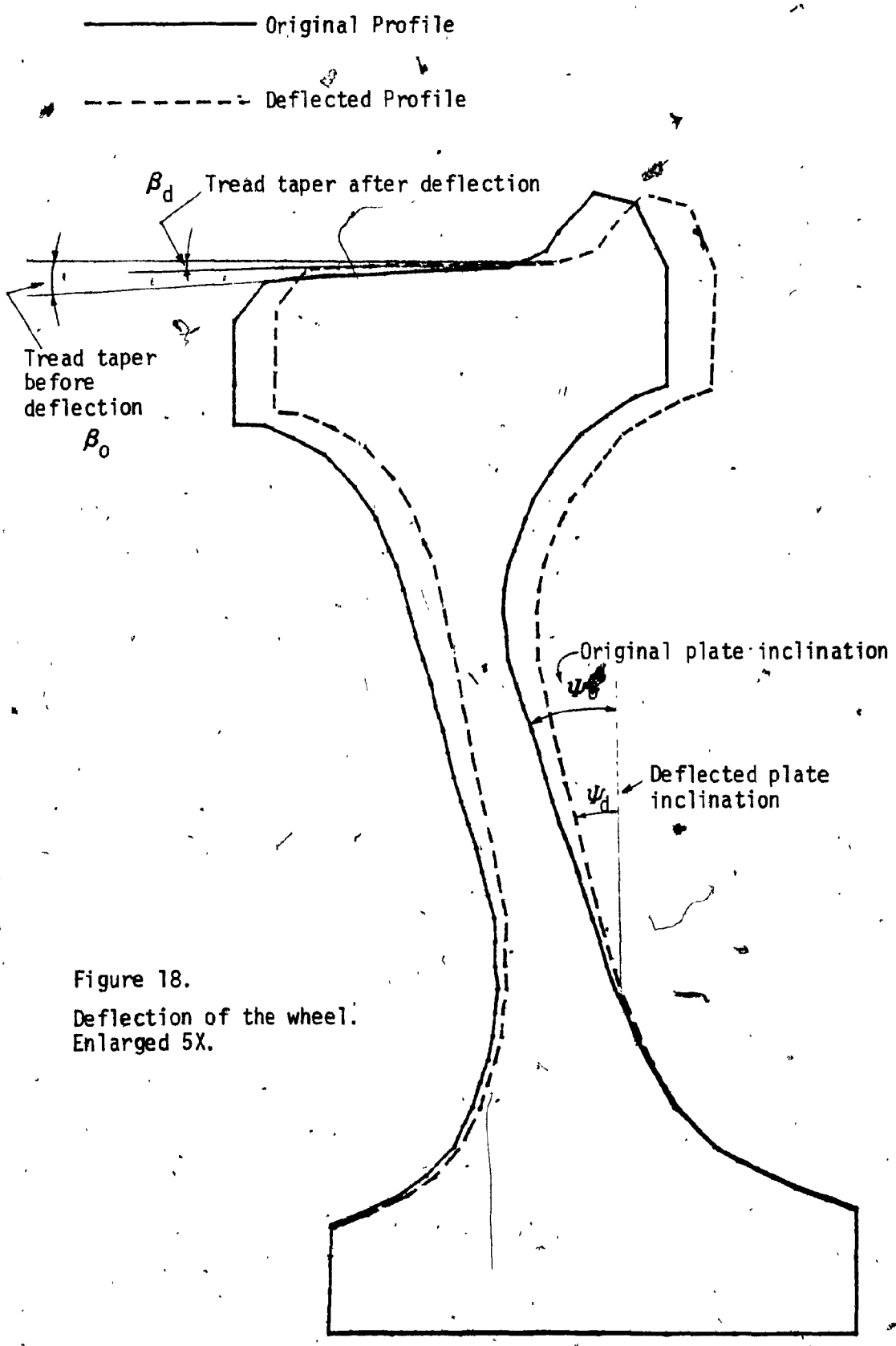

Figure 18.

Deflection of the wheel. Enlarged 5X.

plate inclination, as is evident by the change in angle Ψ in Figure 18.

3.2 STRESS DISTRIBUTION

The displacement of wheel profile results in compressive radial and tangential stresses in the inside-rim-fillet and tensile radial and tangential stresses in the outside-hub-fillet regions, which is illustrated from the elastic stress distribution in a wheel after brake application of 20hp for 30 minutes, as shown in Figure 19. High Von Mises stresses are observed in inside-rim-fillet and outside-hub-fillet regions, causing initiation of yielding in those regions, which is evident from the extent of yielded region for 20hp brake application for 60 minutes, shown in Figure 20, where only outside-hub-fillet and inside-rim-fillet regions are yielded. The triangle represent the yielded regions. Application of higher horsepower brakes cause increase in the yielded region. Since the temperature in the rim section is very high, and wheel material properties are greatly affected by high temperatures, a considerable part of the rim section is found to be yielded due to brake application of 30hp and 40hp for 60 minutes, which is shown in Figure 20.

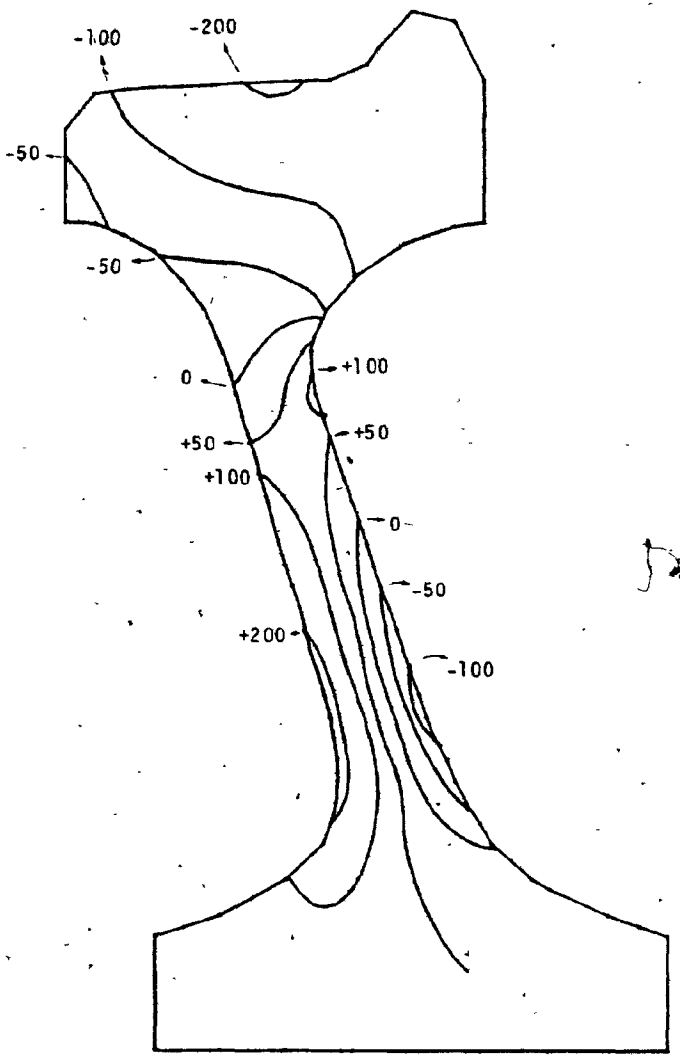

Tangential Stresses
20hp, 30 min.

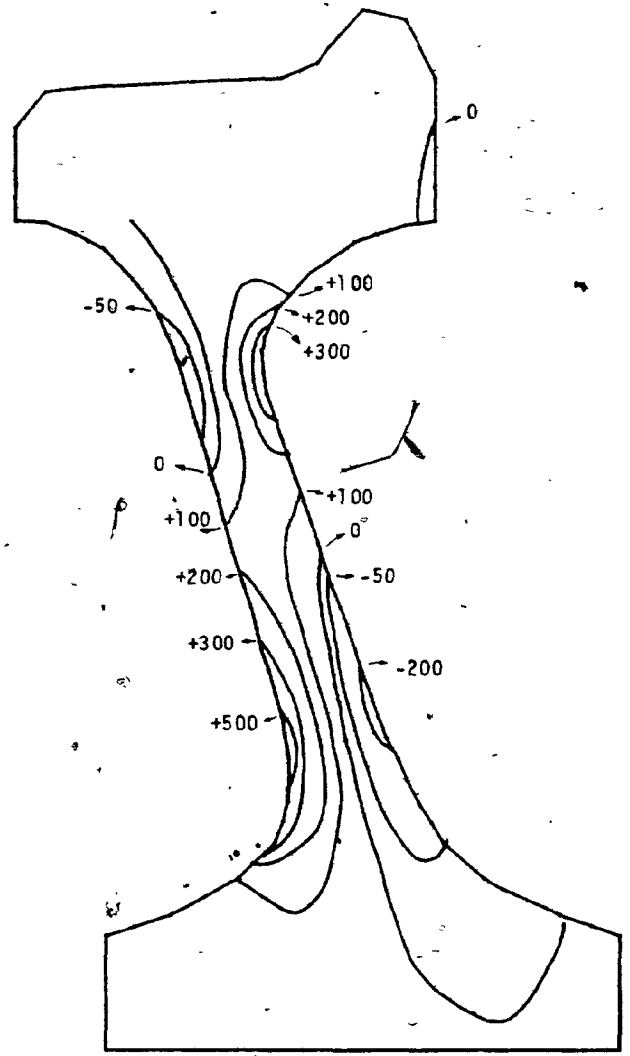

Radial Stresses
20hp, 30 min.

Figure 19. Elastic stress distribution in wheel after 20hp brake application for 30 minutes. All values in MPa.

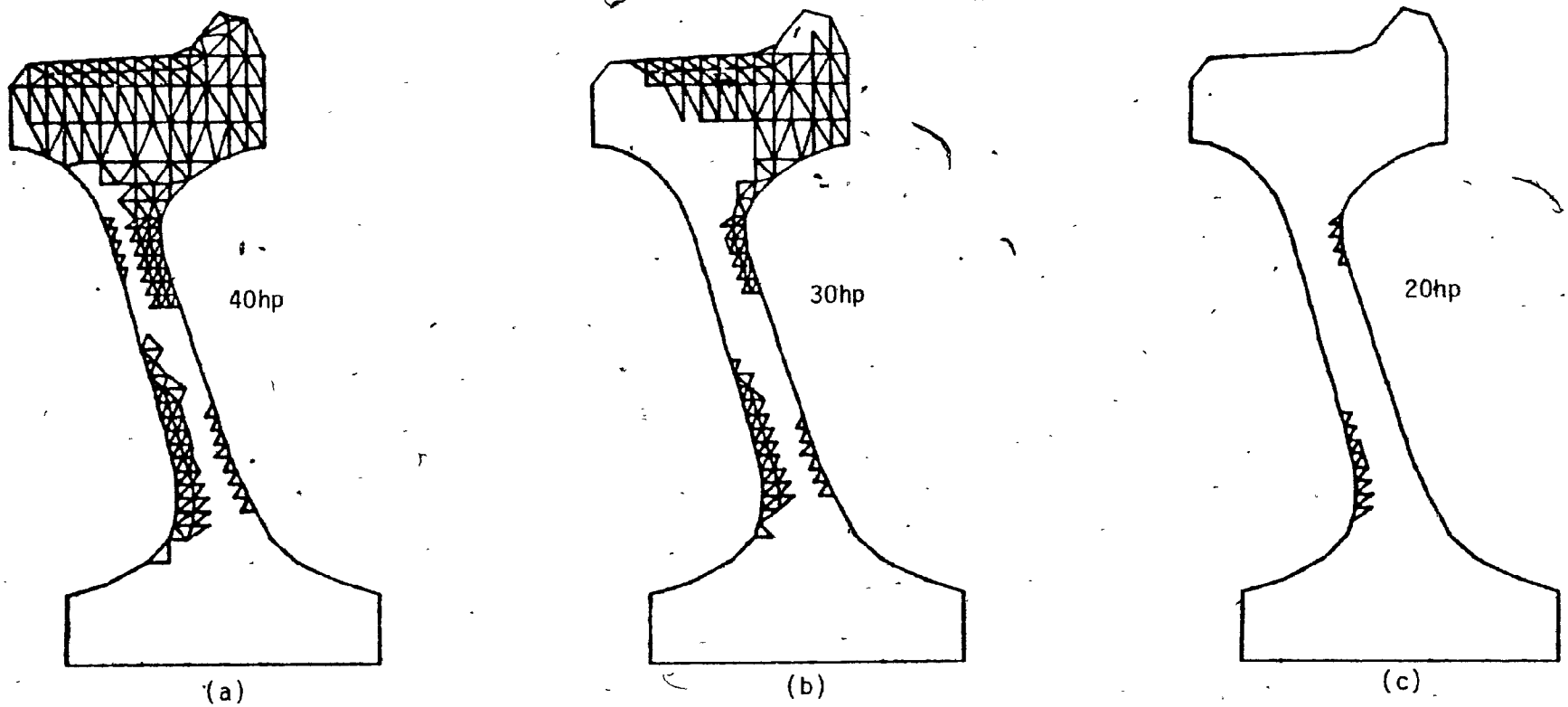

Figure 20. Extent of yield region in wheel after drag brake application for 60 minutes.

Elasto-plastic stresses are obtained for the wheel subjected to yielding, from 20hp, 30hp and 40hp of brake application for 60 minutes, shown in Figure 21. High compressive tangential stresses and tensile radial stresses are found in rim section. Slight reduction is observed in both radial and tangential stresses in this region for 40hp case, Figure 21 (a) and (f), as compared to 30hp, Figure 21 (b) and (e), due to larger yielded region of the former. In outside-hub-fillet and inside-rim-fillet region high tensile radial and tangential stresses are found.

Residual stresses are obtained for the wheel by subtracting the elastic stresses from the elasto-plastic stresses, they are shown in Figure 22. Tensile tangential stresses and compressive radial stresses are found in rim and inside-rim-fillet regions, while tensile radial and compressive tangential stresses are found in outside-hub-fillet regions. Fillet areas are found to be the regions of high stress concentration.

Tensile radial stresses are very important factor in fatigue failure. Their presence contribute towards reduction of fatigue life, since they act as the mean stress. Fatigue strength is seriously reduced by the presence of stress concentration. So it is imperative that the tensile residual stresses around the areas of stress concentration should be reduced.

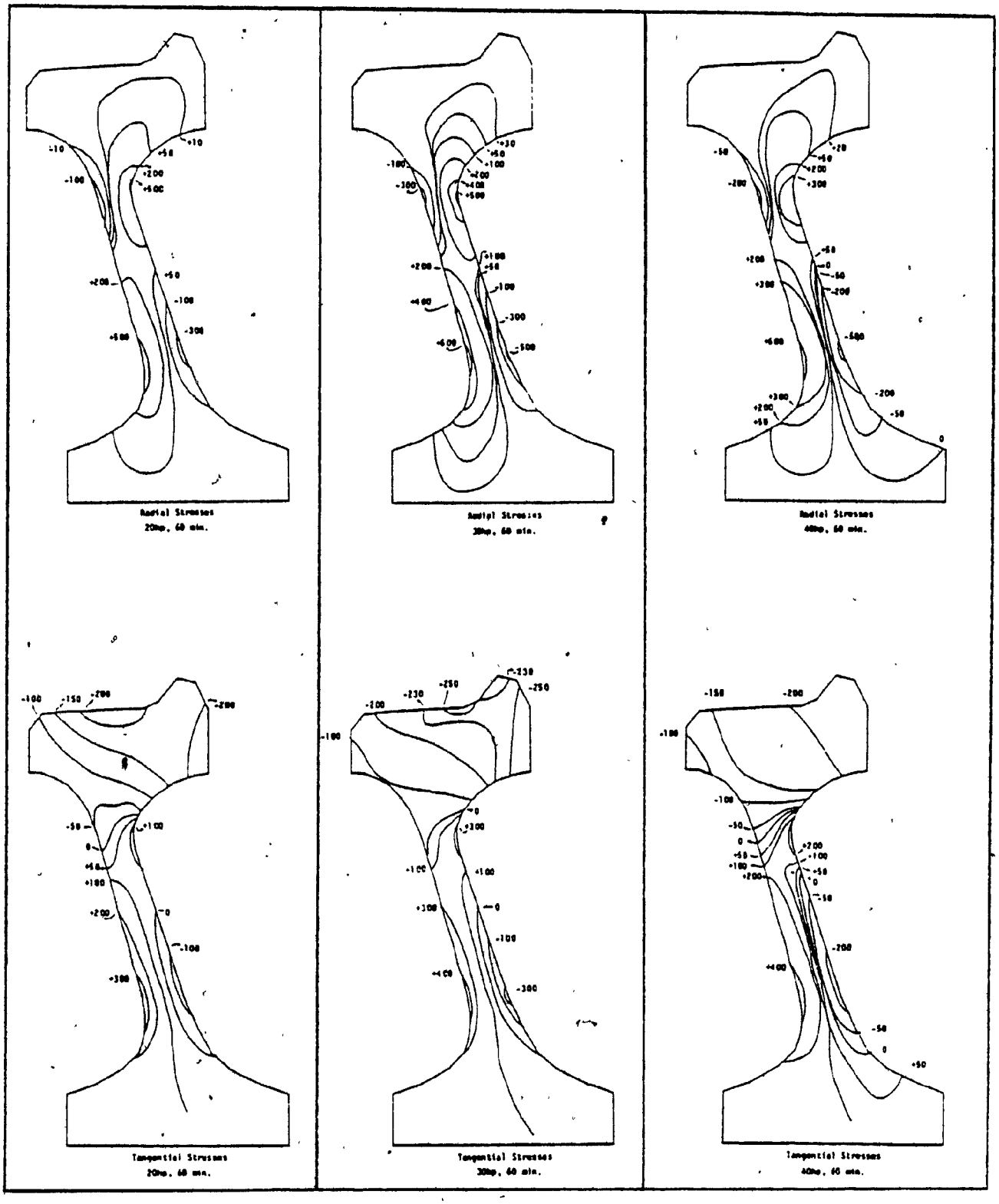

Figure 21. Elasto-plastic, radial and tangential, stress distribution in wheel after 20hp, 30hp and 40hp brake application for 60 minutes. All values in MPa.

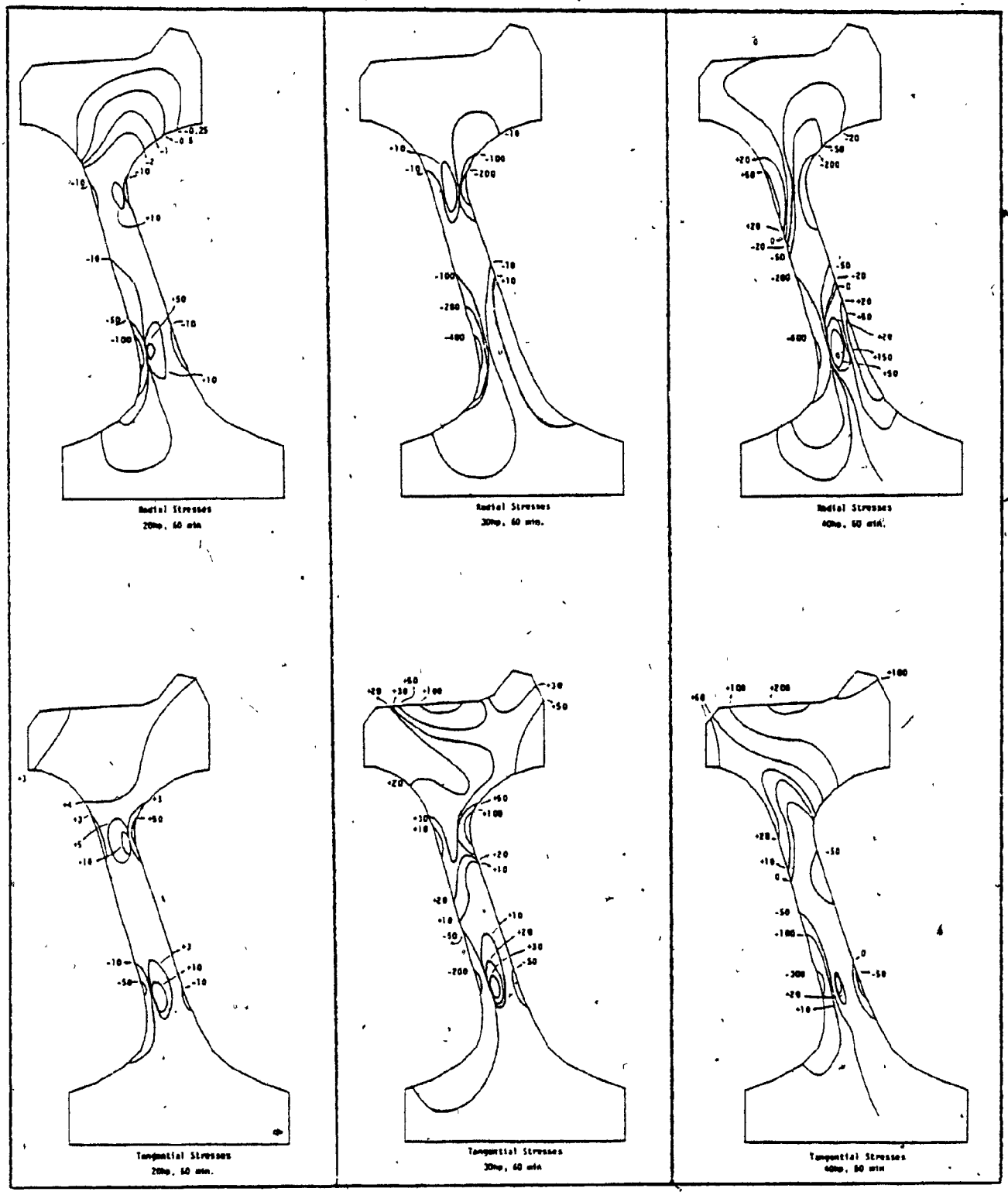

Figure 22. Residual, radial and tangential, stress distribution in wheel after 20hp, 30hp and 40hp brake application for 60 minutes. All values in MPa.

Reduction in tensile residual stresses by improving the profile of wheel fillets will improve the fatigue life of the wheel. For this reason, three new designs are tested. Improvement in profile is done in the inside-rim-fillet and outside-hub-fillet regions, since they are high stress areas. The three new designs are presented in Figure 23 , 24 and 25 , along with the old design. For design #1 and #2 there is no significant change in weight while design #3 has 4% increase in weight. The fillet profiles can be represented by a polynomial:

$$z = ar^3 + br^2 + cr + d \qquad (3.1)$$

where z and r are coordinates, and a, b, c and d are constants given in Table 4. The three new designs are analysed elasto-plastically and residual stresses are obtained for each of them. Brake energy of 30hp for 60 minutes is used for this purpose.

Obviously the design with reduction in high tensile residual stresses is a better one, but reduction in one region may cause an increase in tensile residual stresses in some other regions. For that reason comparison between the residual stresses of the four different designs is done using a "penalty" function, by assigning weights to fifteen different locations on the wheel as shown in Figure 26 and 27. These weights are given in accordance with the relative sensitivity of the location and the stresses, as shown in

– – – – – – – – Original Design

———————— New Design #1.

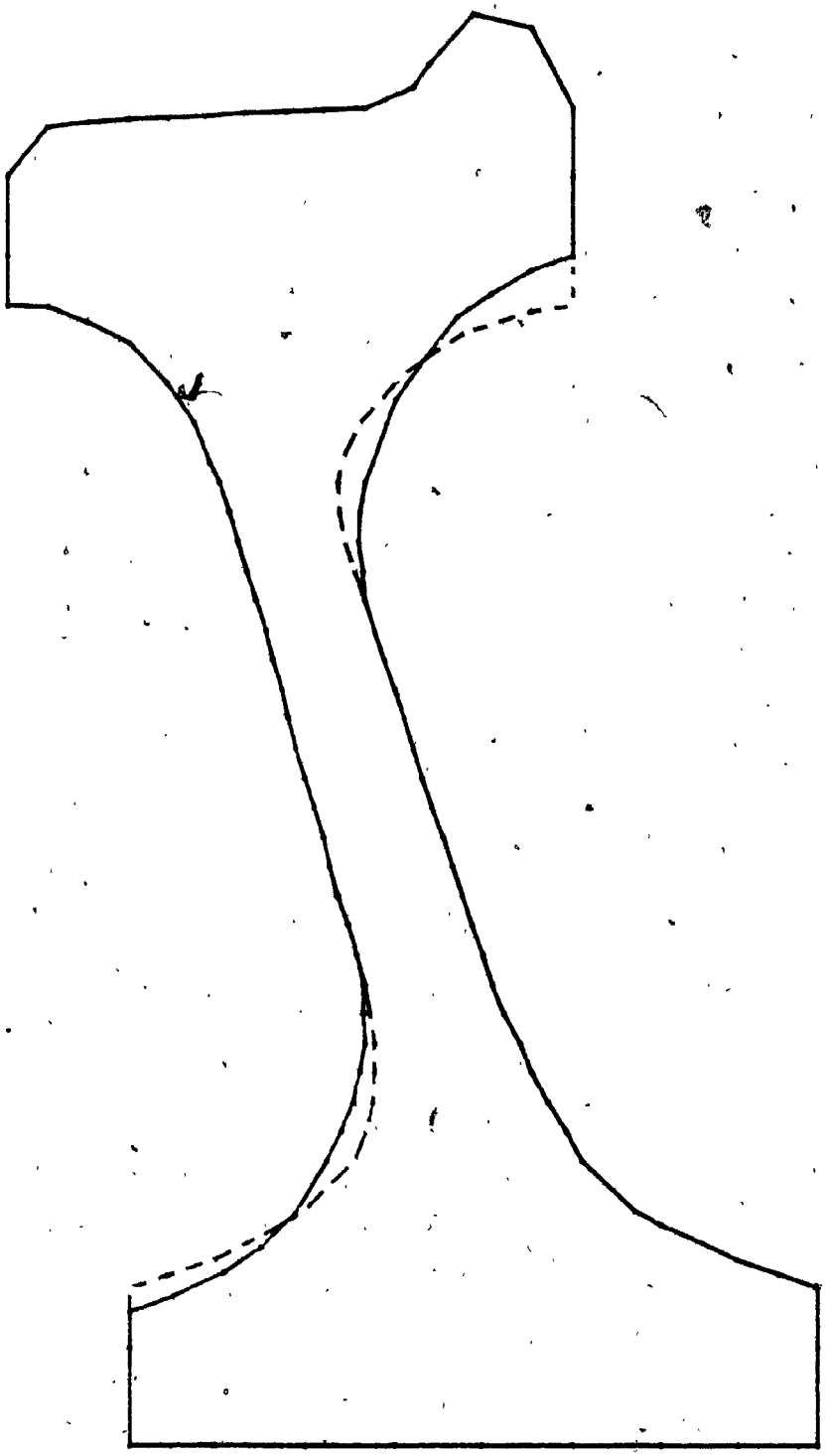

Figure 23.
New Design #1.

- - - - - - - Original Design

——————— New Design #2.

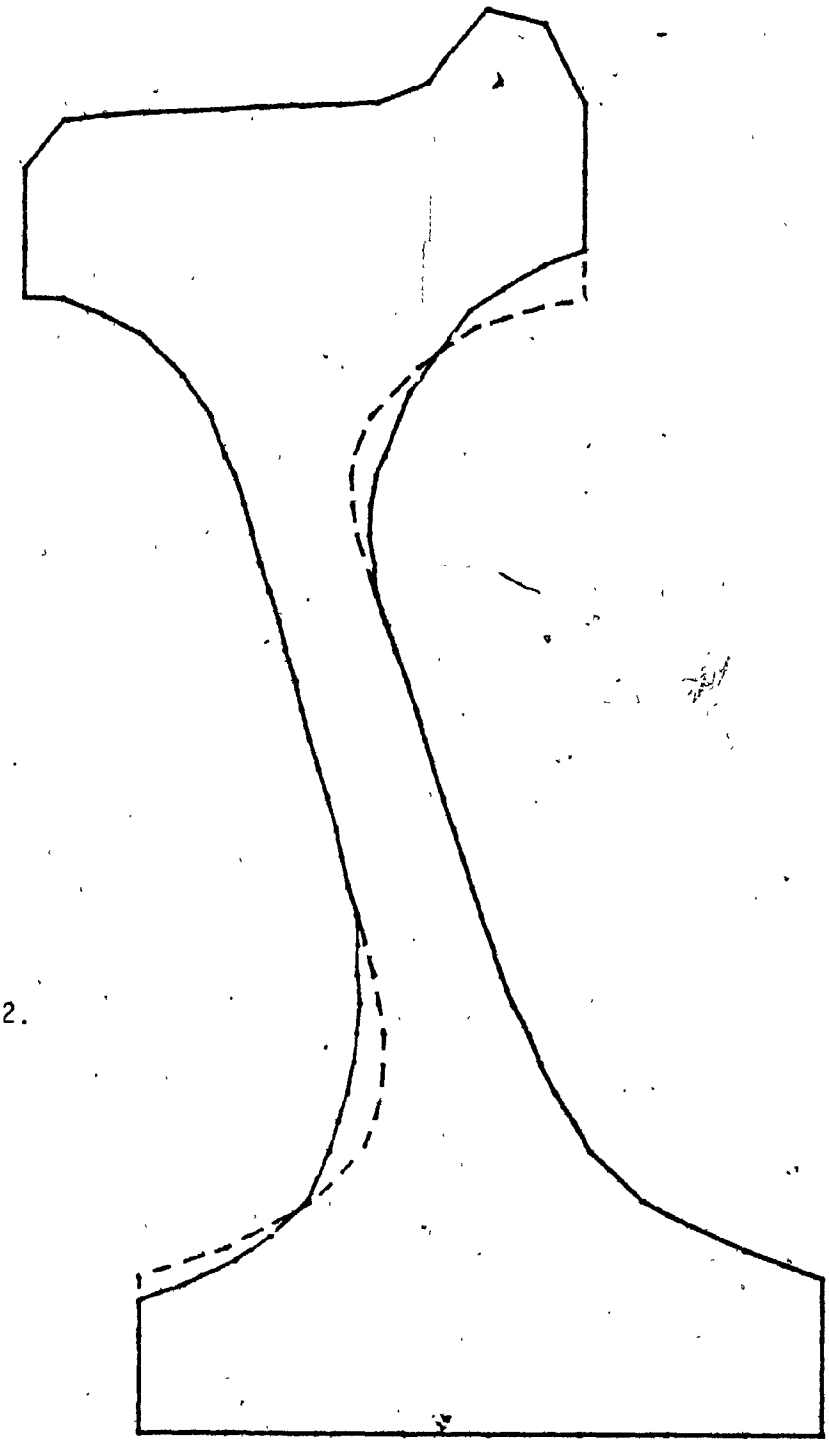

Figure 24.
New Design #2.

---------- Original Design

———————— New Design #3.

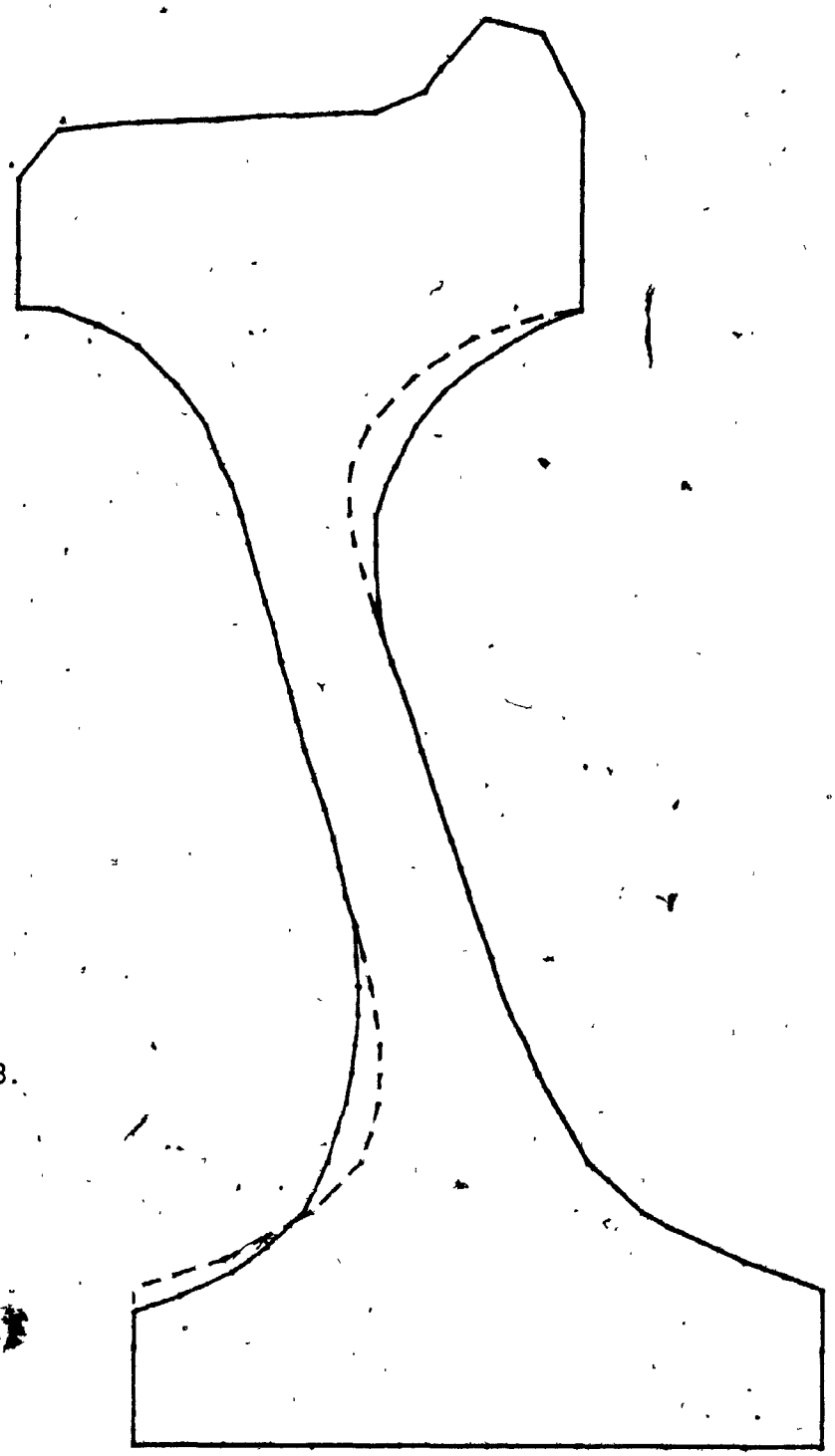

Figure 25.
New design #3.

Design	Inside-Rim-Fillet					Outside-Hub-Fillet				
	a	b	c	d	fillet radius range (cms.)	a	b	c	d	fillet radius range (cms.)
Old	+0.0346	-3.722	+133.12	-1573.82	41.9<r<33.53	-0.02212	+1.5704	-36.88	+298.27	16.5<r<25.9
#1	+0.0073	-0.7297	+24.15	-254.82	43.18<r<33.53	-0.1246	+0.8997	-21.543	+182.95	15.9<r<25.9
#2	+0.0073	-0.7297	+24.15	-254.82	43.18<r<33.53	-0.0168	+1.1589	-26.64	+215.77	15.9<r<25.9
#3	+0.013	+1.335	+45.5	-506.4	41.9<r<33.53	-0.0168	+1.1589	-26.64	+215.77	15.9<r<25.9

Equation: $z = ar^3 + br^2 + cr + d$

Table 4. Constants for equation representing fillet profiles.

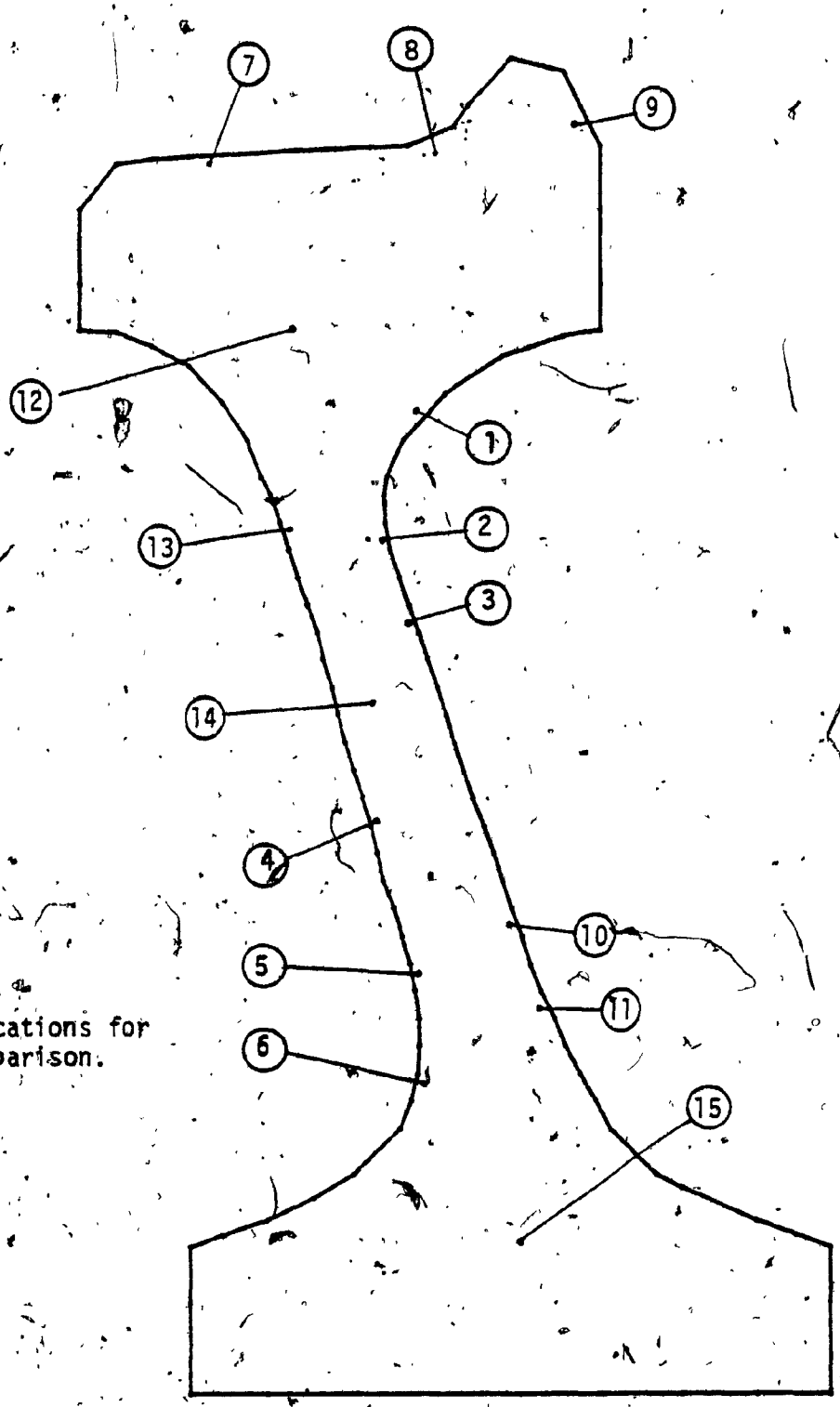

Figure 26.
Fifteen locations for stress comparison.

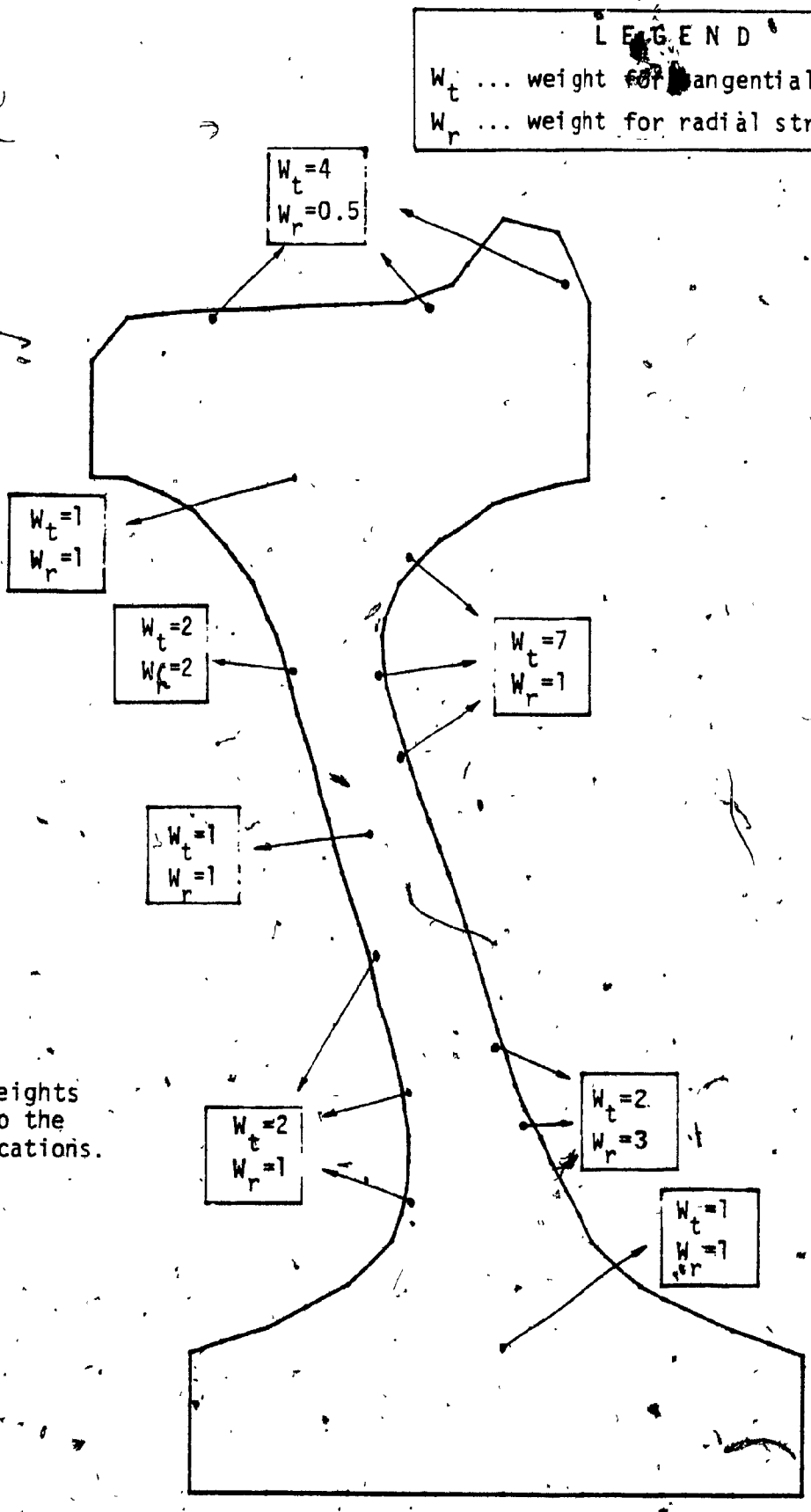

Figure 27.

Relative weights assigned to the fifteen locations.

Table 5. Weights assigned to the fifteen locations for comparison of stresses.

Location	Weights	Remarks
1,2,3	W_t=7	High tangential tensile residual stresses are observed. In practice cracks are found in this region.
	W_r=1	High radial compressive stresses in this region. A little reduction in compressive stresses will not contribute in failure.
4,5,6	W_t=2	Compressive tangential stresses in the region.
	W_r=1	High compressive radial stresses in the region.
7, 8, 9	W_t=4	Tensile tangential stresses. Increase in that will contribute towards fatigue failure.
	W_r=0.5	Very small radial stresses.
10,11	W_t=2	Compressive stresses.
	W_r=3	Tensile radial stresses.
12	W_t=1	Small tensile stresses.
	W_r=1	Compressive radial stresses.
13	W_t=2	Small compressive stresses.
	W_r=2	Small compressive stresses.
14	W_t=1	Small tensile stresses.
	W_r=1	Compressive radial stresses.
15	W_t=1	Compressive stresses.
	W_r=1	Compressive stresses.

Figure 27 and explained in Table 5. For example, the locations with high tensile stresses are given high weights while the locations with high compressive stresses are given low weights. W_t and W_r are the weights assigned to tangential and radial stress at a location respectively. More than one location of comparison is used around yielded region, while for the regions which are not yielded only one location is used. For example outside-hub-fillet region has location 1, 2 and 3 which fall within the yielded region in that area. Similarly loactions 7, 8 and 9 fall within the yielded region in rim section, while the location 12 represents the unyielded region of the rim. The penalty function used is:

$$C_f = \sum_{i=1}^{15} \left[(W_t)_i \, (\Delta\sigma_\theta)_i + (W_r)_i \, (\Delta\sigma_r)_i \right] \qquad (3.2)$$

where $\Delta\sigma$ for a particular location is the difference in stress of the new design being compared and the stress of the old design for the same location. The design with smallest number (greatest negative number) is the best design under these consideration.

The residual stresses obtained in all the four designs at the fifteen locations are presented in Figure 28 to 31. These stresses along with their proper weights are used in the penalty function, equation 3.2, to find the penalty of the new designs. For design #1 the cost is -653, for design #2 the cost is -955 and for design #3 it is -548. Since for

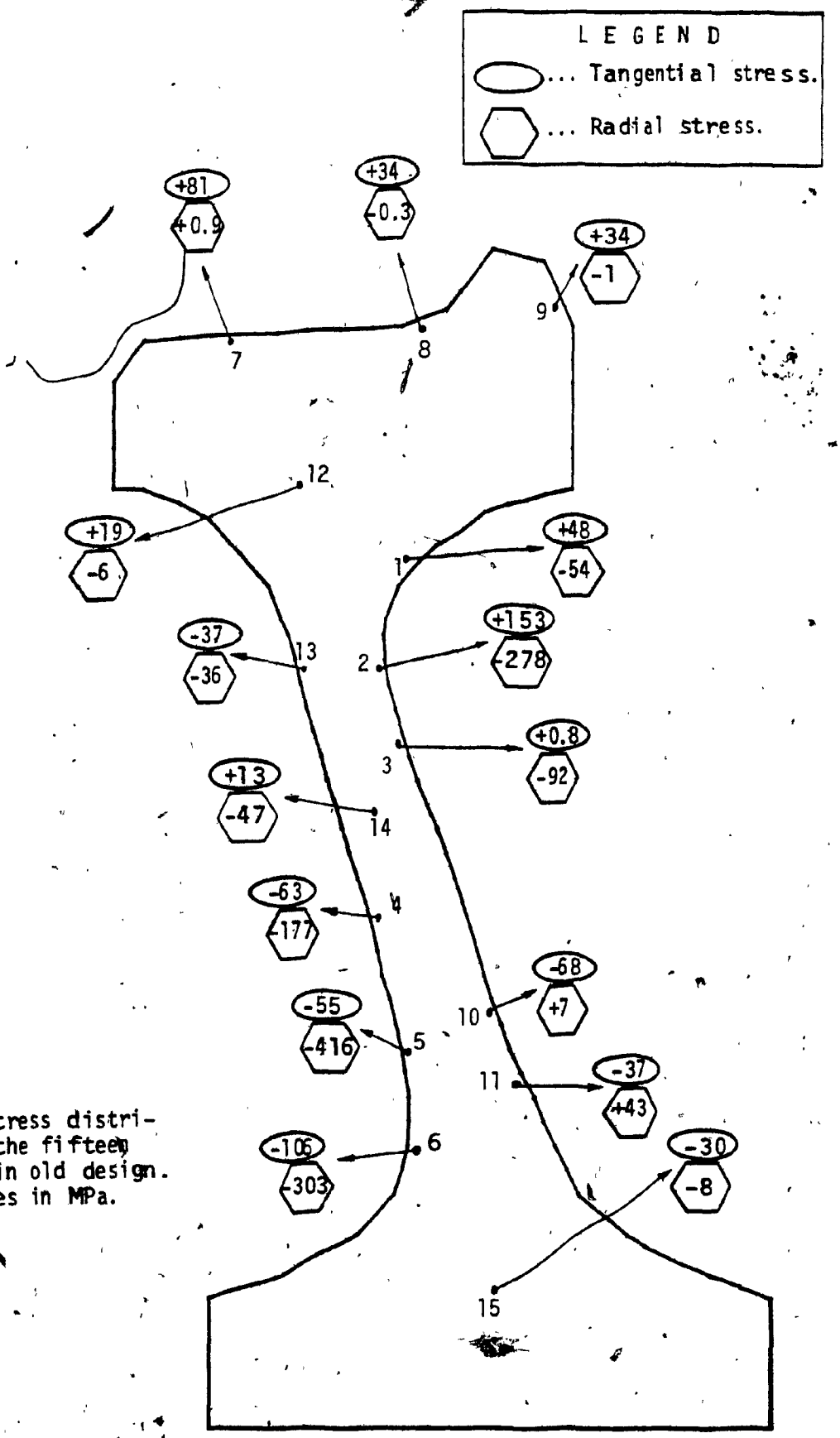

Figure 28.

Residual stress distribution at the fifteen locations in old design. All stresses in MPa.

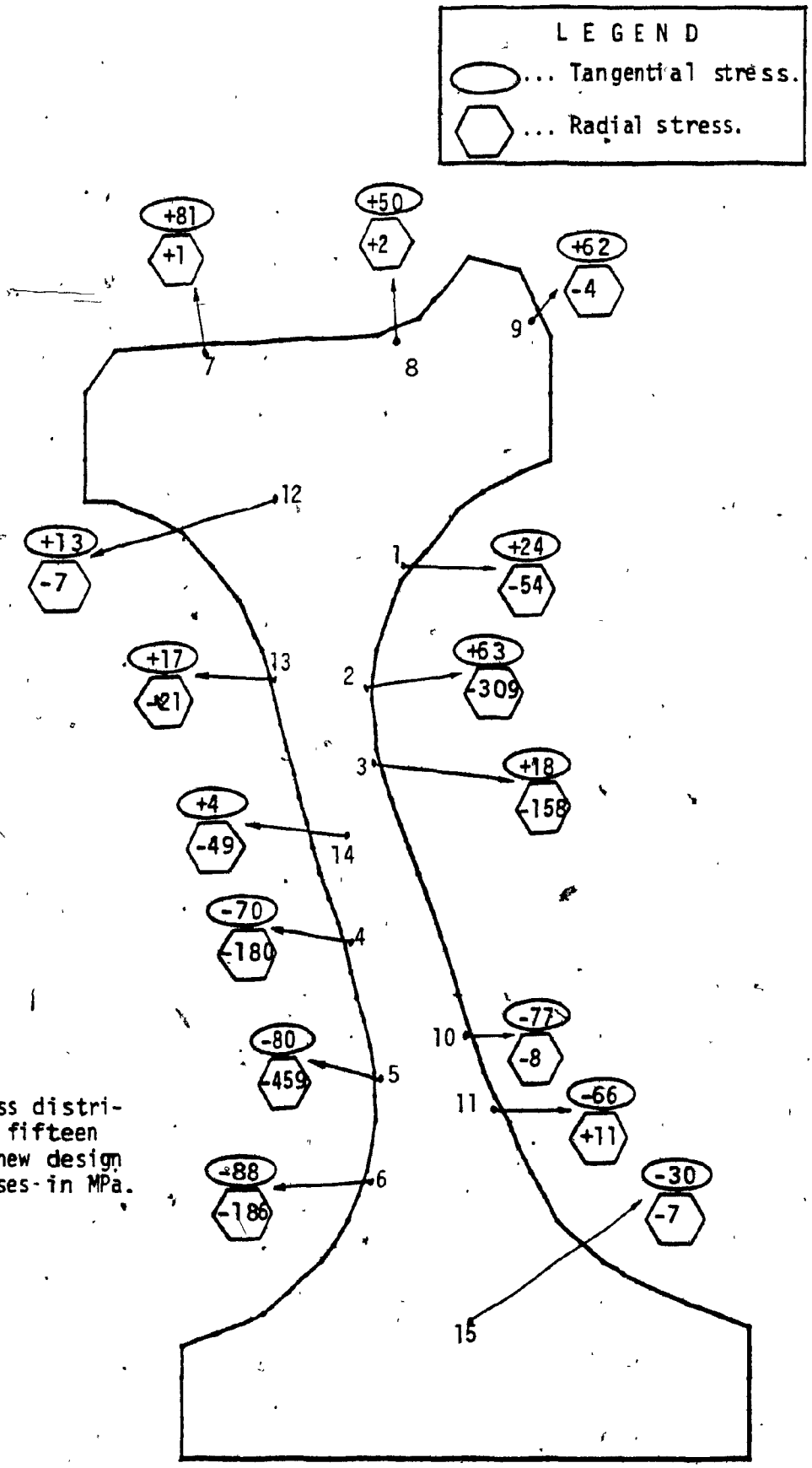

Figure 29.

Residual stress distribution at the fifteen locations in new design #1. All stresses in MPa.

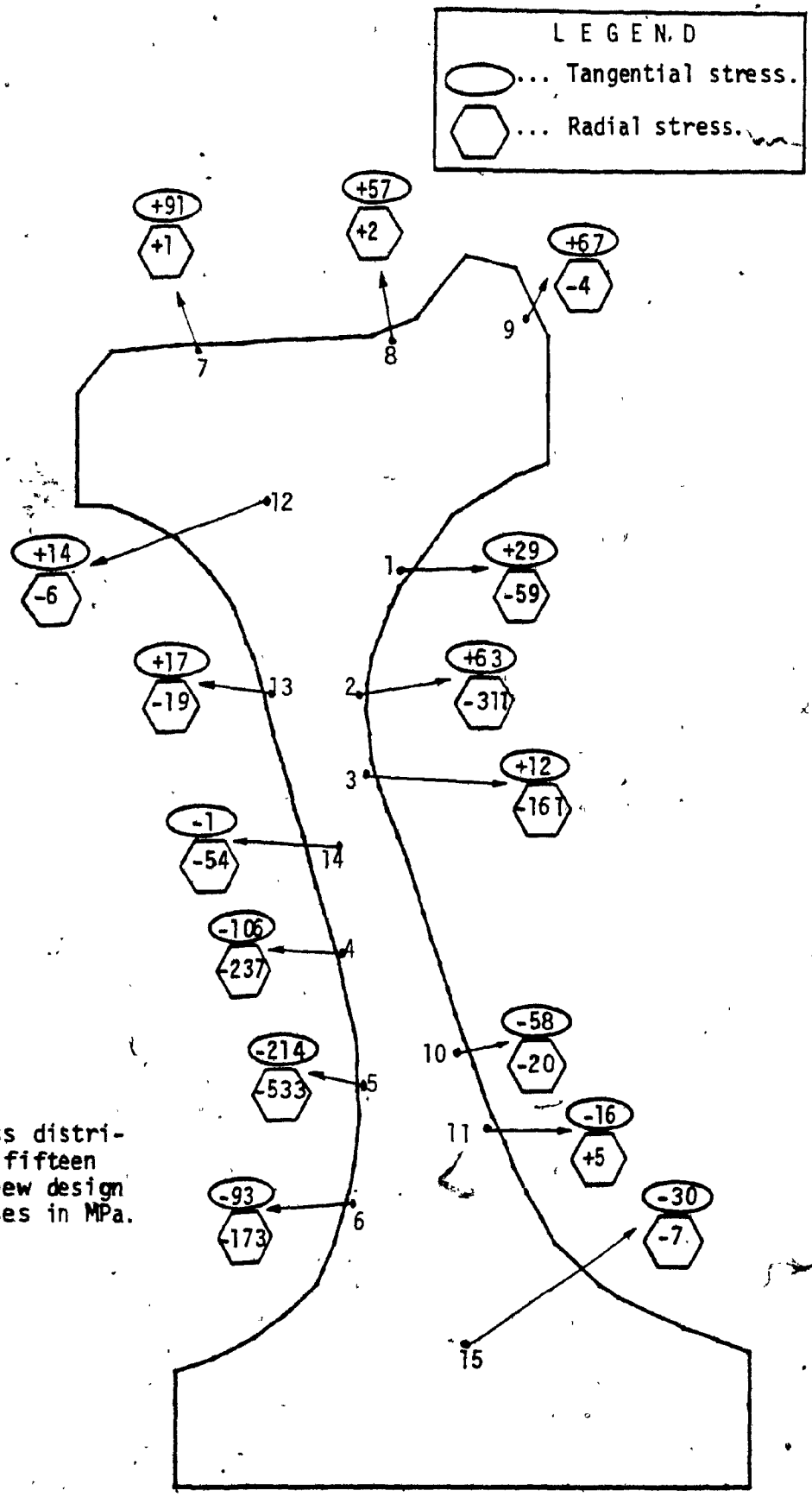

Figure 30.

Residual stress distribution at the fifteen locations in new design #2. All stresses in MPa.

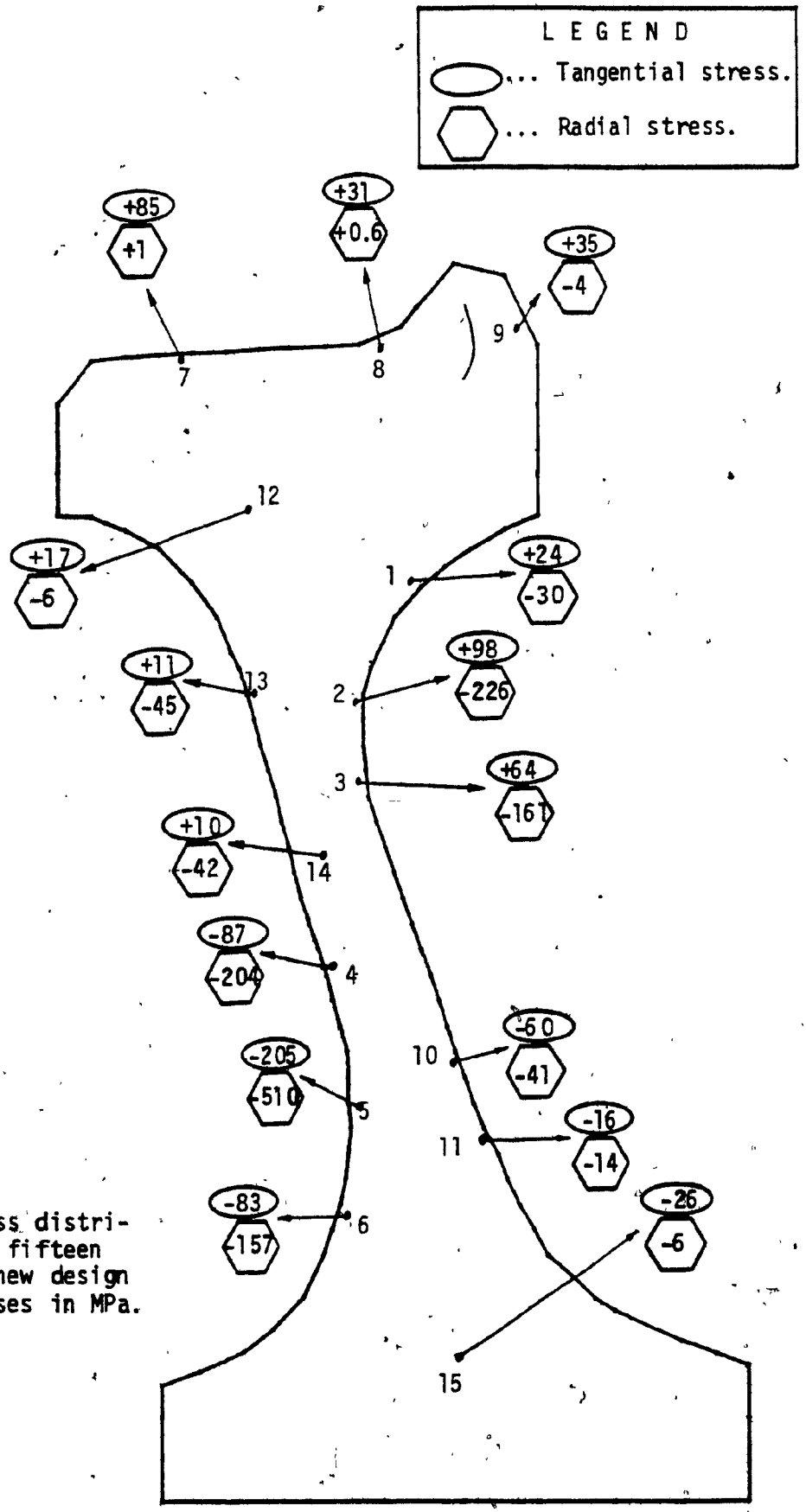

Figure 31.

Residual stress distribution at the fifteen locations in new design #3. All stresses in MPa.

design #2 the penalty is the least, -955, it is the best of the three designs. Considering the cases physically, in rim region, location 7, 8 and 9, design #2 has a slight increase in tensile tangential stresses, as compared to design #1, but in the areas of stress concentration, location 6 and 11, there is a reduction in tensile stresses in design #2. Similarly between design #2 and #3, around critical region of inside-rim-fillet the tensile stresses are lower in #2 than in #3. Moreover, as shown in Table 6, the old design and design #1, undergo more deformation under thermal loads than design #2 and #3, as is observed by the changes in tread taper, ($\beta_o - \beta_d$), (see Figure 18, page 60), and plate inclination, ($\Psi_o - \Psi_d$), angles. And, also, design #2 and #3 have about the same deformation, which further supports that design #2 with considerable reduction in residual stresses and smaller wheel deflection is the best of the four designs.

Design	Change in angles (deg.)	
	($\beta_o - \beta_d$)	($\Psi_o - \Psi_d$)
Old	1.50	2.01
#1	1.05	1.67
#2	0.43	0.78
#3	0.40	0.74

Original tread taper angle, $\beta_o = 3.06^0$
Deflected tread taper angle, β_d
Change in tread taper angle, ($\beta_o - \beta_d$)

Original plate inclination angle, $\Psi_o = 18.95^0$
Deflected plate inclination angle, Ψ_d
Change in plate inclination angle, ($\Psi_o - \Psi_d$)

Table 6. Changes in tread taper angle and plate inclination angle for different designs.

4. CONCLUSIONS

Railway wheel failure has been a major concern to engineers for the past few decades due to increasing trend in heavy train loads and high speed requirements. These wheels not only help in travelling and support car load, but also act as breakdrums. They experience a great deal of stresses during service life. Under severe drag braking, the heat from brake energy travel deep inside the wheel, reducing the tread taper and plate inclination. The stresses caused by thermal gradient are extreemly high..

Due to the irregular shape of the wheel the finite element technique is used for stress analysis. This technique is found to be very useful for elasto-plastic stress analysis. The wheel is divided into more than 430 elements, and the brake energy is simulated as heat flux on a 70 mm wide strip on tread surface. Since the wheel rotates very fast, axisymmetric heat input is assumed. Temperature distribution in the wheels are obtained for 20hp, 30hp and 40hp break application for 60 minutes. Stresses from the temperatures are obtained for the three cases. Yielding is observed in all the three cases. Yielding is initiated in inside-rim-fillet and outside-hub-fillet regions. For 30hp and 40hp a considerable part of the rim section is also yielded.

Residual stresses are obtained for the wheel. Tensile tangential and radial residual stresses are found in inside-rim-fillet and outside-hub-fillet regions respectively. These tensile residual stresses are critical in the fatigue life of a wheel, especially since they are in regions of high stress concentration.

Attempt is made to reduce these tensile residual stresses by modifying fillet profiles. Three new designs with modifications in fillet profiles are tested. Care is taken to avoid significant change in the wheel weight in the new designs. Residual stresses are obtained for the new designs and are compared with residual stresses in the old design. A penalty function is used for the comparision of stresses. The possibility of using penalty function, as a mean of comparison of stress variation with design change, is demonstrated in this thesis. Design #2 is found to be the best of the three new designs, with a considerable reduction in the maximum tensile residual stresses as compared to the old design.

5 FUTURE WORK

Further studies can be done in the area of fatigue failure in wheels having residual stresses from drag braking. The car load on the wheel although negligible compared to thermal loads after drag braking, as well as dynamic-load due to rail irregularities, can contribute significantly to low cycle fatigue failures. Their effect is further enhanced by the presence of tensile residual stresses in the wheel. Better material properties are now available in the literature for class U steels. A recent study by Park and Stone [18] has suggests cyclic softening of class U steel at low strains, causing plastic deformation at stresses below yield strength.

The non-symmetric nature of car load on the wheel requires a three dimensional analysis demanding cosiderably larger computer memory. The point load on the wheel can be incorporated in axisymmetric finite element program with slight modifications in matrices [B] and [D], using the Fourier series. Using the Fourier series to model point load on axisymmetric wheel will reduce the memory required..

Another interesting area of work will be to find the optimum fillet profile. Previous attempts to make optimum wheel design has resulted in an straignt plate wheel to take

the shape of a parabolic plate wheel [20]. Since many of the wheel manufacturers in North America make straight plate wheels, and the manufacturing processes for both straight plate and parabolic plate wheels are considerably different, it is advisable to produce a better wheel from the existing process. The attempt in this report shows that slight variation in the fillet profiles has a significant effect on the stress distribution in the wheel. Only a few designs are tested here since this pilot research project is intended to lay down the ground work and to demonstrate the possibility. In future a good finite element optimization program can handle the task much more speedily.

REFERENCES

1. Berg, N. A. and Alber, R. H., "Tread Break Verses The Wheel", Presented At Air Brake Association Annual Meeting, Chicago, Sept. 1972.

2. Berg, N. A. and Kucera, W. J., "A Review Of Thermal Damage In Railroad Wheels", Presented At The Air Brake Association Annual Meeting, Chicago, Sept. 1970, Griffin Wheel Company.

3. Carter, C. S. and Caton, R. G., "Fracture Resistance Of Railroad Wheels". U. S. Dept. Of Transportation. Report No. FRA-ORD & D-75-12, Sept. 1974.

4. Dieter, G. E., "Mechanical Metallurgy", McGraw-Hill Book Company, New York, 1976, pp 72-102.

5. Godfrey, D. E. R., "Theoratical Elasticity And Plasticity For Engineers", Thames And Hudson, London, pp 246-263.

6. Holeman, J. P., "Heat Transfer", McGraw-Hill Book Company, New York, 1976, pp 3-7.

7. Hornbeck, R. W., "Numerical Methods", Quantum Publishers, Inc., New York, 1975, pp 43-47.

8. Hubner, K. H., "The Finite Element Method for Engineers, John Wiley & Sons, New York, 1975, pp 197-241.

9. Johnson, M. R., Welch, R. E. and Young, K. S., "Analysis Of Thermal Stresses And Residual Stress Changes In Railroad Wheels Caused By Severe Drag Braking". TRANS. ASME, J. Of Engineering For Industry, Feb. 1977, pp 18-23.

10. Kachanov, L. M. "Foundation Of The Theory Of Plasticity", Elsevier Publishing Company, pp 95-122.

11. Leadley, G. L., "An Overview Of Current Efforts To Detect And Prevent Steel Wheel Failures", Natl Bur Stand Spec Publ n 436, 1975, for 22nd Meet of Mech Failures Prev Group, Calif, 1975, pp 261-288.

12. Literature Supplied by Hawker Sidley Canada Ltd., "Railway Wheel Data", Canadian Steel Wheel Division, Montreal.

13. Nayak, G. C. and Zienkiwicz, O. C., "Elasto-Plastic Stress Analysis. A Generalization For Various Constitutive Relations Including Strain Softening", Int. J. Num. Methods In Eng., 1, 1972, pp 113-135.

14. Novak, G. E., Dahlman, G. E., Eck, B. J. and Kucera, W. J., "Thermal Pattern In 36 in. Freight Car Wheels During Service Test", ASME Paper # 76-WA/RT-11.

15. Novak, G. E. and Eck, B. J., "A Three-Dmensional Finite Difference Solution For Theermal Stress In Railcar Wheels", TRANS. ASME, J. Of Engineering For Industry, Aug. 1969, pp 891-896.

16. Novak, G. E. and Stone, D. H., "A Comparison Of Stress Level In One And Two Wear 36 in. Diameter Wheels Under Simulated Service Loads", ASME Paper # 77-RT-13.

17. Novak, G. E. and Eck, B. J., "Cyclic Distortion And Stresses In 36 in. Wheels Under Combined Service Loads", ASME Paper # 75-WA/RT-5.

18. Park, Y. J. and Stone, D. H., "Cyclic Behavior of Class U Wheel Steel", TRANS. ASME, J. Of Engineering For Industry, Feb. 1981, pp 113-118.

19. Redford, R. W., "Wheel/Rail Vertical Forces In High-Speed Railway Operation", TRANS. ASME, J. Of Engineering For Industry, Nov. 1977, pp 849-858.

20. Rusin, T. M., Kleeshulte, D. G. and Coughlin, J. M., "Application Of The Finite Element Method In The Development Of Improved Railroad Car Wheel Design", ASME Paper # 78-WA/RT-5.

21. Segerlind, L. J., "Applied Finite Element Analysis", New York, Wiley, 1976, pp 42-46.

22. Ibid., pp 191-223.

23. Steel Product Manual, "Wrought Steel Wheels and Forged Railway Axles", American Iron and Steel Institute, Washington, Sept 1979.

24. Timoshenko, S. P. and Goodier, J. N., "Theory Of Elasticity", McGraw-Hill Book Company, New York, 1970, pp 380-383.

25. Van Swaaij, J. L., "Thermal Damage To Railway Wheel", Int. Conf. Of Railway Braking, I Mech E. Conf Publ 1979-11, Railway Div of Inst of Mech Engrs., 1979, pp 95-100.

26. Wetenkamp, H. R. and Kipp, R. M., "Thermal Damage And Rail Load Stresses In A 33 in. Railroad Car Wheel", TRANS. ASME, J. Of Engineering For Industry, Aug. 1978, pp 363-369.

27. Wilson, E. L., "Structural Analysis Of Axisymmetric Solids", AIAA Journal, Dec. 1965, pp 2269-2274.

28. Zienkiewicz, O. C., "The Finite Element Method", McGraw-Hill Book Company, New York, 1977, pp 48-52.

29. Ibid., pp 73-89.

30. Ibid., pp 254-273.

31. Ibid., pp 369-390.

32. Ibid., pp 512-513.

33. Zienkiewicz, O. C., Valliapan, S. and King, I. P., "Elasto-Plastic Solution Of Engineering Problems, Initial Stress, Finite Element Approach", Int. J. Num. Methods In Eng., 1, 1969, pp 75-100.

APPENDIX A

Computer program 'TEMPCAL', for calculation of temperature distribution.

```
      PROGRAM TEMPCAL(INPUT,OUTPUT,TAPE5,TAPE6,TAPE3)
      DIMENSION B(3),C(3),AL(3,3),COND(3,3),CONV(3,3),CAPC(3,3)
     1,D(3,3),IPP(3),AB(3,3),F(3),R(3),ND(450,6)
     1,FINALK(267,22),FINALF(300),TN1(300),FORCE(3)
     1,T(300),II(450),JJ(450),KK(450),IR(450,4),FF(300)
     1,KNDTMP(450),RX(300),ZY(300)
*****************************************************************
* PROGRAM TO CALCULATE TEMPERATURE DISTRIBUTION IN AXISYMMETRIC *
* SOLIDS.                                                       *
*****************************************************************
*                                                               *
*                          L E G E N D                          *
*                                                               *
*****************************************************************
*                                                               *
* NC1          BANDWIDTH.                                       *
* NEL          NUMBER OF ELEMENTS.                              *
* NNODES       NUMBER OF NODES.                                 *
* COEFK        THERMAL CONDUCTIVITY.                            *
* COEFH        CONVECTION COEFFICIENT.                          *
* TAMB         AMBIENT TEMPERATURE.                             *
* HFLUX        HEAT FLUX, IN WATTS/CM. SQ.                      *
* CAPC         CAPACITANCE MATRIX.                              *
* COND         CONDUCTION MATRIX.                               *
* CONV         CONVECTION MATRIX.                               *
* FINALK       ACCUMULATED STIFFNESS MATRIX.                    *
* FINALC       ACCUMULATED CAPACITANCE MATRIX.                  *
* RX           COORDINATE "R" OF THE NODE.                      *
* ZY           COORDINATE "Z" OF THE NODE.                      *
* II           ARRAY CONTAINING NODE "I" OF THE ELEMENT.        *
* JJ           ARRAY CONTAINING NODE "J" OF THE ELEMENT.        *
* KK           ARRAY CONTAINING NODE "K" OF THE ELEMENT.        *
*                                                               *
*****************************************************************
*                     SEQUENCE OF DATA                          *
*****************************************************************
*                                                               *
* ICASE:       ICASE=0 .. IF STEADY STATE CASE.                 *
*              ICASE=1 .. IF TRANSIENT CASE.                    *
* NUMBER OF ELEMENTS, "NEL".                                    *
* NUMBER OF NODES, "NNODE".                                     *
* NEL  NUMBER OF LINES CONTAINING "Z" AND "R" COORDINATES       *
*                     OF EACH NODE.                             *
* NNODE NUMBER OF LINES CONTAINING I, J,  AND K FOR             *
*                     EACH ELEMENT.                             *
*                                                               *
*****************************************************************
      REWIND 5
      REWIND 6
      REWIND 3
*
* CONVECTION COEFFICIENT, WATTS/CM.SQ.DEG"C.
      COEFH=0.001987
*
* AMBIENT TEMPERATURE, DEG"K.
      TAMB=297
*
* DENSITY OF THE MATERIAL.
      RHO=7.833E-3
```

```
      TIME=3600
*
* TIME INCREMENT FOR TRANSIENT CASE.
      DT=120
      READ(5,*)ICASE
*************************************************************
* READING OF STRUCTURE DATA AND BANDWIDTH CALCULATION.*
*************************************************************
      READ(5,*)NEL,NNODE
      DO 5 I=1,NNODE
5     READ(5,*)RX(I),ZY(I)
      DO 6 M=1,NEL
      READ(5,*)II(M),JJ(M),KK(M)
      KG=IABS(II(M)-JJ(M))
      IF(IABS(II(M)-KK(M)).GT.KG)  KG=IABS(II(M)-KK(M))
      IF(IABS(JJ(M)-KK(M)).GT.KG)  KG=IABS(JJ(M)-KK(M))
      IF(KG.GT.NBW)  NBW=KG
6     CONTINUE
      NC=NBW-1
*
* TOTAL NUMBER OF ELEMENTS HAVING HEAT FLUX.
      READ(5,*)KT
      IF(KT.EQ.0)  GO TO 13
* HEAT FLUX, WATTS/CM.SQ.
* HORSE POWER.
      HP=746.*40
      HFLUX=HP/(2*3.1415926*2.54*2.54*3*18)
      PRINT*,"   HEAT FLUX  = ",HFLUX,"   WATT/CM.SQ."
* KT ELEMENT NUMBERS HAVING THE HEAT FLUX.
      DO 47 I=1,KT
47    READ(5,*)KNDTMP(I)
*************************************
* FINDS THE ELEMENTS AT THE SURFACE.*
*************************************
13    DO 7 I=1,NEL
      ND(I,1)=II(I)
      ND(I,2)=JJ(I)
      ND(I,3)=JJ(I)
      ND(I,4)=KK(I)
      ND(I,5)=KK(I)
      ND(I,6)=II(I)
7     CONTINUE
      N1=NEL-1
      DO 26 I=1,N1
      DO 27 J=1,5,2
      IF(ND(I,J).EQ.0)  GO TO 27
      A=ND(I,J)
      ND(I,J)=ND(I,J+1)
      ND(I,J+1)=A
      I1=I+1
      DO 30 IA=I1,NEL
      DO 19 JA=1,5,2
      IF(ND(IA,JA).NE.ND(I,J))  GO TO 19
      JA1=JA+1
      J1=J+1
      IF(ND(IA,JA1).NE.ND(I,J1))  GO TO 19
      IF(ND(IA,JA).EQ.0)  GO TO 19
      ND(IA,JA)=0
      ND(IA,JA1)=0
```

```
      ND(I,J)=0
      ND(I,J1)=0
19    CONTINUE
30    CONTINUE
      A=ND(I,J)
      ND(I,J)=ND(I,J+1)
      ND(I,J+1)=A
27    CONTINUE
26    CONTINUE
*
* FINDS SIDES SUBJECTED TO CONVECTION
      DO 11 I=1,NEL
      K=0
      DO 12 J=1,5,2
      IF(ND(I,J).EQ.0) GO TO 12
      K=K+1
      IP(I,K)=ND(I,J)
      K=K+1
      IP(I,K)=ND(I,J+1)
12    CONTINUE
11    CONTINUE
*************************************
* FORMULATION OF ELEMENT MATRICES.*
*************************************
      DO 29 I=1,NEL
      X1=RX(II(I))
      Y1=ZY(II(I))
      X2=RX(JJ(I))
      Y2=ZY(JJ(I))
      X3=RX(KK(I))
      Y3=ZY(KK(I))
      IPP(1)=II(I)
      IPP(2)=JJ(I)
      IPP(3)=KK(I)
      DO 44 K=1,4
      IJ=IP(I,K)
      DO 44 J=1,3
      IF(IJ.NE.IPP(J)) GO TO 44
      IP(I,K)=J
44    CONTINUE
*
* CODE FOR CONVECTIVE ELEMENT.
      IP1=IP(I,1)
      IP2=IP(I,2)
      IP3=IP(I,3)
      IP4=IP(I,4)
*
* AREA OF THE ELEMENT.
      AREA=((X2*Y3)-(Y2*X3)-X1*(Y3-Y2)+Y1*(X3-X2))/2
      IF(AREA.LE.0) PRINT*,"  ERROR IN ELEMENT NO.  ",I
*
* SHAPE FUNCTION
      B(1)=Y2-Y3
      C(1)=X3-X2
      B(2)=Y3-Y1
      C(2)=X1-X3
      B(3)=Y1-Y2
      C(3)=X2-X1
      AL(3,1)=(((X3-X1)**2)+((Y3-Y1)**2))**(0.5)
```

```
      AL(2,3)=(((X2-X3)**2)+((Y2-Y3)**2))**(0.5)
      AL(1,2)=(((X1-X2)**2)+((Y1-Y2)**2))**(0.5)
      RBAR=(X1+X2+X3)/3
*
* CONDUCTION MATRIX
      DO 8 K=1,3
      DO 8 J=1,3
8     COND(K,J)=0
      DO 1 K=1,3
      DO 1 J=1,3
      AB(K,J)=B(K)*B(J)
      COND(K,J)=C(K)*C(J)
      AB(K,J)=AB(K,J)*2*3.1415926*RBAR*COEFK/(4*AREA)
1     COND(K,J)=COND(K,J)*2*3.1415926*RBAR*COEFK/(4*AREA)
      DO 2 IA=1,3
      DO 2 JA=1,3
      COND(IA,JA)=COND(IA,JA)+AB(IA,JA)
2     AB(IA,JA)=0
      DO 10 J=1,3
10    FORCE(J)=0
*
* FORCE VECTOR DUE TO HEAT INPUT.
      R(1)=X1
      R(2)=X2
      R(3)=X3
      KZ=0
      DO 50 K=1,KT
      IF(KNDTMP(K).EQ.1) KZ=1
50    CONTINUE
      IF(KZ.EQ.0) GO TO 51
      F(1)=F(2)=F(3)=0
      F(IP1)=2*R(IP1)+R(IP2)
      F(IP2)=R(IP1)+2*R(IP2)
      DO 52 K=1,3
52    F(K)=F(K)*2*3.1415926*HFLUX*AL(IP1,IP2)/6
*
* NO CONVECTION FOR ELEMENT WITH HEAT FLUX(INPUT).
      IP1=IP2=0
51    IF(IP1.EQ.0)  GO TO 28
*
* CONVECTION MATRIX
      D(IP1,IP1)=3*R(IP1)+R(IP2)
      D(IP2,IP2)=3*R(IP2)+R(IP1)
      D(IP1,IP2)=D(IP2,IP1)=R(IP1)+R(IP2)
      DO 20 K=1,3
      DO 20 J=1,3
20    D(K,J)=D(K,J)=3.1415926*AL(IP1,IP2)*COEFH/6
      DO 23 K=1,3
      DO 23 J=1,3
      CONV(K,J)=CONV(K,J)+D(K,J)
23    D(K,J)=0
      IF(IP3.EQ.0)  GO TO 21
      D(IP3,IP3)=3*R(IP3)+R(IP4)
      D(IP4,IP4)=3*R(IP4)+R(IP3)
      D(IP3,IP4)=D(IP4,IP3)=R(IP3)+R(IP4)
      DO 22 K=1,3
      DO 22 J=1,3
22    D(K,J)=D(K,J)*3.1415926*AL(IP3,IP4)*COEFH/6
      DO 24 K=1,3
```

```
      DO 24 J=1,3
      CONV(K,J)=CONV(K,J)+D(K,J)
24    D(K,J)=0
      PRINT*,IP3,IP4
21    DO 4 IA=1,3
      DO 4 JA=1,3
      COND(IA,JA)=COND(IA,JA)+CONV(IA,JA)
4     CONV(IA,JA)=0
*
* FORCE MATRIX DUE TO CONVECTION
      DO 14 K=1,3
      F(K)=0
14    FORCE(K)=0
      F(IP1)=2*R(IP1)+R(IP2)
      F(IP2)=2*R(IP2)+R(IP1)
      DO 15 K=1,3
15    F(K)=F(K)*3.1415926*COEFH*TAMB*AL(IP1,IP2)/3
      DO 16 K=1,3
      FORCE(K)=FORCE(K)+F(K)
16    F(K)=0
      IF(IP3.EQ.0) GO TO 28
      F(IP3)=2*R(IP3)+R(IP4)
      F(IP4)=2*R(IP4)+R(IP3)
      DO 17 K=1,3
17    F(K)=F(K)*3.1415926*COEFH*TAMB*AL(IP3,IP4)/3
      DO 18 K=1,3
      FORCE(K)=FORCE(K)+F(K)
18    F(K)=0
*
* ACCUMULATES STIFFNESS MATRIX.
28    CALL ACCUMK(FINALK,NNODE,NBW,COND,I,II,JJ,KK,NEL)
*
* ACCUMULATES FORCE MATRIX
      CALL ACCUMF(FINALF,NNODE,FORCE,I,II,JJ,KK,NEL)
*
* FOR STEADY STATE CASE.
      IF(ICASE.EQ.0) GO TO 29
*
* THERMAL CONDUCTIVITY, WATTS/CM.DEG"C.
      TAVG=(TN1(II(I))+TN1(JJ(I))+TN1(KK(I)))/3
      TTT=(9*(TAVG-273)/5)+460
      COEFK=(30-(5.5*TTT/1000))*0.01731
* HEAT CAPACITANCE.
      CP=(0.07+(0.06*TTT/1000))*4.18674*1000
      ALAMDA=RHO*CP
*
* ELEMENT CAPACITANCE MATRIX.
      CAPC(1,1)=6*X1+2*X2+2*X3
      CAPC(2,2)=2*X1+6*X2+2*X3
      CAPC(3,3)=2*X1+2*X2+6*X3
      CAPC(1,2)=CAPC(2,1)=2*X1+2*X2+X3
      CAPC(1,3)=CAPC(3,1)=2*X1+X2+2*X3
      CAPC(2,3)=CAPC(3,2)=X1+2*X2+2*X3
      DO 57 K=1,3
      DO 57 J=1,3
57    CAPC(K,J)=CAPC(K,J)*4*ALAMDA*3.1415926*A/(120*DT)
*
      WRITE(3,*)((CAPC(K,J),J=1,3),K=1,3)
29    CONTINUE
```

```
*
      IF(ICASE.EQ.0)  GO TO 9
**********************
* TRANSIENT CASE.....*
**********************
      REWIND 3
      DO 25 I=1,NNODE
      DO 25 J=1,NBW
25    FINALK(I,J)=(-1.)*FINALK(I,J)/2
      WRITE(6,*)((FINALK(I,J),J=1,NBW),I=1,NNODE)
*
      DO 31 I=1,NEL
      READ(3,*)((CAPC(K,J),J=1,3),K=1,3)
      CALL ACCUMK(FINALK,NNODE,NBW,COND,I,II,JJ,KK,NEL)
31    CONTINUE
      REWIND 5
      WRITE(5,*)((FINALK(I,J),J=1,NBW),I=1,NNODE)
*
      REWIND 6
      READ(6,*)((FINALK(I,J),J=1,NBW),I=1,NNODE)
      DO 32 I=1,NNODE
      DO 32 J=1,NBW
32    FINALK(I,J)=FINALK(I,J)*(-1.)
      REWIND 3
      DO 33 I=1,NEL
      READ(3,*)((CAPC(K,J),J=1,3),K=1,3)
      CALL ACCUMK(FINALK,NNODE,NBW,COND,I,II,JJ,KK,NEL)
33    CONTINUE
      WRITE(5,*)(FINALF(I),I=1,NNODE)
      WRITE(5,*)((FINALK(I,J),J=1,NBW),I=1,NNODE)
*
      PRINT*," ENTER NUMBER OF TIME INCREMENTS REQUIRED. "
      READ*,K
71    ITER=ITER+1
      REWIND 5
      READ(5,*)((FINALK(I,J),J=1,NBW),I=1,NNODE)
      CALL VMULOF(FINALK,NNODE,NC,L,TN1,1,NNODE,FF,NNODE)
      READ(5,*)(FINALF(I),I=1,NNODE)
      DO 66 I=1,NNODE
66    FINALF(I)=FINAL(I)+FF(I)
      READ(5,*)((FINALK(I,J),J=1,NBW),I=1,NNODE)
      IDGT=10
      CALL LEQ1PB(FINALK,NNODE,NC,NNODE,FINALF,
     1NNODE,1,IDGT,D1,D2,IER)
      DO 34 I=1,NNODE
34    TN1(I)=FINALF(I)
      IF(ITER.EQ.K)  GO TO 68
      GO TO 71
*********
*
9     IF(ICASE.EQ.1)  GO TO 55
      PRINT*,"OK"
      PRINT*," ENTER TOTAL NUMBER OF NODES WITH SPECIFIED "
      PRINT*," TEMPERATURES. IF NONE ENTER 0. "
* TOTAL NUMBER OF NODES WITH SPECIFIED TEMPERATURE.
      READ*,KT
      IF(KT.EQ.0)  GO TO 55
* NODE NUMBER AND ITS TEMPERATURE.
      DO 3 I=1,KT
```

```
      PRINT*," ENTER NODE NUMBER(INTEGER) AND "
      PRINT*," ITS TEMPERATURE(REAL), "
      READ*,K,T(K)
      CALL MODYSBS(K,T,NNODE,FINALK,FINALF,NBW)
3     CONTINUE
*
* CALCULATION OF TEMPERATURE,STORED IN F.
*
55    IDGT=10
      CALL LEQ1PB(FINALK,NNODE,NC,NNODE,FINALF,
     1NNODE,1,IDGT,D1,D2,IER)
*
68    REWIND 6
      WRITE(6,*)NEL,NNODE
      DO 48 I=1,NNODE
48    WRITE(6,*)RX(I),ZY(I),FINALF(I)
      DO 49 I=1,NEL
49    WRITE(6,*)II(I),JJ(I),KK(I)
      PRINT*," NOW THE STRUCTURE DATA AND ITS TEMPERATURES "
      PRINT*," ARE WRITTEN ON TAPE6. "
1000  STOP
      END
```

```
      SUBROUTINE ACCUMK(FK,NNODE,NBW,AK,IN,II,JJ,KK,NEL)
      DIMENSION AK(3,3),FK(NNODE,NBW),II(NEL),JJ(NEL),KK(NEL),N(3)
*****************************************************************
* SUBROUTINE TO ACCUMULATE 3X3 ELEMENT STIFFNESS MATRIX IN      *
* GLOBAL STIFFNESS MATRIX OF NNODEXNNODE. STORED IN SYMMETRIC   *
* BAND STORAGE MODE.                                            *
*****************************************************************
*                        L E G E N D                            *
*****************************************************************
* AK                  ELEMENT STIFFNESS MATRIX.                 *
* FK                  GLOBAL STIFFNESS MATRIX.                  *
* NNODE               TOTAL NUMBER OF DEGREES OF FREEDOM.       *
* II, JJ, KK          VECTORS CONTAINING I, J AND K NODE NUMBERS *
*                     OF ELEMENTS, RESPECTIVELY.                *
*****************************************************************
      N(1)=II(IN)
      N(2)=JJ(IN)
      N(3)=KK(IN)
      DO 1,I=1,3
1     FK(N(I),NBW)=FK(N(I),NBW)+AK(I,I)
      DO 2 I=1,2
      I1=I+1
      DO 2 J=I1,3
      IF(N(J).GT.N(I))  GO TO 4
      J1=NBW-(N(I)-N(J))
      FK(N(I),J1)=FK(N(I),J1)+AK(J,I)
      GO TO 2
4     J2=NBW-(N(J)-N(I))
      FK(N(J),J2)=FK(N(J),J2)+AK(J,I)
2     CONTINUE
      RETURN
      END
      SUBROUTINE ACCUMF(FF,L,F,IN,ITI,ITJ,ITK,IL)
      DIMENSION FF(L),F(3),ITI(IL),ITJ(IL),ITK(IL)
*****************************************************************
* SUBROUTINE TO STORE 3X1 ELEMENT FORCE VECTOR IN GLOBAL FORCE  *
* VECTOR OF LX1.                                                *
*****************************************************************
*                        L E G E N D                            *
*****************************************************************
* FF                  GLOBAL FORCE VECTOR.                      *
* F                   ELEMENT FORCE VECTOR.                     *
* L                   TOTAL NUMBER OF DEGREES OF FREEDOM.       *
* IL                  TOTAL NUMBER OF ELEMENTS.                 *
* ITI, ITJ, ITK       VECTORS CONTAINING ELEMENT NODE NUMBERS,  *
*                     I, J AND K, RESPECTIVELY.                 *
*****************************************************************
      FF(ITI(IN))=FF(ITI(IN))+F(1)
      FF(ITJ(IN))=FF(ITJ(IN))+F(2)
      FF(ITK(IN))=FF(ITK(IN))+F(3)
      RETURN
      END
```

```
      SUBROUTINE MODFYSBS(NO,T,L,FK,F,NC1)
      DIMENSION FK(L,NC1),F(L),T(L)
C*****************************************************************
C* SUBROUTINE TO MODIFY STIFFNESS MATRIX, STORED IN SYMMETRIC    *
C* BAND STORAGE MODE, IF SOME NODAL VALUES ARE KNOWN, OTHER THAN *
C* ZERO. T(NO) CONTAINS THE KNOWN VALUE.                         *
C*****************************************************************
C*                        L E G E N D                            *
C*****************************************************************
C*FK                GLOBAL STIFFNESS MATRIX LXNC1.              *
C* F                 GLOBAL FORCE VECTOR.                        *
C* NO                NUMBER OF THE NODE WITH KNOWN VALUE.        *
C* T                 VECTOR CONTAINING NODAL VALUES.             *
C* NC1               BANDWIDTH.                                  *
C* L                 TOTAL NUMBER OF DEGREES OF FREEDOM.         *
C*****************************************************************
      F(NO)=FK(NO,NC1)*T(NO)
      NC=NC1-1
      J=L-NC1+1
      IF(NO.GT.J)  GO TO 6
      KK=-1
      J=NC+NO
      DO 1 I=1,NC
      KK=KK+1
      M=J-KK
      F(M)=F(M)-FK(M,I)*T(NO)
    1 FK(M,I)=0
      GO TO 3
    6 K=NO-(L-NC1)
      KK=-1
      IF(K.GT.NC)  GO TO 3
      DO 2 I=K,NC
      KK=KK+1
      M=L-KK
      F(M)=F(M)-FK(M,I)*T(NO)
    2 FK(M,I)=0
    3 K=NO-NC-1
      J=1
      IF(NO.GE.NC1)  GO TO 4
      K=0
      J=NC1-NO+1
      IF(J.GT.NC)  GO TO 8
    4 DO 5 I=J,NC
      K=K+1
    5 F(K)=F(K)-FK(NO,I)*T(NO)
    8 DO 7 I=1,NC
    7 FK(NO,I)=0
      RETURN
      END
```

APPENDIX B

Computer program 'PLASTIC', for elasto-plastic stress analysis.

```
      PROGRAM PLASTIC(INPUT,OUTPUT,TAPE5,TAPE6,TAPE11,TAPE15
     1,TAPE9)
      DIMENSION ITI(450),ITJ(450),ITK(450),NNODE(450,6)
     1,FK(523,36),FF(523),RSDF(523),R(523),Z(523),T(300)
     1,B(4,6),D(4,4),BTD(6,4),AK(6,6),NN(6),EPSZERO(4),F(6)
     1,DF(4),DFD(1,4),DD(4,4),DEP(4,4),DEPS(6),DSGMA(6)
     1,DELTA(6),P(6),DSGMA3(6),DSGMA2(6)
     1,YPI(17),PT(17),TI(17),FTI(17),HPI(17)
C*****************************************************
C* PROGRAM FOR AXISYMMETRIC ELASTO-PLASTIC STRESS ANALYSIS OF *
C* STRUCTURE.  INITIAL STRESS METHOD.                *
C*****************************************************
C*                                                   *
C*****************************************************
C*                      L E G E N D                  *
C*****************************************************
C* ITI,ITJ,ITK      ELEMENT NODE NUMBERS, I, J, K RESPECTIVELY *
C* R,Z              VECTOR CONTAINING R AND Z COORDINATES OF A *
C*                  NODE.                            *
C* NNODE            ELEMENT DEGREES OF FREEDOM       *
C* FK               GLOBAL STIFFNESS MATRIX, L2XNBW  *
C* L2               TOTAL DEGREES OF FREEDOM.        *
C* NBW              BANDWIDTH.                       *
C* FF               GLOBAL FORCE VECTOR.             *
C* AK               ELEMENT STIFFNESS MATRIX.        *
C* F                ELEMENT FORCE VECTOR.            *
C* T                VECTOR CONTAINING NODAL TEMPERATURES. *
C*****************************************************
C*****************************************************
C
C VONMISES STRESS FUNCTION.
      VONMS(S1,S2,S3,S4)=((0.5*((S1-S2)**2))+(0.5*((S2-S3)**2))
     1+(0.5*((S3-S1)**2))+3*(S4**2))**0.5
C
C DATA FOR FUNCTION VALUES AT DIFFERENT TEMPERATURE, USING
C LAGRANGE POLYNOMIAL.
C
C TEMPERATURE POINTS.
      DATA TI/-400.,-300.,-200.,-100.,0.,100.,200.,300.,400.
     1,500.,600.,700.,800.,900.,1000.,1100.,1200./
C
C VALUES FOR ELASTIC MODULUS.
      DATA FTI/2.,2.,2.,2.,2.,1.99999,1.94,1.92,1.86666,
     11.83333,1.75,1.67,1.56666,1.46666,1.33333,1.13333,0.93333/
C
C VALUES FOR YIELD POINT.
      DATA YPI/400.,400.,400.,400.,400.,397.,394.,390.,385.
     1,377.,340.,300.,250.,210.,185.,140.,113./
C
C VALUES FOR PLASTIC MODULUS.
      DATA HPI/4.3,4.3,4.3,4.3,4.3,4.27,4.2,4.13,4.0,3.85,3.7
     1,3.46,3.19,2.9,2.47,2.0/
C
      REWIND 5
      REWIND 6
      REWIND 9
      REWIND 11
      REWIND 15
C
```

```
*****************************************************
*  READ DATA OF THE STRUCTURE, AND FIND BANDWIDTH.*
*****************************************************
*
      READ(5,*)N,L
      DO 1 I=1,L
1     READ(5,*)Z(I),R(I),T(I)
      DO 2 I=1,N
      READ(5,*)ITI(I),ITJ(I),ITK(I)
2     CONTINUE
      DO 3 I=1,N
      DO 6 J=1,6
6     READ(5,*)NNODE(I,J)
      K1=K2=NNODE(I,1)
      DO 10 J=2,6
      IF(NNODE(I,J).EQ.0)  GO TO 10
      IF(NNODE(I,J).GT.K1)  K1=NNODE(I,J)
      IF(NNODE(I,J).LT.K2)  K2=NNODE(I,J)
10    CONTINUE
      IF((K1-K2+1).GT.NBW)  NBW=K1-K2+1
3     CONTINUE
      NC1=NBW
*
**
*****************************************************
*
      NC=NBW-1
      PRINT*," BANDWIDTH = ",NBW
*
* AMBIENT TEMPERATURE
      TAMB=24+273
*
* POISSON'S RATIO.
      V=0.3
*
*********************************************
* FIND TOTAL NUMBER OF DEGREES OF FREEDOM.*
*********************************************
      L2=NNODE(1,1)
      DO 47 I=1,N
      DO 47 J=1,6
      IF(NNODE(I,J).GT.L2)  L2=NNODE(I,J)
47    CONTINUE
      PRINT*," TOTAL NUMBER OF ELEMENTS = ",N
      PRINT*," TOTAL DEGREES OF FREEDOM = ",L2
*
      PRINT*,"KIND OF LOADING**********"
      PRINT*,"IF ONLY MECHANICAL LOADING, ENTER 1"
      PRINT*,"IF ONLY THERMAL LOADING, ENTER 2"
      PRINT*,"IF BOTH MECHANICAL AND THERMAL LOADING, ENTER 3"
      READ*,LOADING
      IF(LOADING.EQ.2)  GO TO 46
      PRINT*,"ENTER TOTAL NUMBER OF NODES SUBJECTED TO
     1MECHANICAL LOADING (INTEGER)."
      READ(5,*)J
      DO 21 I=1,J
21    READ(5,*)K,FF(K)
*
```

```
*************************************************
*/ ELEMENT STIFFNESS AND FORCE MATRICES FORMULATION.*
*************************************************
*
46      DO 8 I=1,N
        Z1=Z(ITI(I))
        R1=R(ITI(I))
        Z2=Z(ITJ(I))
        R2=R(ITJ(I))
        Z3=Z(ITK(I))
        R3=R(ITK(I))
C
C AREA AND VOLUME OF THE ELEMENT.
        AREA=((R2*Z3)-(Z2*R3)-R1*(Z3-Z2)+Z1*(R3-R2))/2
        VOL=AREA*2*3.1415926*(R1+R2+R3)/3
C
C AVERAGE TEMPERATURE OF THE ELEMENT.
        TEMP=(T(ITI(I))+T(ITJ(I))+T(ITK(I)))/3
C
C B-MATRIX.
        B(1,2)=B(4,1)=R3-R2
        B(1,4)=B(4,3)=R1-R3
        B(1,6)=B(4,5)=R2-R1
        B(2,1)=B(4,2)=Z2-Z3
        B(2,3)=B(4,4)=Z3-Z1
        B(2,5)=B(4,6)=Z1-Z2
        B(3,1)=((R2*Z3-R3*Z2)+((Z2-Z3)*(R1+R2+R3)/3)+((R3-R2)
       1*(Z1+Z2+Z3)/3))*3/(R1+R2+R3)
        B(3,3)=((R3*Z1-R1*Z3)+((Z3-Z1)*(R1+R2+R3)/3)+((R1-R3)
       1*(Z1+Z2+Z3)/3))*3/(R1+R2+R3)
        B(3,5)=((R1*Z2-R2*Z1)+((Z1-Z2)*(R1+R2+R3)/3)+((R2-R1)
       1*(Z1+Z2+Z3)/3))*3/(R1+R2+R3)
        DO 13 K=1,4
        DO 13 J=1,6
13      B(K,J)=B(K,J)/(2*AREA)
C
C MODULUS OF ELASTICITY OF THE ELEMENT .
        E=PROPS(TEMP,ETI,PT,TI)
        E=E*1E+7
C
C ELASTICITY MATRIX OF THE ELEMENT.
        D(1,1)=D(2,2)=D(3,3)=1-V
        D(2,1)=D(1,2)=D(1,3)=D(3,1)=D(2,3)=D(3,2)=V
        D(4,4)=(1-2*V)/2
        DO 4 I1=1,4
        DO 4 J=1,4
4       D(I1,J)=D(I1,J)*E/((1+V)*(1-2*V))
C
C MULTIPLIES TRANSPOSE OF B TO D , STORED IN BTD.
        CALL VMULFM(B,D,4,6,4,4,4,BTD,6,IER)
C
        F(1)=F(2)=F(3)=F(4)=F(5)=F(6)=0
        IF(LOADING.EQ.1)  GO TO 20
C COEFFICIENT OF THERMAL EXPANSION.
        ALPHA=(11.15+((TEMP-255.22)*(4.65)/666.666))*1E-6
```

```
C
C NODAL FORCES DUE TO INITIAL STRAIN
      EPSZERO(1)=EPSZERO(2)=EPSZERO(3)=ALPHA*(TEMP-TAMB)
      CALL VMULFF(BTD,EPSZERO,6,4,1,6,4,F,6,IER)
      DO 11 J=1,6
11    F(J)=F(J)*VOL
C
C MULTIPLIES BTD TO B , STORED IN AK
20    CALL VMULFF(BTD,B,6,4,6,6,4,AK,6,IER)
C
C ELEMENT STIFFNESS MATRIX AK.
      DO 9 IK=1,6
      DO 9 IL=1,6
9     AK(IK,IL)=AK(IK,IL)*VOL
C ACCUMULATION OF STIFFNESS MATRIX.
      CALL ACCUMK(FK,L2,NBW,AK,I,NNODE)
C
* ACCUMULATION OF FORCE MATRIX.
      CALL ACCUMF(FF,L2,F,I,NNODE)
      WRITE(11,*)VOL
      WRITE(11,*)((B(K,J),J=1,6),K=1,4),((D(K,J),J=1,4),K=1,4)
      WRITE(11,*)(EPSZERO(M),M=1,4)
8     CONTINUE
*****************************************************************
* END OF ELEMENT STIFFNESS AND FORCE MATRICES FORMULATION.*
*****************************************************************
*
*******************************************
* START OF ELASTO-PLASTIC STRESS ANALYSIS.*
*******************************************
      IDGT=10
      LAST=SUM=ITER=0
      INCR=1
      REWIND 15
      WRITE(15,*)((FK(K,J),J=1,NBW),K=1,L2)
C FIRST INCREMENT OF THE LOAD.
      SUM=FACTOR=0.5
      DO 5 I=1,L2
      R(I)=0
      Z(I)=FF(I)
5     FF(I)=FF(I)*FACTOR
*********************************
* CALCULATION OF DISPLACEMENTS.*
*********************************
      CALL LEQ1PB(FK,L2,NC,L2,FF,L2,1,IDGT,D1,D2,IER)
      IF(IER.EQ.129)  STOP
      GO TO 1000
*
1005  INCR=INCR+1
      SUM=SUM+FACTOR
      IF(SUM.GT.1)  FACTOR=FACTOR-(SUM-1)
      IF(SUM.GE.1)  LAST=1
      DO 1015 I=1,L2
1015  FF(I)=Z(I)*FACTOR
      REWIND 15
      READ(15,*)((FK(K,J),J=1,NBW),K=1,L2)
      CALL LEQ1PB(FK,L2,NC,L2,FF,L2,1,IDGT,D1,D2,IER)
      IF(IER.EQ.129)   STOP
```

```
      ****************************
      * CALCULATION OF STRESSES.*
      ****************************
 1000 ITER=ITER+1
      MAXCHK=0
      AP=0
      REWIND 11
 3000 DO 119 I=1,N
   50 READ(11,*) VOL
      READ(11,*)((R(K,J),J=1,6),K=1,4),((D(K,J),J=1,4),K=1,4)
      READ(11,*)(EPSZERO(M),M=1,4)
C
C  AVERAGE TEMPERATURE OF THE ELEMENT.
      TEMP=(T(ITI(I))+T(ITJ(I))+T(ITK(I)))/3
C
C  YIELD STRENGTH OF THE ELEMENT.
      YS=PROPS(TEMP,YPI,PT,TI)*1E+2
C
      DO 150 J=1,6
  150 NN(J)=NNODE(I,J)
      DO 114 J=1,6
      IF(NN(J).EQ.0)     DELTA(J)=0
      IF(NN(J).EQ.0)    GO TO 114
      DELTA(J)=FF(NN(J))
  114 CONTINUE
C
      CALL VMULFF(R,DELTA,4,6,1,4,6,DEPS,4,IER)
      IF(RSD.EQ.1)  GO TO 3001
      DO 123 JA=1,4
  123 DEPS(JA)=DEPS(JA)-(EPSZERO(JA)*FACTOR)
C
 3001 CALL VMULFF(D,DEPS,4,4,1,4,4,DSGMA,4,IER)
      IF(RSD.EQ.1)  GO TO 3002
      S1=S2=S3=S4=0
      IF(INCR.GT.1)  READ(6,*)S1,S2,S3,S4
C
      F(1)=S1
      F(2)=S2
      F(3)=S3
      F(4)=S4
C
      SI=VONMS(S1,S2,S3,S4)
C
C FINAL STRESS
      S1=S1+DSGMA(1)
      S2=S2+DSGMA(2)
      S3=S3+DSGMA(3)
      S4=S4+DSGMA(4)
      FMS=VONMS(S1,S2,S3,S4)-YS
C
C IF THE ELEMENT IS NOT YIELDED, STORE THE VALUE OF STRESSES.
      IF(FMS.LT.0)  WRITE(9,*)S1,S2,S3,S4
      IF(FMS.LT.0)  GO TO 119
```

```
C
C ELESTC-PLASTIC STIFFNESS MATRIX OF THE ELEMENT.
C
      FS=VONMS(S1,S2,S3,S4)
C
C  PLASTIC MODULUS OF THE ELEMENT.
      HP=PROPS(TEMP,HPI,PT,TI)*1E+6
      DO 1027 IA=1,4
      DEPS(IA)=DEPS(IA)*(FS-YS)/(FS-SI)
1027  DSGMA(IA)=DSGMA(IA)*(FS-YS)/(FS-SI)
      AVGS=(S1+S2+S3)/3
      DF(1)=3*(S1-AVGS)/(2*FS)
      DF(2)=3*(S2-AVGS)/(2*FS)
      DF(3)=3*(S3-AVGS)/(2*FS)
      DF(4)=3*S4/FS
      CALL VMULFM(DF,D,4,1,4,4,4,DFD,1,IER)
      HH=DFD(1,1)*DF(1)+DFD(1,2)*DF(2)+DFD(1,3)*DF(3)
     1+DFD(1,4)*DF(4)
      CALL VMULFF(DF,DFD,4,1,4,4,1,DD,4,IER)
      CALL VMULFF(D,DD,4,4,4,4,4,DEP,4,IER)
      DO 106 J=1,4
      DO 106 K=1,4
106   DEP(J,K)=D(J,K)-DEP(J,K)/(HP+HH)
      CALL VMULFF(DEP,DEPS,4,4,1,4,4,DSGMA2,4,IER)
C
      DO 126 JA=1,4
126   DSGMA3(JA)=DSGMA(JA)-DSGMA2(JA)
C
C CURRENT VALUE OF PLASTIC STRESSES.
      S1=S1-DSGMA3(1)
      S2=S2-DSGMA3(2)
      S3=S3-DSGMA3(3)
      S4=S4-DSGMA3(4)
      WRITE(9,*)S1,S2,S3,S4
C
      P(1)=ABS((F(1)-S1)/F(1))*100
      P(2)=ABS((F(2)-S2)/F(2))*100
      P(3)=ABS((F(3)-S3)/F(3))*100
      P(4)=ABS((F(4)-S4)/F(4))*100
      DO 7 IA=1,4
      IF(P(IA).GT.MAXCHK)  MAXCHK=P(IA)
7     CONTINUE
C
*   RESIDUAL FORCE VECTOR OF THE ELEMENT.
      CALL VMULFM(B,DSGMA3,4,6,1,4,4,P,6,IER)
      DO 128 IA=1,6
128   P(IA)=P(IA)*VOL
      CALL ACCUMF(RSDF,L2,P,6,1,NNODF,N)
      GO TO 119
C
3002  READ(9,*)S1,S2,S3,S4
      S1=S1-DSGMA(1)
      S2=S2-DSGMA(2)
      S3=S3-DSGMA(3)
      S4=S4-DSGMA(4)
      WRITE(6,*)S1,S2,S3,S4
119   CONTINUE
```

```
**
**
**
***************
*
      IF(RSD.EQ.1)  STOP
      REWIND 6
      REWIND 9
      DO 12 I=1,N
      READ(9,*)S1,S2,S3,S4
12    WRITE(6,*)S1,S2,S3,S4
      REWIND 6
      REWIND 9
C
C CHECK FOR CONVERGENCE OF STRESSES..
      IF(MAXCHK.LT.5)  GO TO 1010
      DO 130 I=1,L2
      FF(I)=RSDF(I)
130   RSDF(I)=0
      REWIND 15
      READ(15,*)((FK(K,J),J=1,NBW),K=1,L2)
      CALL LEQ1PB(FK,L2,NC,L2,FF,L2,1,IDGT,D1,D2,IER)
      GO TO 1000
1010  STRS=0
      FACTOR=0.5
      IF(LAST.EQ.1)  GO TO 1014
      GO TO 1005
*****************************************************
* ELASTO-PLASTIC STRESS CALCULATION IS NOW OVER.*
*****************************************************
*************************************
*  CALCULATION OF RESIDUAL STRESSES.*
*************************************
* RESIDUAL STRESS=ELASTO-PLASTIC STRESS-ELASTIC STRESS.
*  RSD  ...  CODE FOR CALCULATION OF RESIDUAL STRESSES.
*
1014  REWIND 15
      READ(15,*)((FK(K,J),J=1,NBW),K=1,L2)
      DO 3010 I=1,L2
3010  FF(I)=Z(I)
      CALL LEQ1PB(FK,L2,NC,L2,FF,L2,1,IDGT,D1,D2,IER)
      RSD=1
      REWIND 11
      REWIND 6
      GO TO 3000
***
***
***
***************
      END
```

```
      FUNCTION PROPS(TEMP,FTI,PT,TI)
      DIMENSION FTI(17),PT(17),TI(17)
*****************************************************
* SUBROUTINE TO FIND FUNCTION VALUES USING LAGRANGE *
* POLYNOMIAL.                                       *
*****************************************************
      TT=(9*(TEMP-273)/5)+32
      DO 16 J=1,17
      PROD1=PROD2=1
      DO 17 I1=1,17
      IF(I1.EQ.J) GO TO 17
      PROD1=PROD1*(TT-TI(I1))
      PROD2=PROD2*(TI(J)-TI(I1))
17    CONTINUE
      PT(J)=PROD1/PROD2
16    CONTINUE
      PROPS=0
      DO 18 I1=1,17
18    PROPS=PROPS+FTI(I1)*PT(I1)
      I1=TT/100
      I1=I1+5
      J=I1+1
      IF(PROPS.GT.FTI(I1))  GO TO 28
      IF(PROPS.LT.FTI(J))  GO TO 28
      GO TO 29
28    PROPS=(FTI(I1)+FTI(J))/2
29    RETURN
      END
      SUBROUTINE ACCUMF(FF,L,F,IN,NNODE)
      DIMENSION FF(L),F(6),NNODE(450,6)
*****************************************************************
* SUBROUTINE TO STORE 6X1 ELEMENT FORVE VECTOR IN GLOBAL FORCE  *
* VECTOR OF LX1.                                                *
*****************************************************************
*                          L E G E N D                          *
*****************************************************************
* FF                GLOBAL FORCE VECTOR.                        *
* F                 ELEMENT FORCE VECTOR.                       *
* L                 TOTAL NUMBER OF DEGREES OF FREEDOM.         *
* IN                ELEMENT NUMBER.                             *
* NNODE             MATRIX CONTAINING ELEMENT DEGREES OF FREEDOM*
*****************************************************************
      FF(NNODE(IN,1))=FF(NNODE(IN,1))+F(1)
      FF(NNODE(IN,2))=FF(NNODE(IN,2))+F(2)
      FF(NNODE(IN,3))=FF(NNODE(IN,3))+F(3)
      FF(NNODE(IN,4))=FF(NNODE(IN,4))+F(4)
      FF(NNODE(IN,5))=FF(NNODE(IN,5))+F(5)
      FF(NNODE(IN,6))=FF(NNODE(IN,6))+F(6)
      RETURN
      END
```

```
      SUBROUTINE ACCUMK(FK,NDOF,NBW,AK,IN,NNODE)
      DIMENSION AK(6,6),FK(NDOF,NBW),NNODE(450,6),N(6)
*****************************************************************
* SUBROUTINE TO ACCUMULATE 6X6 ELEMENT STIFFNESS                *
* MATRIX IN GLOBAL STIFFNESS MATRIX OF NDOFXNDOF.               *
* STORED IN SYMMETRIC BAND STORAGE MODE.                        *
*****************************************************************
* AK            ELEMENT STIFFNESS MATRIX.                       *
* FK            GLOBAL STIFFNESS MATRIX.                        *
* NNODE         MATRIX CONTAINING ELEMENT DEGREES OF FREEDOM.   *
* NBW           BANDWIDTH.                                      *
*****************************************************************
      DO 7 IA=1,6
7     N(IA)=NNODE(IN,IA)
11    DO 1 I=1,6
      IF(N(I).EQ.0)  GO TO 1
      FK(N(I),NBW)=FK(N(I),NBW)+AK(I,I)
1     CONTINUE
      DO 5 I=1,5
      IF(N(I).EQ.0)  GO TO 5
      I1=I+1
      DO 2 J=I1,6
      IF(N(J).EQ.0)  GO TO 2
      IF(N(J).GT.N(I))  GO TO 4
      J1=NBW-(N(I)-N(J))
      FK(N(I),J1)=FK(N(I),J1)+AK(J,I)
      GO TO 2
4     J2=NBW-(N(J)-N(I))
      FK(N(J),J2)=FK(N(J),J2)+AK(J,I)
2     CONTINUE
5     CONTINUE
      RETURN
      END
```